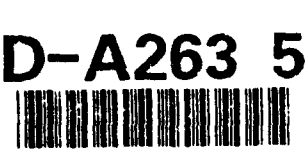

NAVAL POSTGRADUATE SCHOOL
Monterey, California

THESIS

SWAY, YAW, AND ROLL COUPLING EFFECTS ON STRAIGHT LINE STABILITY OF SUBMERSIBLES

by

Daniel J. Cunningham, II

March, 1993

Thesis Advisor: Fotis A. Papoulias

Approved for public release; distribution is unlimited

REPORT DOCUMENTATION PAGE

Form Approved
OMB No 0704-0188

1. AGENCY USE ONLY (Leave blank)	2. REPORT DATE	3. REPORT TYPE AND DATES COVERED
	March 1993	Master's Thesis

4. TITLE AND SUBTITLE
Sway, Yaw, and Roll Coupling Effects on Straight Line Stability of Submersibles

5. FUNDING NUMBERS

6. AUTHOR(S)
Cunningham, Daniel J. II

7. PERFORMING ORGANIZATION NAME(S) AND ADDRESS(ES)
Naval Postgraduate School
Monterey, California 93943-5000

8. PERFORMING ORGANIZATION REPORT NUMBER

9. SPONSORING/MONITORING AGENCY NAME(S) AND ADDRESS(ES)

10. SPONSORING/MONITORING AGENCY REPORT NUMBER

11. SUPPLEMENTARY NOTES
The views expressed in this thesis are those of the author and do not reflect the official policy or position of the Department of Defense or the U.S. government.

12a. DISTRIBUTION/AVAILABILITY STATEMENT
Approved for public release; distribution is unlimited.

12b. DISTRIBUTION CODE

13. ABSTRACT (Maximum 200 words)

This thesis analyzes the sway, yaw, and roll dynamic stability of neutrally buoyant submersibles. Utilizing the hydrodynamic coefficients for a Mark IX Swimmer Delivery Vehicle (SDV) as a base-line model, the linearized equations of motion for the decoupled steering and roll systems are compared to the coupled system. Two different configurations of hydrodynamic coefficients are considered along with the effects of varying the vertical (Z_g) and longitudinal (X_g) centers of gravity of the vehicle while the longitudinal center of buoyancy (X_b) is held constant. Results demonstrate the significant effects on stability of coupling the steering and roll equations of motion, and the importance of Z_g and X_g selection in minimizing those effects while retaining stability. Perturbation analysis results confirm the essential dependence of the linearized coupled equations on the separation of X_g and X_b.

14. SUBJECT TERMS	15. NUMBER OF PAGES
Straight Line Stability of Neutrally Buoyant Submersibles; Dynamic Coupling; Submersibles; Steering and Roll Equations	84
	16. PRICE CODE

17. SECURITY CLASSIFICATION OF REPORT	18. SECURITY CLASSIFICATION OF THIS PAGE	19. SECURITY CLASSIFICATION OF ABSTRACT	20. LIMITATION OF ABSTRACT
Unclassified	Unclassified	Unclassified	UL

NSN 7540-01-280-5500

Standard Form 298 (Rev 2-89)
Prescribed by ANSI Std 239-18

Approved for public release; distribution is unlimited.

Sway, Yaw, and Roll Coupling Effects on

Straight Line Stability of Submersibles

by

Daniel J. Cunningham, II
Lieutenant, United States Navy
B.A., The University of Vermont, 1983

Submitted in partial fulfillment of the
requirements for the degree of

MASTER OF SCIENCE IN MECHANICAL ENGINEERING

from the

NAVAL POSTGRADUATE SCHOOL

March, 1993

Author: 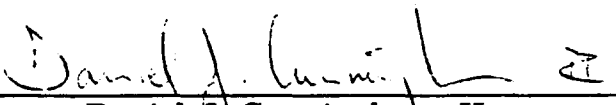

Daniel J. Cunningham, II

Approved by: 

Fotis A. Papoulias, Thesis Advisor

Matthew D. Kelleher, Chairman
Department of Mechanical Engineering

ABSTRACT

This thesis analyzes the sway, yaw, and roll dynamic stability of neutrally buoyant submersibles. Utilizing the hydrodynamic coefficients for a Mark IX Swimmer Delivery Vehicle (SDV) as a base-line model, the linearized equations of motion for the decoupled steering and roll systems are compared to the coupled system. Two different configurations of hydrodynamic coefficients are considered along with the effects of varying the vertical (Z_g) and longitudinal (X_g) centers of gravity of the vehicle while the longitudinal center of buoyancy (X_b) is held constant. Results demonstrate the significant effects on stability of coupling the steering and roll equations of motion, and the importance of Z_g and X_g selection in minimizing those effects while retaining stability. Perturbation analysis results confirm the essential dependence of the linearized coupled equations on the separation of X_g and X_b.

TABLE OF CONTENTS

LIST OF FIGURES

I. INTRODUCTION

A. GENERAL

As the missions for submersibles become more complex and demanding, the requirement for a highly stable platform becomes increasingly important so the operator(s) can concentrate on matters other than station-keeping. Submersible simulators have not been employed to any great extent thus far, since the actual system is relatively inexpensive and the dynamics are usually very non-linear and difficult to model. The analysis of a submersible can be significantly more complex than the analysis of a conventional submarine or aircraft, since the presence of ancillary equipment such as manipulators, video devices, and tethers introduce extra cross-coupling terms usually absent in other, more symmetric, vehicle dynamic analyses. [Ref. 1] Additionally, all mathematical models include simplifying assumptions and errors in the model's hydrodynamic coefficients.

Submersibles typically have a variety of complex dynamic interactions that can severely inhibit maneuverability and control performance. The goal of this thesis is to present an understanding of the coupling effects on straight line motion stability in the horizontal plane using a linearized model, and the primary means of minimizing these effects. Development of the mathematical models for both the coupled and uncoupled maneuvering and roll equations of motion is presented in Chapter II. Utilizing two different configurations of hydrodynamic coefficients, the degree of stability, regions of stability, and linear simulations for the coupled and uncoupled

systems are presented in Chapter III. A Hamming method nonlinear simulation [Ref. 2], which is similar to a fourth order Runge-Kutta integration technique, is conducted on both configurations to compare with the results obtained for the linearized models. Chapter IV develops a perturbation analysis to demonstrate the strong degree of dependence on the separation between the longitudinal centers of buoyancy and gravity to the solution of the linearized coupled equations of motion. Chapter V summarizes the results and provides recommendations for future submersible modelling research. Appendix A contains the computer programs utilized for the linear and nonlinear simulations.

B. PARAMETER DEFINITION

The values for the hydrodynamic derivatives and vehicle dimensions are from Smith, Crane, and Summey [Ref. 3], with the following exceptions:

- Y_r - the force in sway due to a change in yaw rate
- N_v - the moment due to a change in sway velocity.

These two coefficients were modified to produce two different models that would have one eigenvalue change sign for a reasonable range of longitudinal and vertical centers of gravity. A comparison between the actual non-dimensional values and those used in this thesis is as follows:

	Y_r	N_v
Configuration 'A'	-3.500E-02	-1.484E-03
Configuration 'B'	-5.940E-02	-1.484E-03
Actual SDV	2.970E-02	-7.420E-03

The effects of changing these coefficients are illustrated in Figures 1 and 2 on the following pages. Additionally, the analysis presented herein is conducted in dimensional form; hence the nominal forward longitudinal velocity 'U' appears in the equations of motion. All calculations and simulations utilize a value of 5 ft/sec for 'U'. The coordinate system convention is the standard body-fixed, right -hand orthogonal axis system employing the Euler angle approach.

1. Variables

x, y, z	Distances along the body fixed principal axes.
u, v, w	Translational velocity components of model relative to fluid along body axes.
p, q, r	Rotational velocity components of model along body axes.
X, Y, Z	Hydrodynamic force components along body axes.
K, M, N	Hydrodynamic moment components along body axes.
ψ, θ, ϕ	Yaw, pitch, and roll angles; positive values following the right-hand rule.
X_g, Y_g, Z_g	Center of gravity coordinates along principal axes.
X_b, Y_b, Z_b	Center of buoyancy coordinates along principal axes.
I_{xx}, I_{yy}, I_{zz}	Moments of inertia about the principal axes.
X_{nose}, X_{tail}	Distances from body center along the longitudinal axis used in the crossflow force and moment integrals. Values are located within the nonlinear computer simulation program in Appendix A.
h(x), b(x)	Model width and height values used in the crossflow force and moment integrals. Values are located within the nonlinear computer simulation program in Appendix A.

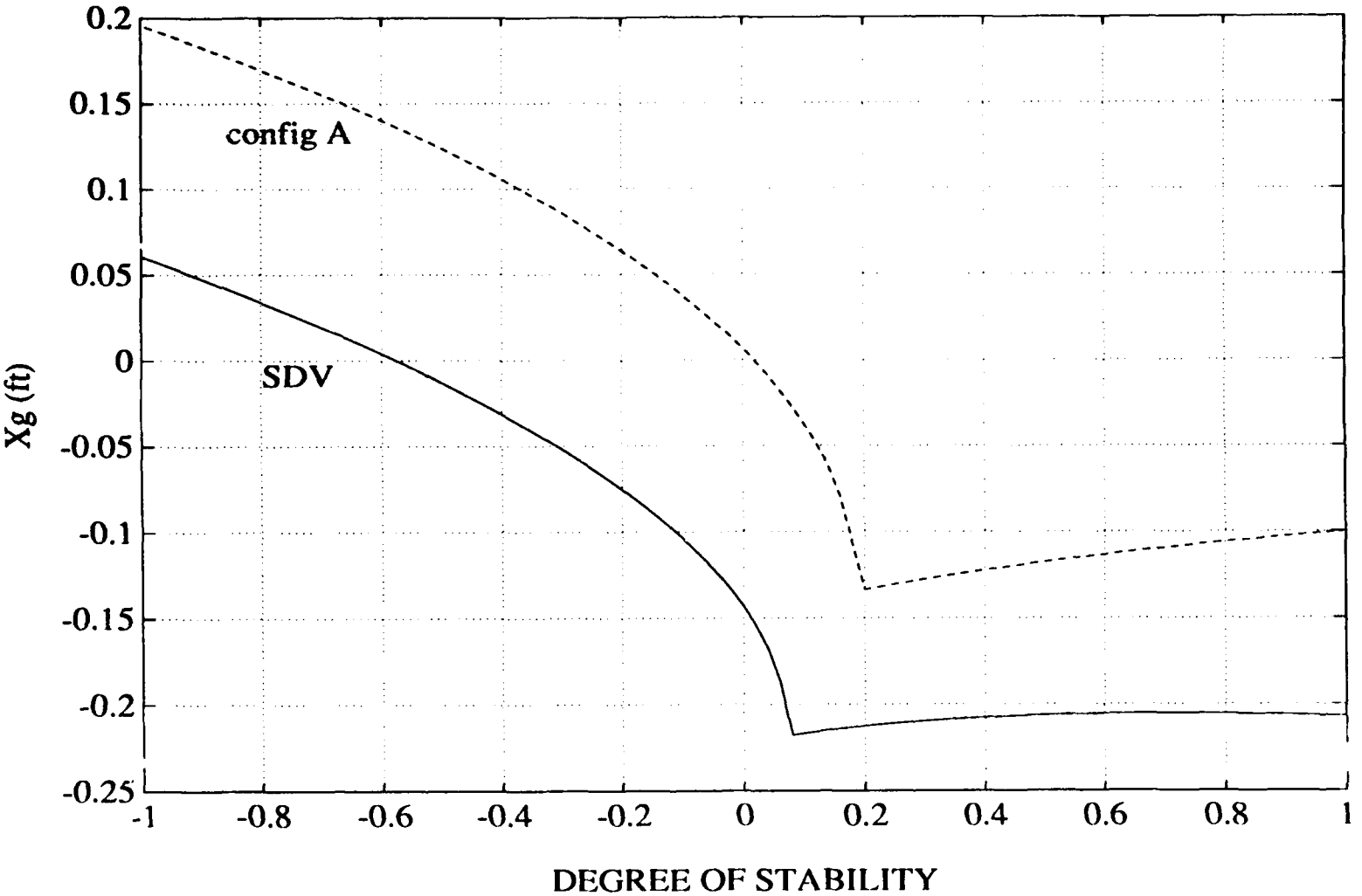

Figure 1: Effect on Degree of Stability for Change in Y_r and N_v - Configuration 'A' (Z_g = 0.10 ft)

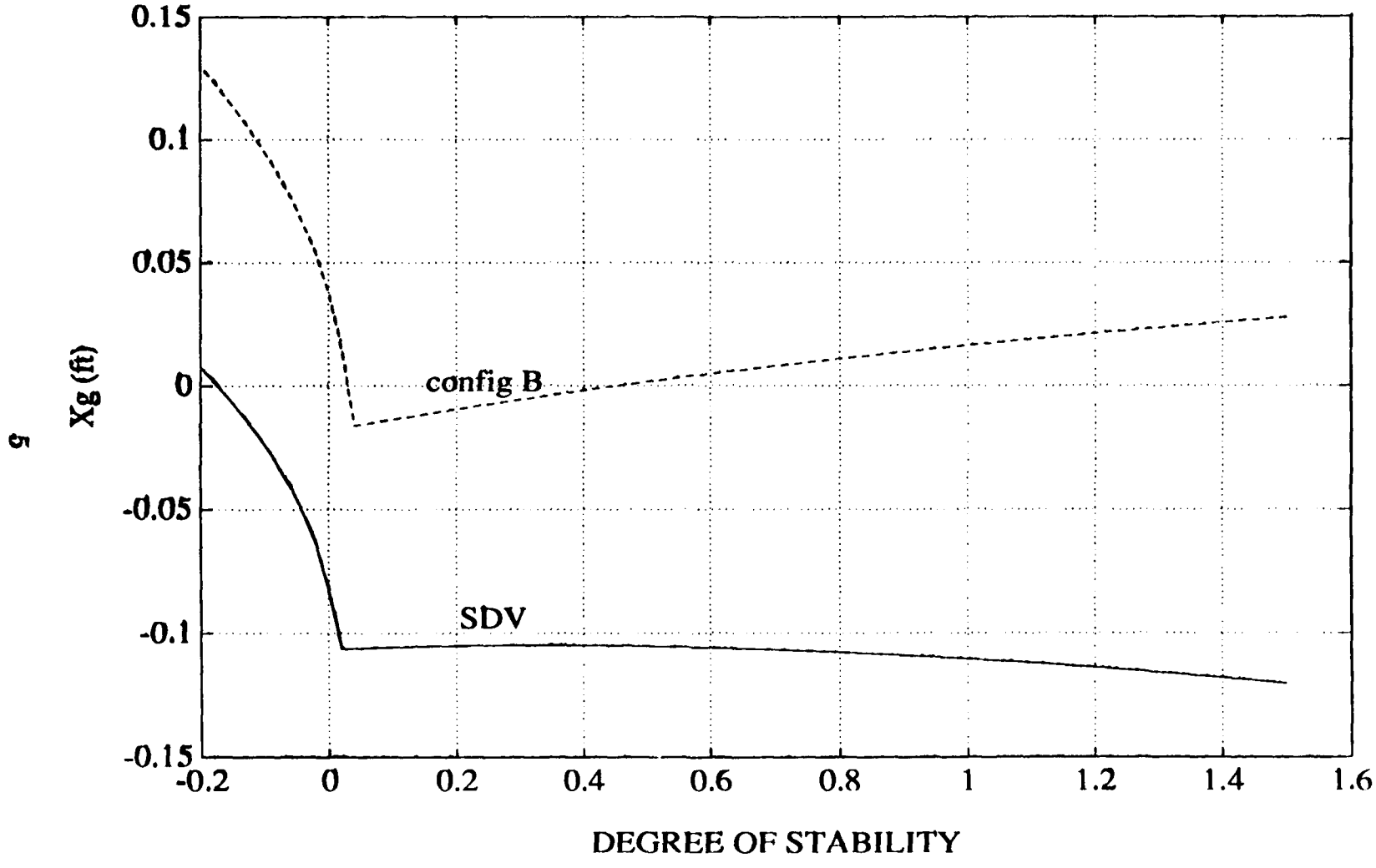

Figure 2: Effect on Degree of Stability for Change in Y_r and N_v - Configuration 'B' (Z_g = 0.03 ft)

II. STABILITY OF MOTION

A. EQUATIONS OF MOTION

The horizontal plane, nonlinear equations of motion for a submersible as developed by Smith, Crane, and Summey [Ref. 1] are shown below in Equations (2.1).

Sway: (2.1a)

$$m[\dot{v} + ur - wp + X_g(pq + \dot{r}) - Y_g(p^2 + r^2) + Z_g(qr - \dot{p})] =$$
$$[Y_{\dot{p}}\dot{p} + Y_{\dot{r}}\dot{r} + Y_{pq}pq + Y_{qr}qr] + [Y_v uv + Y_{vw}vw + Y_{\delta r}u^2\delta r] +$$
$$[Y_{\dot{v}}\dot{v} + Y_p up + Y_r ur + Y_{vq}vq + Y_{wp}wp + Y_{wr}wr] + (W - B)\cos\theta \sin\phi -$$
$$\int_{X_{tail}}^{X_{nose}} [C_{Dy}\, h(x)(v + xr)^2 + C_{Dz}\, b(x)(w - xq)^2] \frac{(v + xr)}{U_{cf}(x)}\, dx$$

Yaw: (2.1b)

$$I_{zz}\dot{r} + (I_{yy} - I_{xx})pq - I_{xy}(p^2 - q^2) - I_{yz}(pr + \dot{q}) +$$
$$I_{xz}(qr - \dot{p}) + m[X_g(\dot{v} + ur - wp) - Y_g(\dot{u} - vr + wq)] =$$
$$[N_{\dot{p}}\dot{p} + N_{\dot{r}}\dot{r} + N_{pq}pq + N_{qr}qr] +$$
$$[N_{\dot{v}}\dot{v} + N_p up + N_r ur + N_{vq}vq + N_{wp}wp + N_{wr}wr] +$$
$$[N_v uv + N_{vw}vw + N_{\delta r}u^2\delta r] + (X_g W - X_b B)\cos\theta \sin\phi + (Y_g W - Y_b B)\sin\theta -$$
$$\int_{X_{tail}}^{X_{nose}} [C_{Dy}\, h(x)(v + xr)^2 + C_{Dz}\, b(x)(w - xq)^2] \frac{(v + xr)}{U_{cf}(x)}(x)\, dx + u^2 N_{prop}$$

Roll:
(2.1c)

$$I_{xx}\dot{p} + qr(I_{zz} - I_{yy}) + I_{xy}(pr - \dot{q}) - I_{yz}(q^2 - r^2) -$$
$$I_{xz}(pq + \dot{r}) + m[Y_g(\dot{w} - uq + vp) - Z_g(\dot{v} + ur - wp)] =$$
$$[K_{\dot{p}}\dot{p} + K_{\dot{r}}\dot{r} + K_{pq}pq + K_{qr}qr] +$$
$$[K_{\dot{v}}\dot{v} + K_{p}up + K_{r}ur + K_{vq}vq + K_{wp}wp + K_{wr}wr] +$$
$$[K_{v}uv + K_{vw}vw] + (Y_gW - Y_bB)\cos\theta\cos\phi -$$
$$(Z_gW - Z_bB)\cos\theta\sin\phi + u^2K_{prop}$$

B. SIMPLIFICATIONS

In order to obtain the linearized equations of motion about a level flight path, the following simplifications were utilized:

- The translational velocity (w) and acceleration ($\dot{w}$) in the z-direction are zero.
- The rotational velocity (q) and acceleration ($\dot{q}$) in the y-direction are zero.
- The acceleration in the longitudinal direction ($\dot{u}$) is zero.
- The cross-products of inertia are zero by virtue of a body-centered coordinate system.
- The submersible is neutrally buoyant so B = W.
- The longitudinal center of buoyancy (X_b) and the vertical center of buoyancy (Z_b) are located at the origin of the body-fixed coordinate system.
- The lateral center of buoyancy (Y_b) and the lateral center of gravity (Y_g) are located at the origin of the body-fixed coordinate system.
- Dynamic stability analysis is performed with all controls fixed; hence, all forces and moments due to control surfaces are zero.
- The angle of pitch (θ) is sufficiently small for $\sin(\theta)$ to equal zero.

- From Smith, Crane, and Summey [Ref. 1] the propeller coefficients K_{prop} and N_{prop} are zero.

C. COUPLED STABILITY EQUATIONS

When the simplifying assumptions from the preceeding section are applied, the resulting linearized equations are:

(2.2a) Sway: $$m\left[\dot{v} + ur + X_g(\dot{r}) - Z_g(\dot{p})\right] = Y_f$$

(2.2b) Yaw: $$I_{zz}\dot{r} + mX_g(\dot{v} + ur) = N_f$$

(2.2c) Roll: $$I_{xx}\dot{p} - mZ_g(\dot{v} + ur) = K_f$$

where the force and moment representations are given by:

(2.3a) Sway Force: $$Y_f = Y_{\dot{v}}\dot{v} + Y_v v + Y_{\dot{r}}\dot{r} + Y_r r + Y_{\dot{p}}\dot{p} + Y_p p$$

(2.3b) Yaw Moment: $$N_f = N_{\dot{v}}\dot{v} + N_v v + N_{\dot{r}}\dot{r} + N_r r + N_{\dot{p}}\dot{p} + N_p p + (X_g W - X_b B)\varphi$$

(2.3c) Roll Moment: $$K_f = K_{\dot{v}}\dot{v} + K_v v + K_{\dot{r}}\dot{r} + K_r r + K_{\dot{p}}\dot{p} + K_p p + (Z_g W - Z_b B)\varphi$$

Equations 2.2 and 2.3 may be combined to form the state space representation:

$$A\dot{x} = Bx \qquad (2.4a)$$

where $$x = [p \;\; \phi \;\; v \;\; r]^T \qquad (2.4b)$$

$$A = \begin{bmatrix} I_{xx} - K_{\dot{p}} & 0 & -(K_{\dot{v}} + MZ_g) & -K_{\dot{r}} \\ 0 & 1 & 0 & 0 \\ -(Y_{\dot{p}} + MZ_g) & 0 & M - Y_{\dot{v}} & MX_g - Y_{\dot{r}} \\ -N_{\dot{p}} & 0 & MX_g - N_{\dot{v}} & I_{zz} - N_{\dot{r}} \end{bmatrix}, \qquad (2.4c)$$

$$B = \begin{bmatrix} K_pU & Z_bB - Z_gW & K_vU & U(MZ_g + K_r) \\ 1 & 0 & 0 & 0 \\ Y_pU & 0 & Y_vU & U(Y_r - M) \\ N_pU & X_gW - X_bB & N_vU & U(N_r - MX_g) \end{bmatrix} \qquad (2.4d)$$

The stability of the coupled, linearized system depends on the location of the four eigenvalues of $\det(\mathbf{B} - \lambda\mathbf{A}) = 0$, which has a characteristic equation of the form

$$A\lambda^4 + B\lambda^3 + C\lambda^2 + D\lambda + E = 0, \qquad (2.4e)$$

where the coefficients are complicated permutations of the elements in matrices A and B. The values for A, B, C, D, and E are given in Equations (2.4f - 2.4j) in terms of lower case letters that represent entries in matrices A and B; they are explicitly defined in Table 1.

$$A = a\cdot(j\cdot u - l\cdot r) + d\cdot(u\cdot h + o\cdot l) - f\cdot(r\cdot h + o\cdot j) \qquad (2.4f)$$

$$\begin{aligned} B = {} & e\cdot(u\cdot h + o\cdot l) - d\cdot(u\cdot i - w\cdot h + o\cdot m - p\cdot l) - a\cdot(j\cdot w + k\cdot u - l\cdot x - r\cdot m) \\ & - b\cdot(j\cdot u - l\cdot r) + f\cdot(r\cdot i - x\cdot h + o\cdot k - p\cdot j) - g\cdot(r\cdot h + o\cdot j) \end{aligned} \qquad (2.4g)$$

$$\begin{aligned} C = {} & a\cdot(k\cdot w - m\cdot x) + b\cdot(j\cdot w + k\cdot u - l\cdot x - r\cdot m) + g\cdot(r\cdot i - x\cdot h + o\cdot k - p\cdot j) \\ & + c\cdot(j\cdot u - l\cdot r) - d\cdot(q\cdot l - w\cdot i + m\cdot p) - e\cdot(u\cdot i - w\cdot h + o\cdot m - p\cdot l) \\ & + f\cdot(q\cdot j - x\cdot i + p\cdot k) \end{aligned} \qquad (2.4h)$$

$$D = g\cdot(q\cdot j - x\cdot i + p\cdot k) - f\cdot q\cdot k + d\cdot q\cdot m - e\cdot(q\cdot l - w\cdot i + m\cdot p) - b\cdot(k\cdot w - m\cdot x) - c\cdot(j\cdot w + k\cdot u - l\cdot x - r\cdot m) \quad (2.4i)$$

$$E = c\cdot(k\cdot w - m\cdot x) + e\cdot q\cdot m - g\cdot q\cdot k \quad (2.4j)$$

TABLE 1. COEFFICIENT DESCRIPTOR VALUES

$a = I_{xx} - K_{\dot{p}}$	$b = K_pU$	$c = Z_gW - Z_bB$	$d = MZ_g + K_{\dot{v}}$
$e = K_vU$	$f = K_{\dot{r}}$	$g = MZ_gU$	$h = MZ_g + Y_{\dot{p}}$
$i = Y_pU$	$j = M - Y_{\dot{v}}$	$k = Y_vU$	$l = MX_g - Y_{\dot{r}}$
$m = U(Y_r - M)$	$o = N_{\dot{p}}$	$p = N_pU$	$q = X_bB - X_gW$
$r = MX_g - N_{\dot{v}}$	$u = I_{zz} - N_{\dot{r}}$	$w = U(N_r - MX_g)$	$x = N_vU$

D. UNCOUPLED STABILITY EQUATIONS

Using matrices A and B from the preceeding section (Equations 2.4c and 2.4d), uncoupling the steering and roll equations is straightforward:

STEERING EQUATIONS

$$\begin{bmatrix} M - Y_{\dot{v}} & MX_g - Y_{\dot{r}} \\ MX_g - N_{\dot{v}} & I_{zz} - N_{\dot{r}} \end{bmatrix} \begin{bmatrix} \dot{v} \\ \dot{r} \end{bmatrix} = \begin{bmatrix} Y_vU & U(Y_r - M) \\ N_vU & U(N_r - MX_g) \end{bmatrix} \begin{bmatrix} v \\ r \end{bmatrix} \quad (2.5a)$$

ROLL EQUATIONS

$$\begin{bmatrix} I_{xx} - K_{\dot{p}} & 0 \\ 0 & 1 \end{bmatrix} \begin{bmatrix} \dot{p} \\ \dot{\phi} \end{bmatrix} = \begin{bmatrix} K_pU & Z_bB - Z_gW \\ 1 & 0 \end{bmatrix} \begin{bmatrix} p \\ \phi \end{bmatrix} \quad (2.5b)$$

The characteristic equations for the uncoupled steering and roll equations are much simpler than that for the coupled system, and are given as Equations (2.5c and 2.5d) in terms of the hydrodynamic parameters rather than the descriptors used in the previous section.

The steering characteristic equation form is: $A_L\lambda^2 + B_L\lambda + C_L = 0$, where

$$A_L = (M - Y_{\dot{v}})(I_{zz} - N_{\dot{r}}) - (MX_g - Y_{\dot{r}})(MX_g - N_{\dot{v}})$$

$$B_L = -[(I_{zz} - N_{\dot{r}})(Y_v U) + (M - Y_{\dot{v}})(N_r - MX_g)(U) + (Y_r - M)(N_{\dot{v}} - MX_g)(U) + (Y_{\dot{r}} - MX_g)(N_v U)] \quad (2.5c)$$

$$C_L = (Y_v U^2)(N_r - MX_g) - (N_v U^2)(Y_r - M)$$

The roll characteristic equation form is: $A_R\lambda^2 + B_R\lambda + C_R = 0$, where

$$A_R = I_{xx} - K_{\dot{p}}$$

$$B_R = -K_p U \quad (2.5d)$$

$$C_R = Z_g W$$

III. RESULTS AND DISCUSSION

A. DEGREE OF STABILITY

The effects of changing the longitudinal and vertical centers of gravity (while keeping the center of buoyancy fixed at the vehicle center) on the degree of stability for configuration 'A' is illustrated in Figure 3. Degree of stability as utilized in this thesis is defined as the maximum real value of all characteristic roots, with negative values indicating a stable situation. The degree of stability for the uncoupled system is represented by the dashed line. It can be seen that the critical value of X_g for which motions become unstable is clearly a function of the metacentric height Z_g, whereas the uncoupled system predicts a constant value of X_g. Figure 4 displays the variation of the imaginary part of the root value for configuration 'A'.

Figures 5 and 6 are analogous to Figures 3 and 4 for configuration 'B'; they show the degree of stability for varying X_g and Z_g values. For this configuration, the degree of stability has a stronger dependence on the location of X_g and the value of Z_g. For almost all positive values of X_g, the complex conjugate roots are increasing in value and eventually becoming positive; this indicates an oscillatory response that diverges when the degree of stability is positive.

B. REGIONS OF STABILITY

Figure 7 shows the region of stability for configuration 'A', with the uncoupled system represented by a dashed line. The uncoupled system predicts stability for all values of X_g greater than 0.18 ft, while the coupled system predicts an additional region enclosed by the triangular area to the

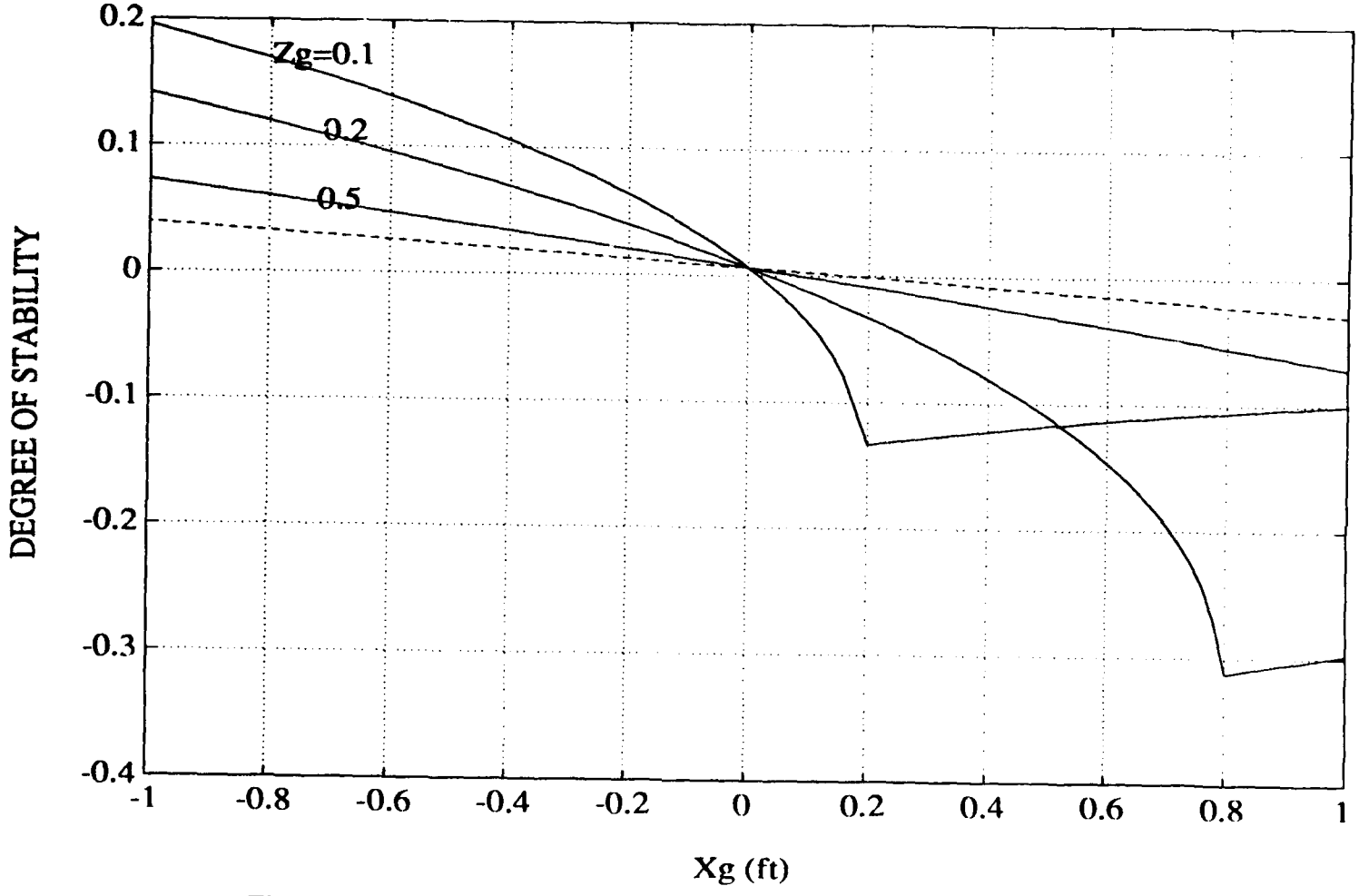

Figure 3: Effects of X_g and Z_g on Degree of Stability for Configuration A

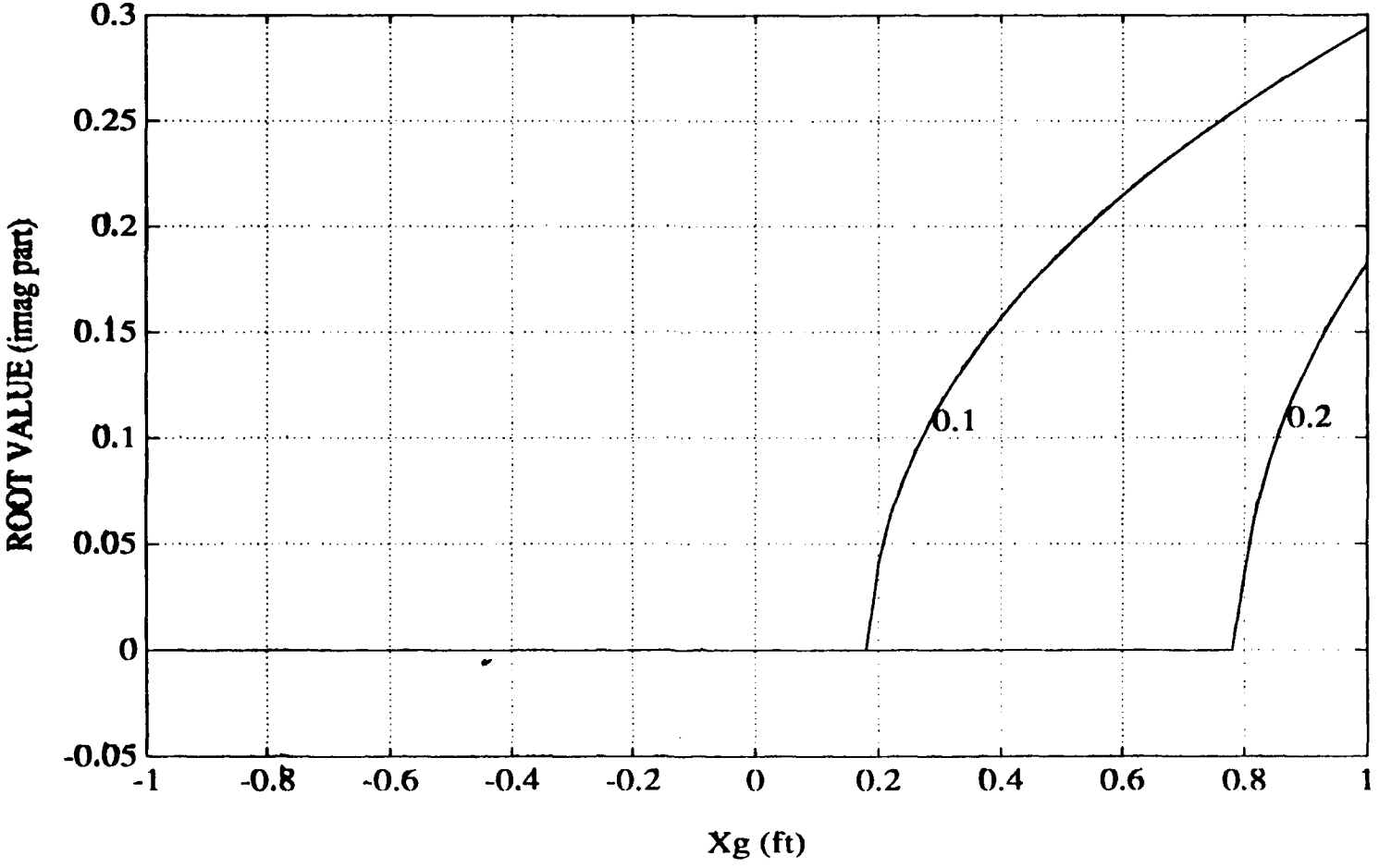

Figure 4: Effects of X_g and Z_g on Imaginary Part of Root for Configuration A

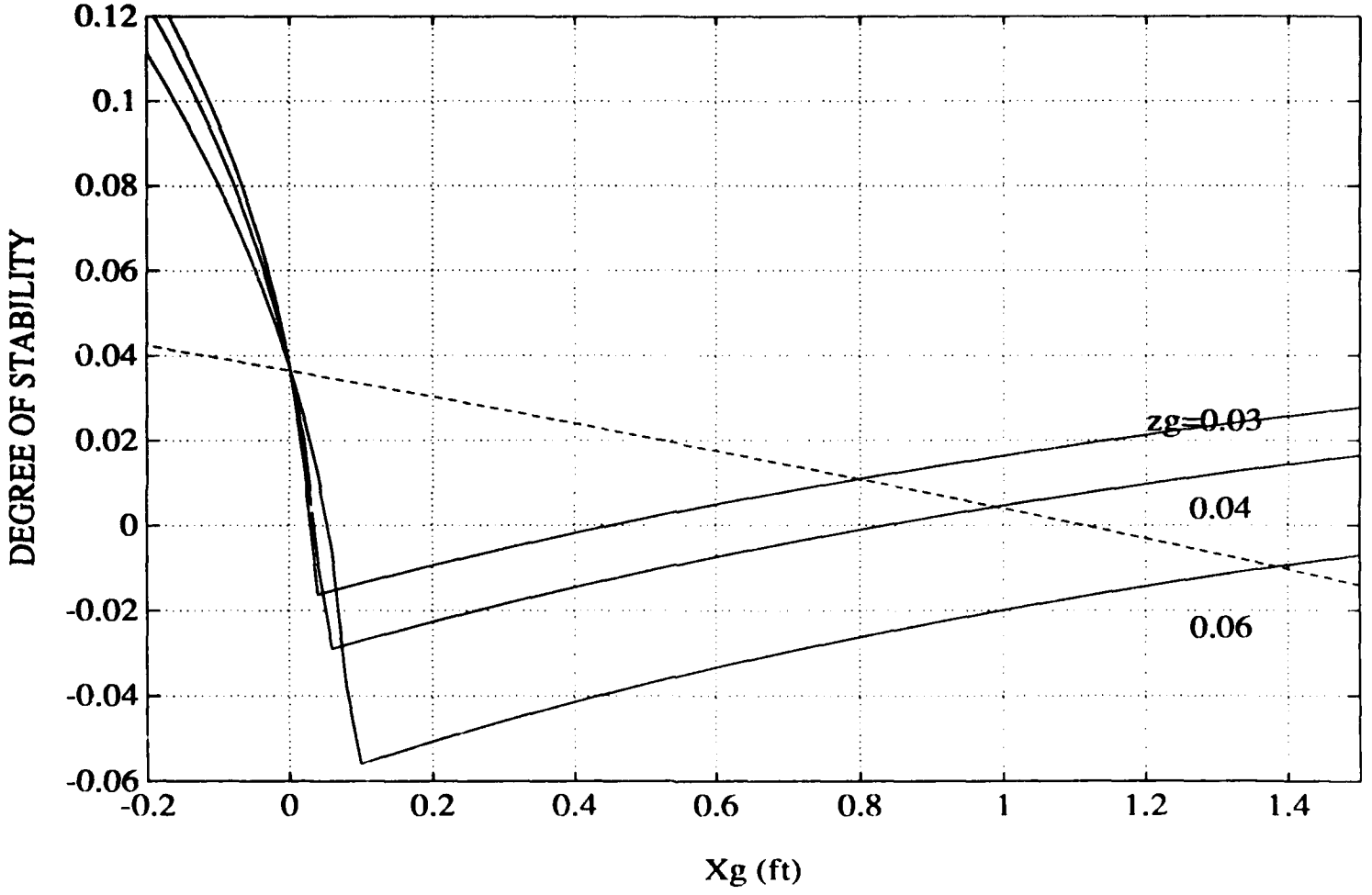

Figure 5: Effects of X_g and Z_g on Degree of Stability for Configuration 'B'

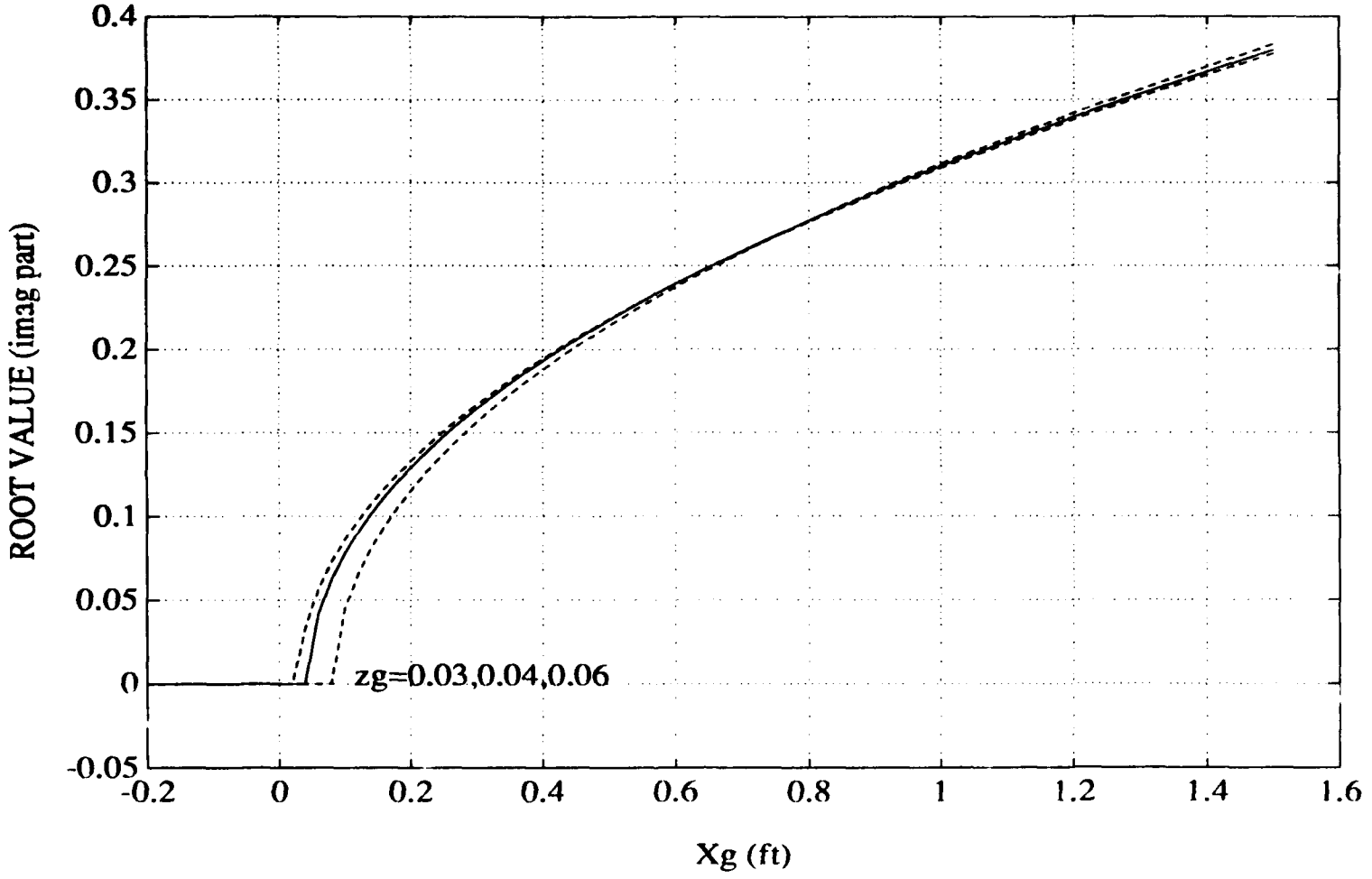

Figure 6: Effects of X_g and Z_g on Imaginary Part of Root for Configuration 'B'

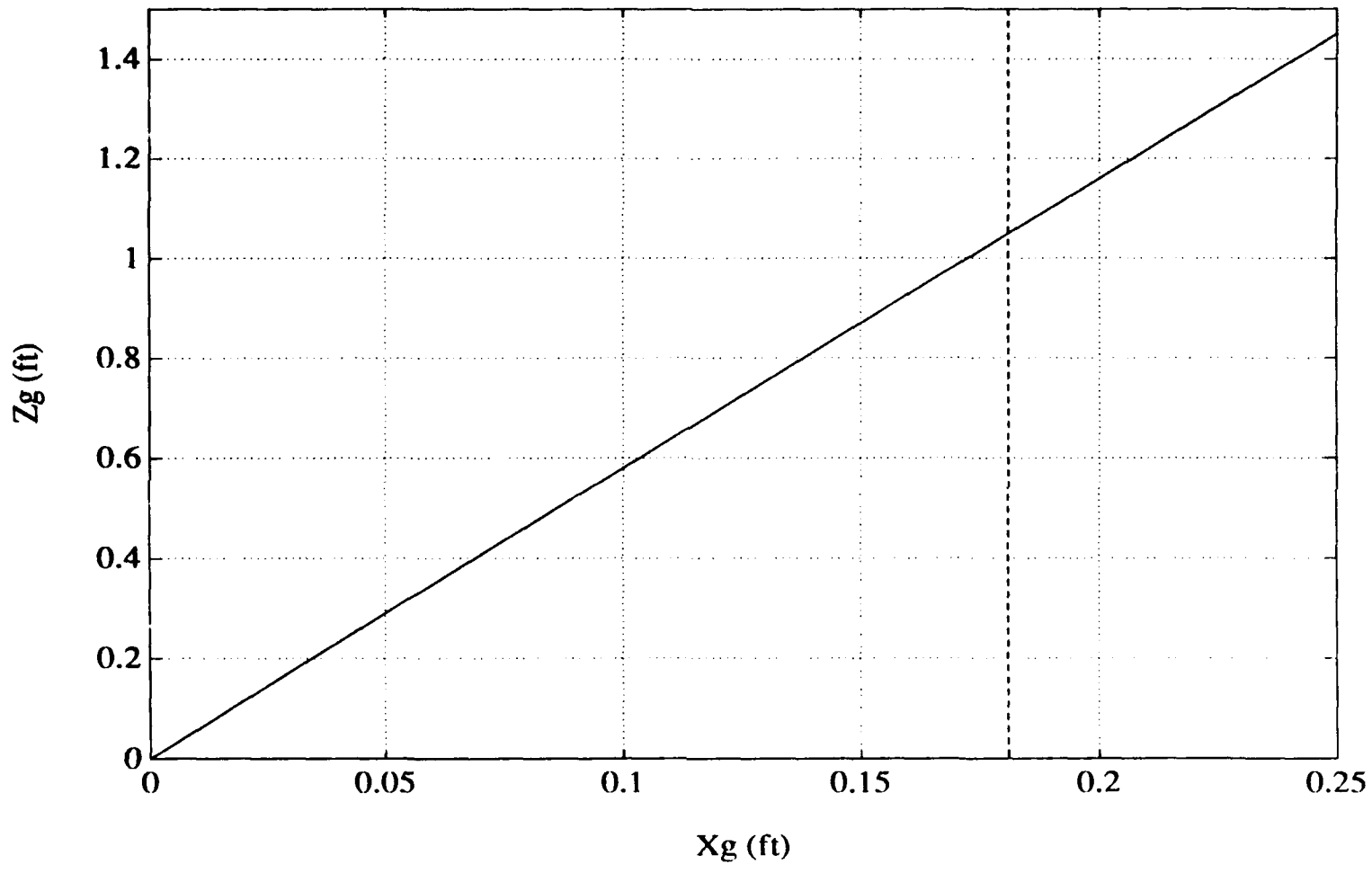

Figure 7: Calculated Z_g Location vs X_g for Configuration 'A'

left of the dashed line. Figure 8 is analogous to Figure 7 for configuration 'B'. The large discrepancies between the predicted regions of stability in this case occur for Z_g values less than 0.045 ft. For small values of Z_g, there are corresponding small regions of X_g where stability is predicted by the coupled equations but not by the uncoupled equations. The root values in this region are complex conjugates with very small real parts. Figures 9(a) and 9(b) illustrate the effect of co-locating X_b and X_g. This results in a degree of stability for the coupled system that is nearly identical to the uncoupled system.

C. INTERPRETATION OF RESULTS

It may be shown by applying Routh's criterion [Ref. 4: pp. 211-218] that for a fourth order equation of the form $A\lambda^4 + B\lambda^3 + C\lambda^2 + D\lambda + E$ to have roots with all negative real parts the following must apply:

$$\text{i.)}\ BCD - AD^2 - EB^2 > 0$$

$$\text{ii.)}\ E > 0.$$

If the quantity 'E' is less than zero, the system will become unstable and the resulting motion will be a simple divergence. If, however, the value of the quantity $BCD - AD^2 - EB^2$ is negative, the resulting instability will result in an oscillatory motion due to the presence of complex conjugate roots with positive real parts.

For the coupled system of equations, the condition $E = 0$ yields:

$$Z_g = X_g \cdot [K_v(Y_r - M)/(Y_v N_r - N_v(Y_r - M))].$$

while the uncoupled system of equations reduces to a constant term expression for X_g:

$$X_g = [(MY_v)/(Y_v N_r - N_v(Y_r - M))].$$

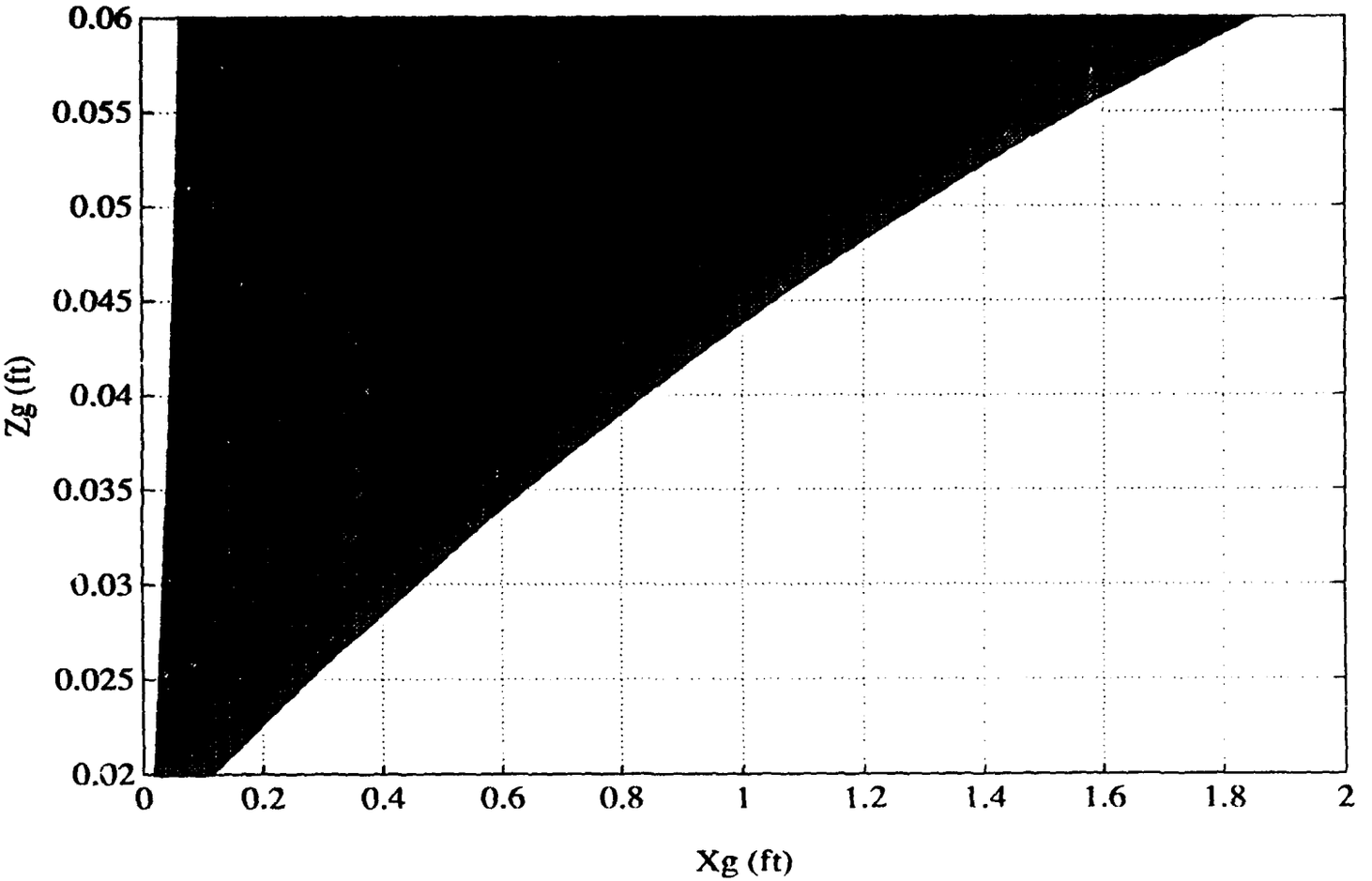

Figure 8: Calculated Z_g Location vs X_g for Configuration 'B'

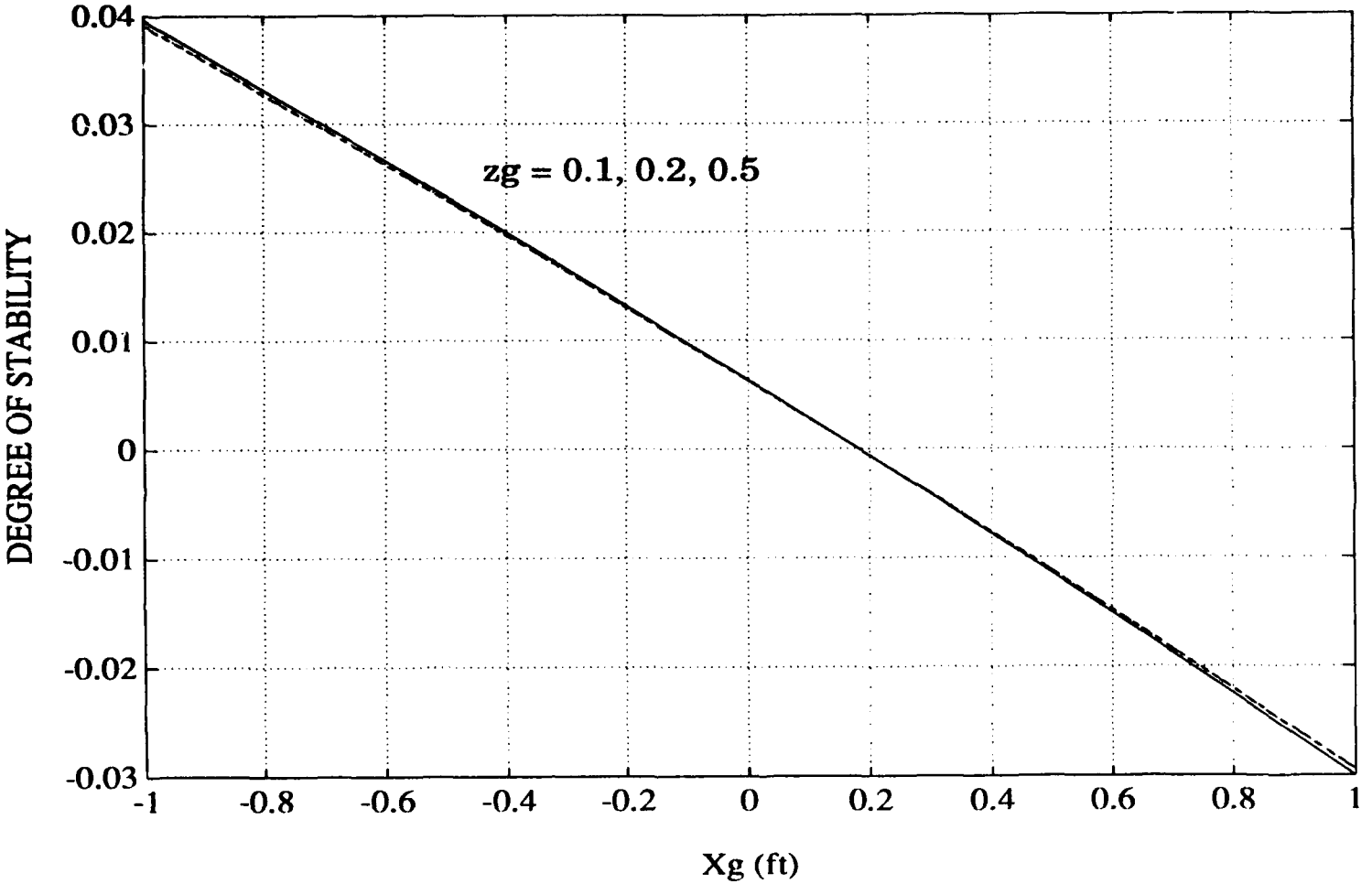

Figure 9(a): Effects of X_g and Z_g on Degree of Stability when X_b Equals X_g for Configuration 'A'

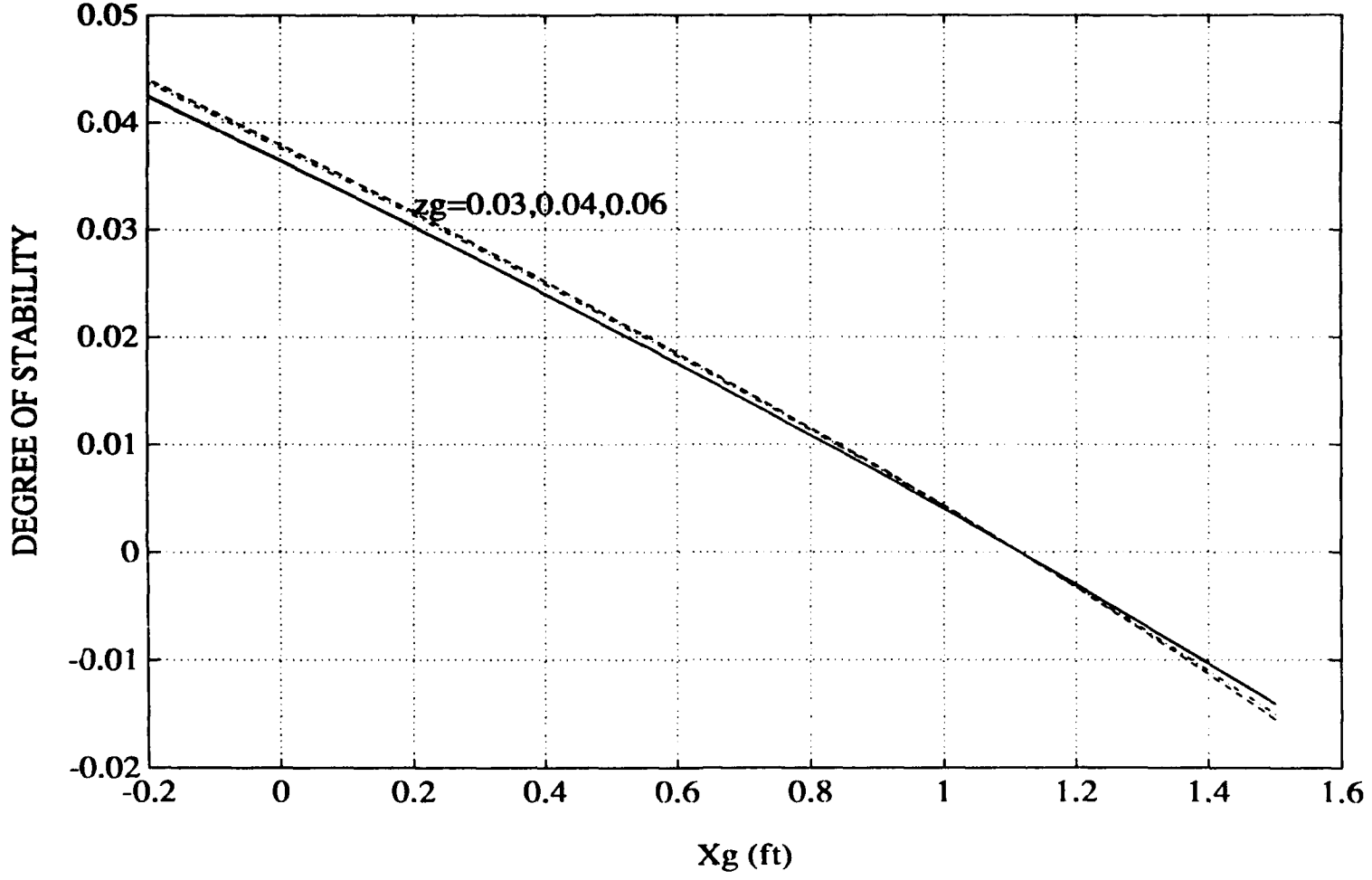

Figure 9(b): Effects of X_g and Z_g on Degree of Stability when X_b Equals X_g for Configuration 'B'

This explains the differences in the regions of stability illustrated in Figure 7, since the above equations show a linear relationship between Z_g and X_g for the coupled equations and a constant value for X_g for the uncoupled equations. When the value for X_g coincides with the value for X_b, the constant term 'E' in the coupled equations is reduced to that of the constant associated with the uncoupled equations, and the resulting predicted degree of stability no longer depends on the value of Z_g. Substituting the coefficient values for 'E' serves to clearly illustrate the reduction:

$$E = (Z_gW)[(Y_vU^2)(N_r\text{-}MX_g) - (N_vU^2)(Y_r\text{-}M)] + (K_vU^2)(Y_r\text{-}M)(X_bB\text{-}X_gW) - (MZ_gU)(Y_vU)(X_bB\text{-}X_gW).$$

When $X_b = X_g$ and B = W for the neutrally buoyant case, the second and third terms are reduced to zero. When 'E' is then set equal to zero (the condition for determining where the real roots change from negative to positive), the dependence on the value Z_g is removed and the expression for X_g is the constant given for the uncoupled equations. This reduction is the explanation for the appearance of Figures 9(a) and 9(b). When the longitudinal centers of buoyancy and gravity coincide for a neutrally buoyant vehicle, the degree of stability for the coupled system of equations covering all metacentric height values is equivalent to the uncoupled system of equations.

A simple reduction of the equation resulting from Routh's criterion to determine when a pair of complex conjugate roots crosses the zero axis is not easily accomplished. Figure 10 is presented as confirmation that the locations of X_g for which $BCD - AD^2 - EB^2 = 0$ matches the locations given graphically in Figure 5.

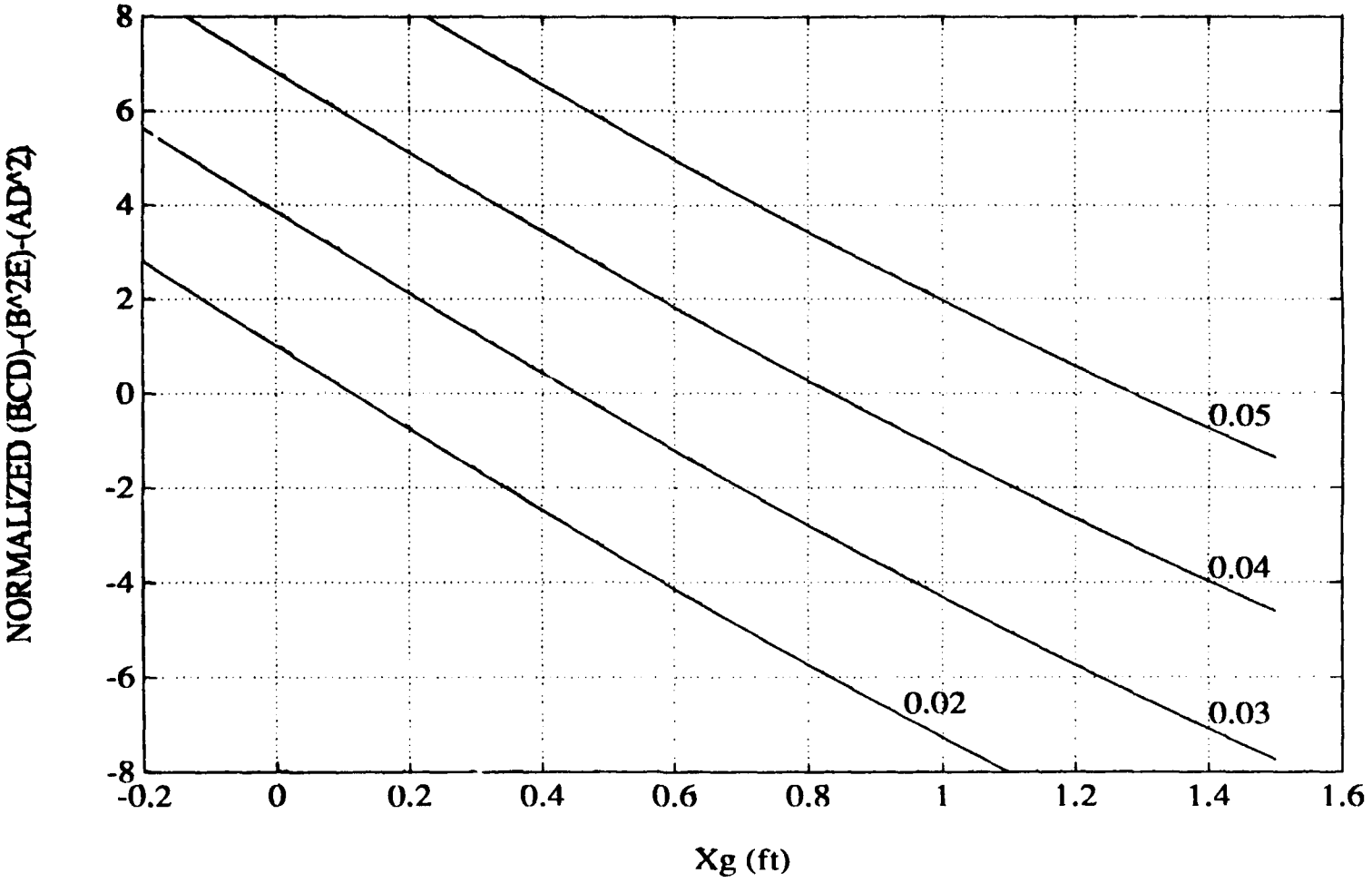

Figure 10: Normalized Routh Criterion Values vs X_g for Varying Z_g Values - Configuration 'B'

D. LINEAR SIMULATIONS

Figures 11 through 14 present comparisons of the coupled and uncoupled system responses for configuration 'A'. For the stable cases X_g = 0.40 ft and for the unstable cases X_g = -0.20 ft, while Z_g is 0.20 ft for both. The unstable coupled case (Figure 11) illustrates a simple divergence for both angle of drift and roll angle. This is expected since the roots are not complex conjugates. The unstable, uncoupled case accurately predicts the divergence in angle of drift, but the roll response is predicted to be stable. This may be explained by examining the uncoupled equation of motion in roll:

$$\phi'' - \phi' (K_p U)/(I_{xx} - K_{\dot{p}}) + \phi (Z_g W)/(I_{xx} - K_{\dot{p}}) = 0.$$

Substituting values for configuration 'A' yields:

$$\phi'' + \phi' (1.475) + \phi (0.720) = 0.$$

The solution of this equation results in a natural frequency of 0.85 rad/sec and a damping factor of 0.869. This is an underdamped case, since both roots have negative real parts and are complex conjugates. Substituting values for configuration 'B' yields:

$$\phi'' + \phi' (1.475) + \phi (0.144) = 0.$$

The solution for this case results in a natural frequency of 0.380 rad/sec and a damping factor of 1.941, which represents an overdamped situation. This also demonstrates that a vehicle's natural frequency in roll may be increased by increasing the metacentric height. The effects of the underdamping may be seen in Figures 12 through 14.

Figures 15 through 20 provide a comparison between the coupled and uncoupled equations for configuration 'B'. The effects of the overdamping are evident in figures 15 through 17. This set of figures demonstrate the

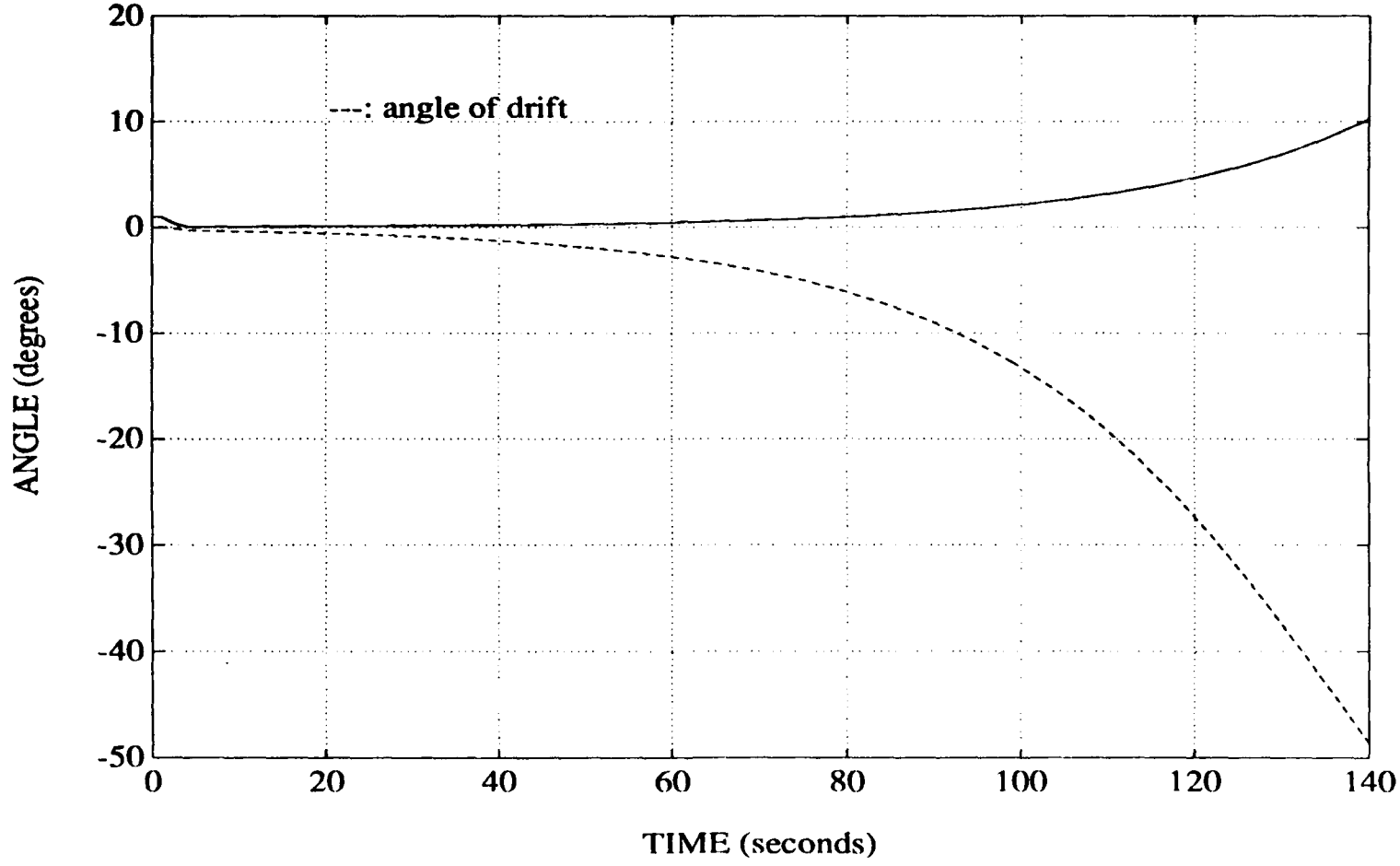

Figure 11: Roll and Angle of Drift vs Time for Configuration 'A' Coupled System
Z_g = 0.20 ft X_g = -0.20 ft Initial Roll Angle = 1.0 degree

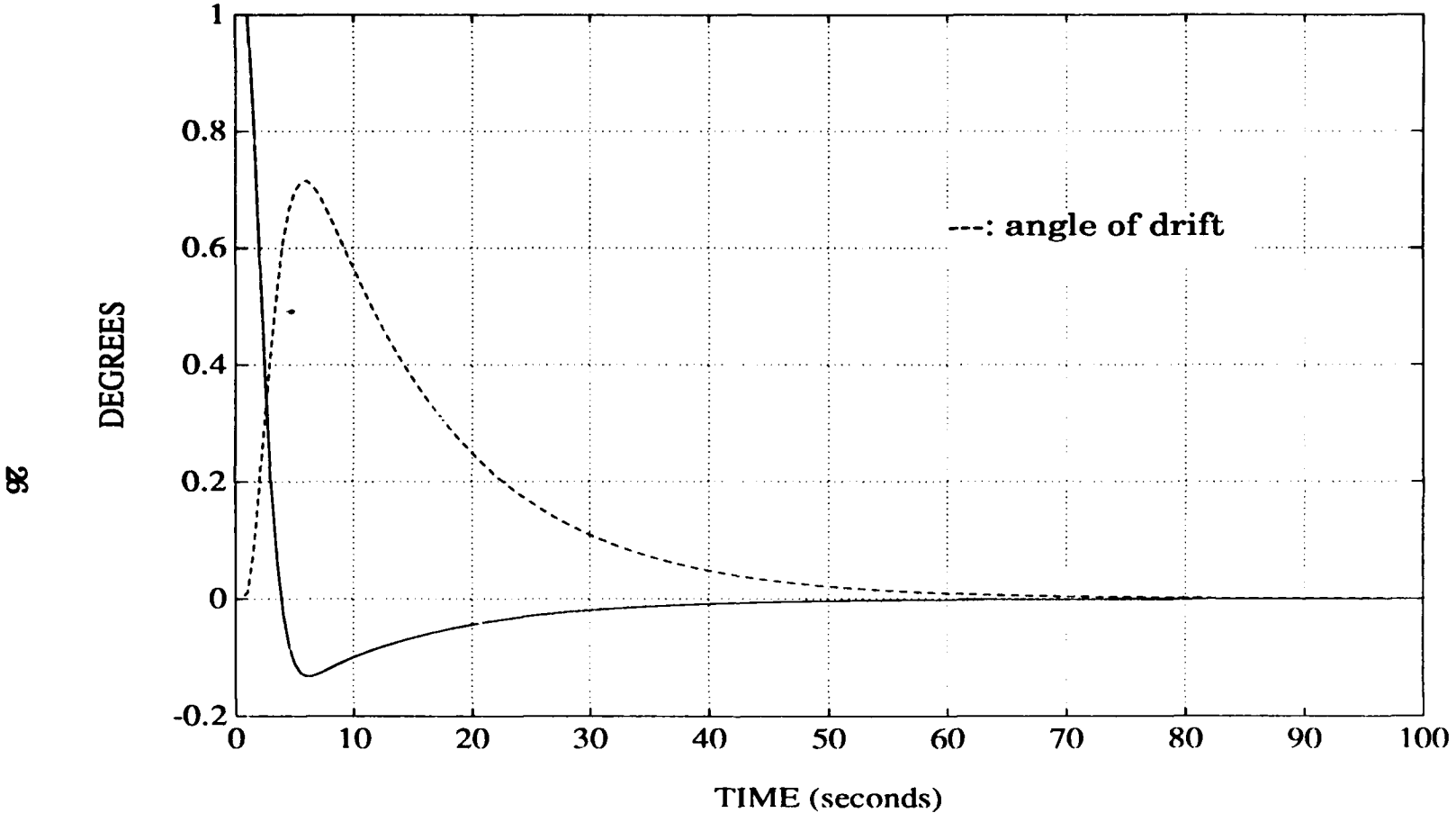

Figure 12: Roll and Angle of Drift vs Time for Configuration 'A' Coupled System
Z_g = 0.20 ft X_g = 0.40 ft Initial Roll Angle = 1.0 degree

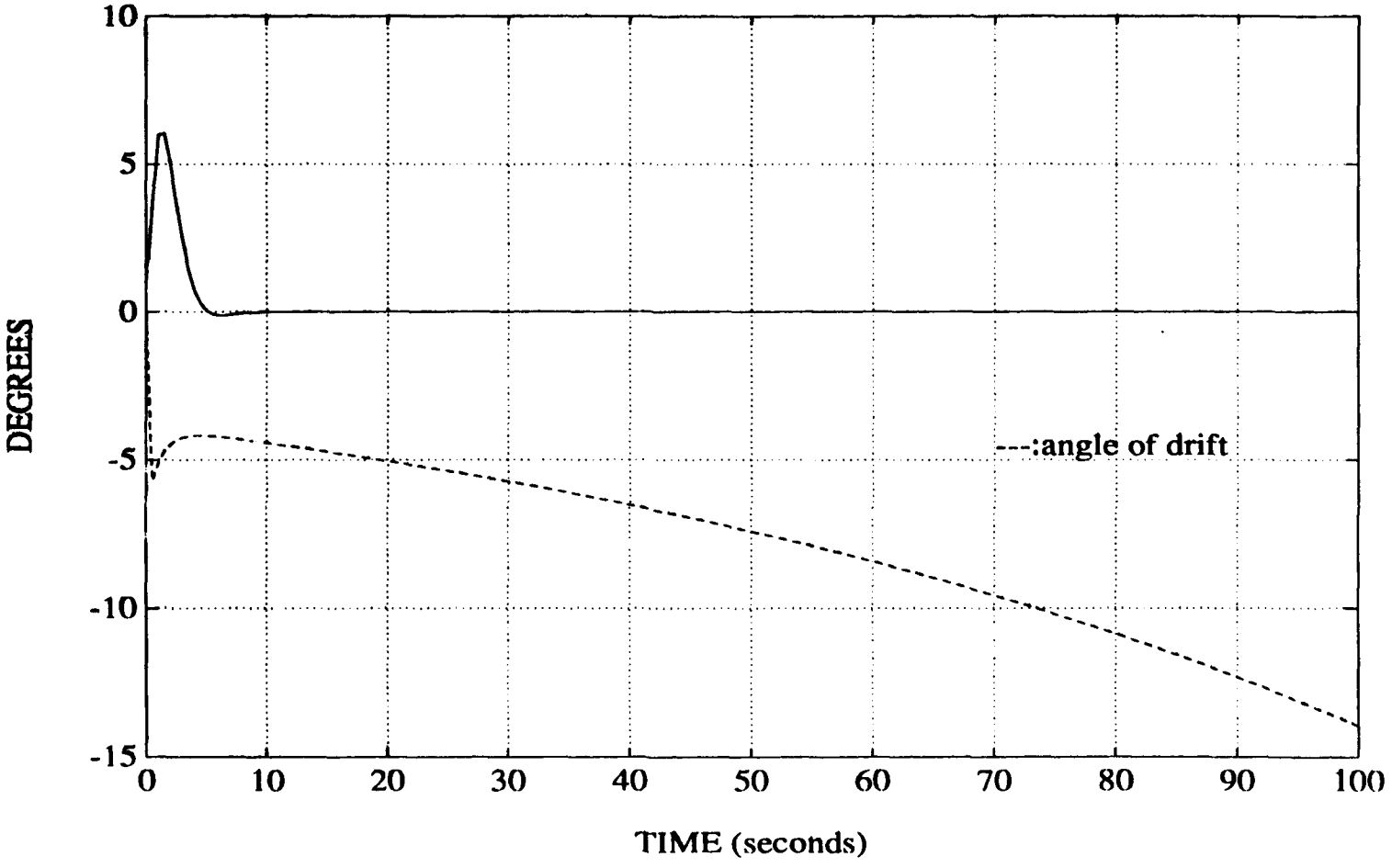

Figure 13: Roll and Angle of Drift vs Time for Configuration 'A' Uncoupled System
Z_g = 0.20 ft X_g = -0.20 ft

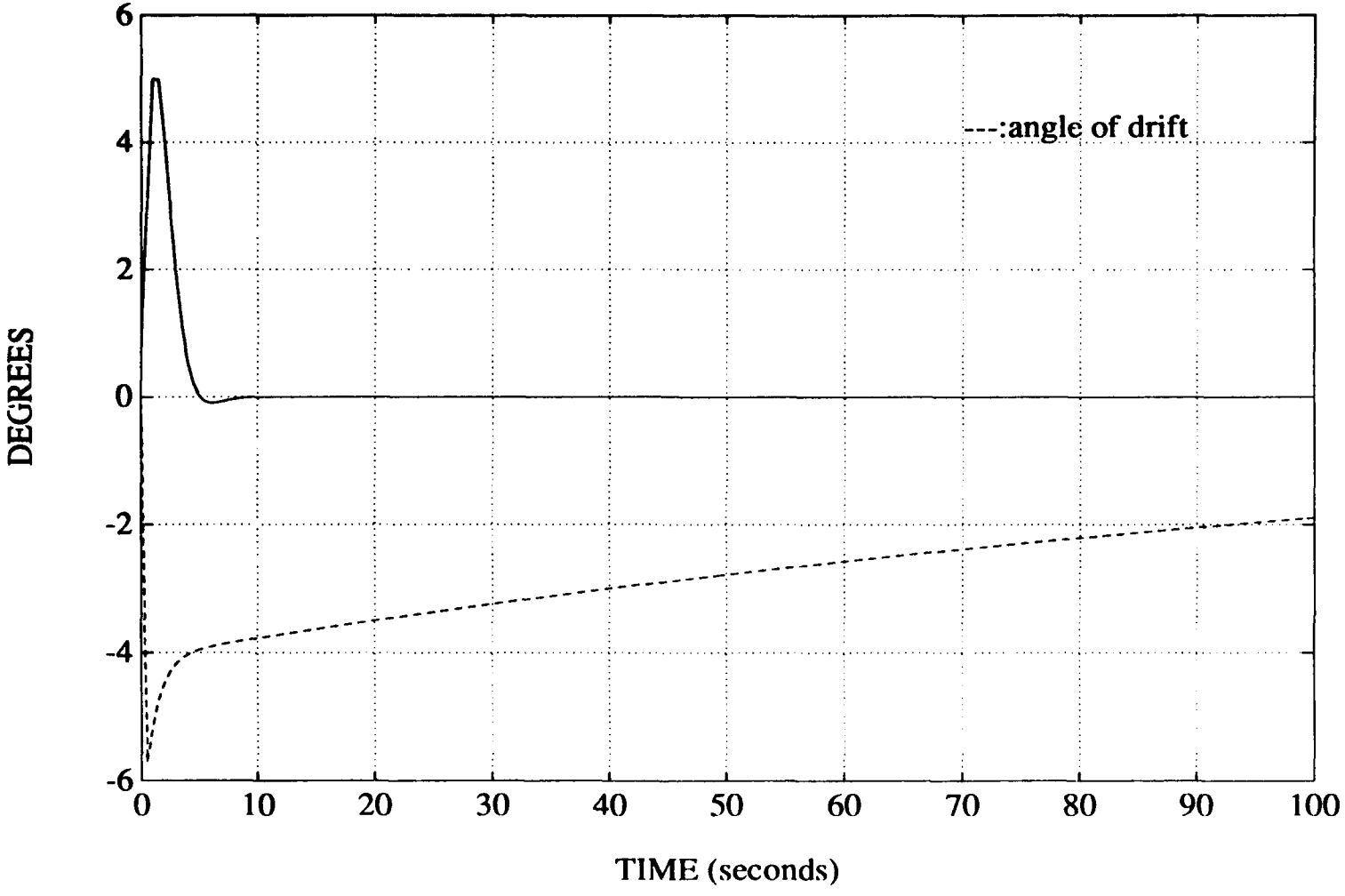

Figure 14: Roll and Angle of Drift vs Time for Configuration 'A' Uncoupled System
$Z_g = 0.20$ ft $X_g = 0.40$ ft

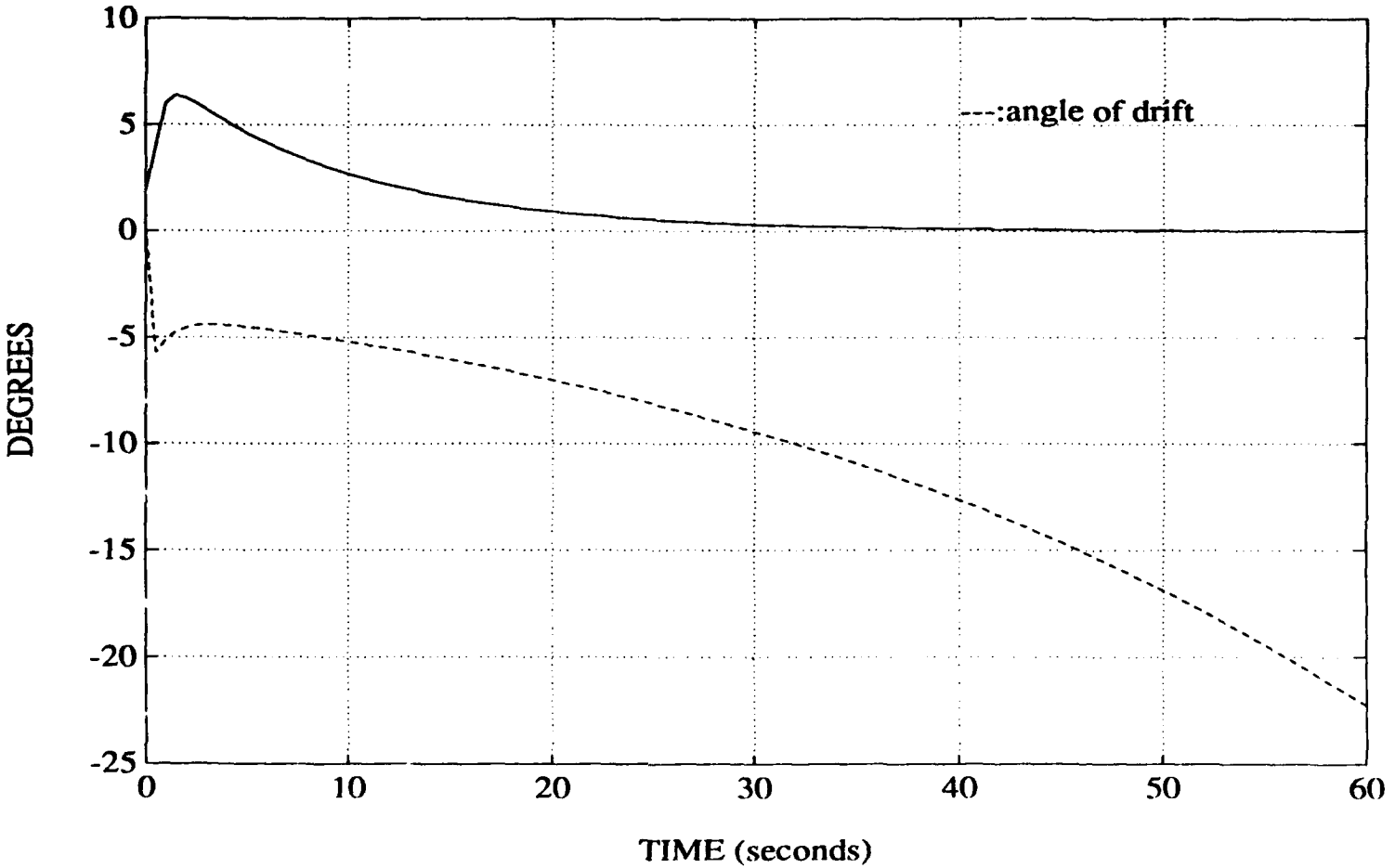

Figure 15: Roll and Angle of Drift vs Time for Configuration 'B' Uncoupled System
$Z_g = 0.04$ ft $X_g = 0.20$ ft

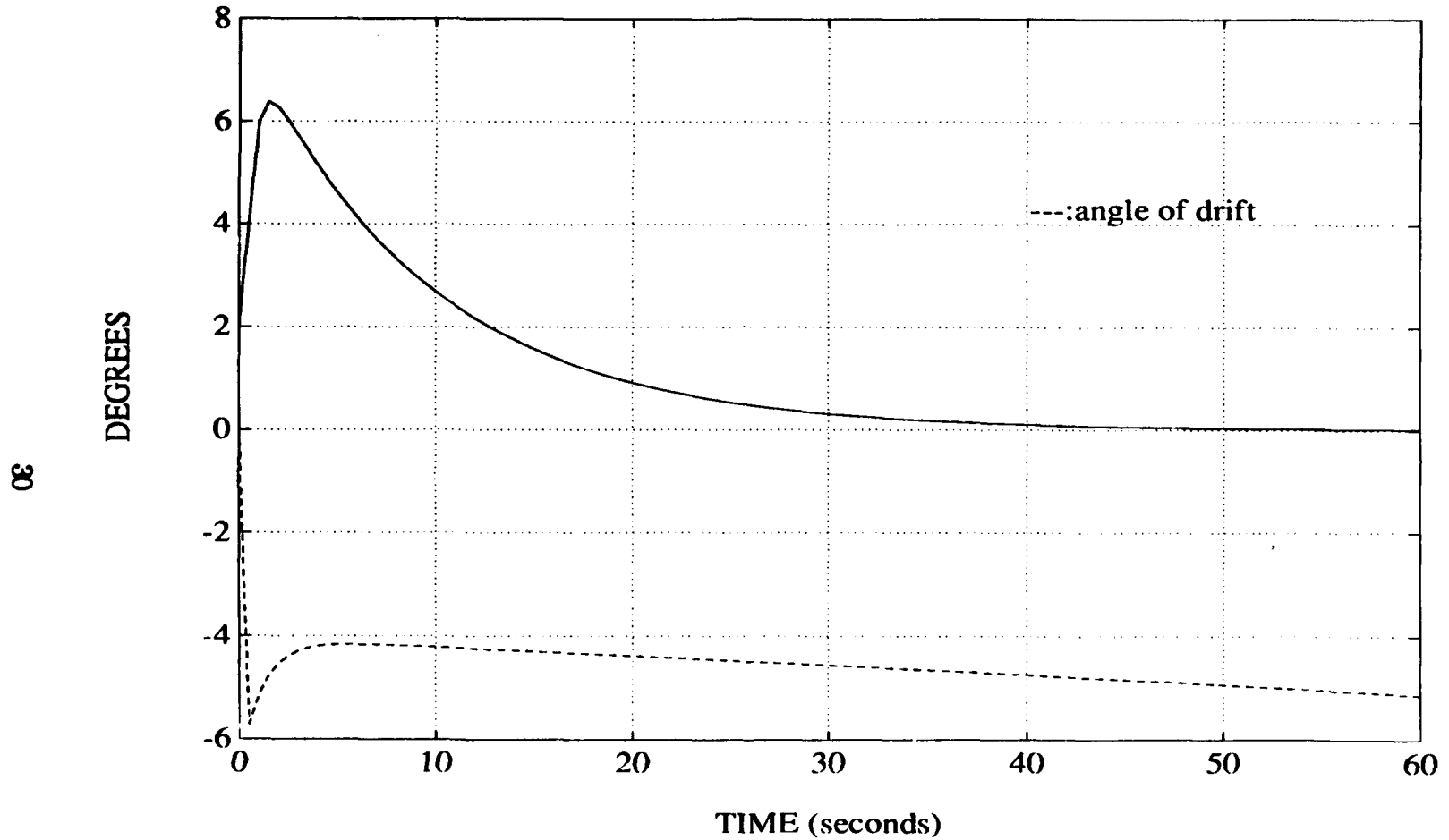

Figure 16: Roll and Angle of Drift vs Time for Configuration 'B' Uncoupled System
Z_g = 0.04 ft X_g = 1.00 ft

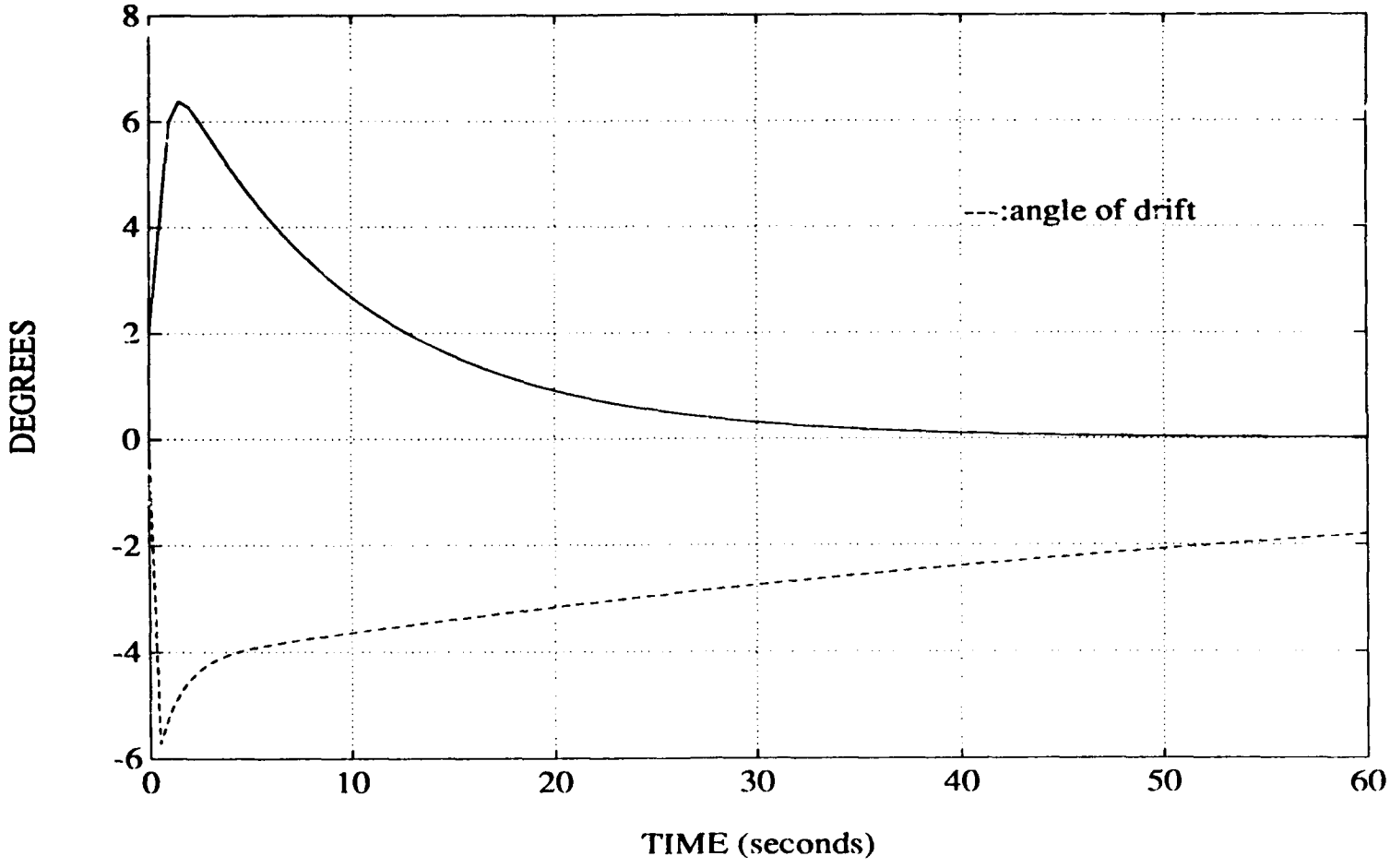

Figure 17: Roll and Angle of Drift vs Time for Configuration 'B' Uncoupled System
Z_g = 0.04 ft X_g = 1.50 ft

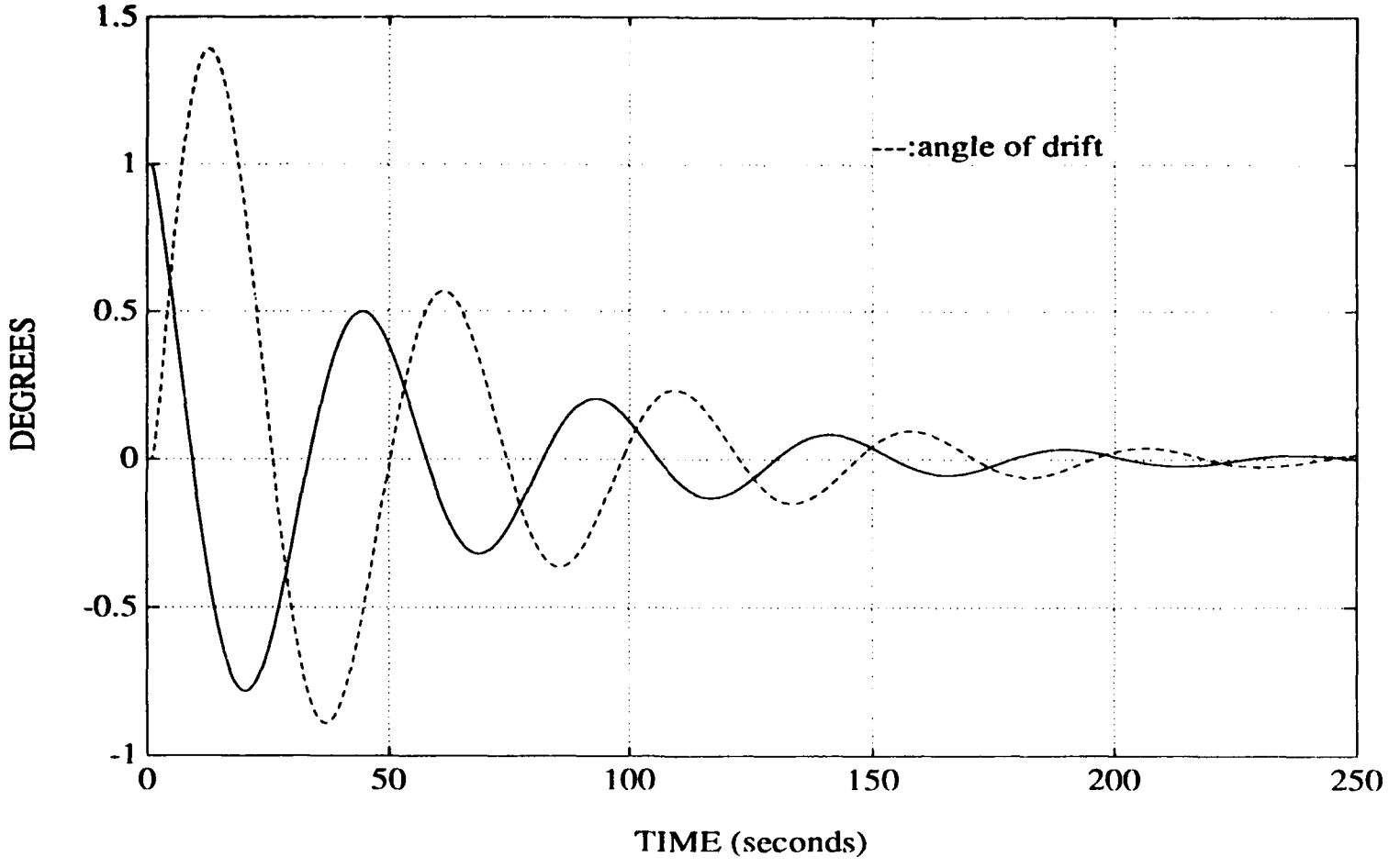

Figure 18: Roll and Angle of Drift vs Time for Configuration 'B' Coupled System
Z_g = 0.04 ft X_g = 0.20 ft Initial Roll Angle = 1.0 degree

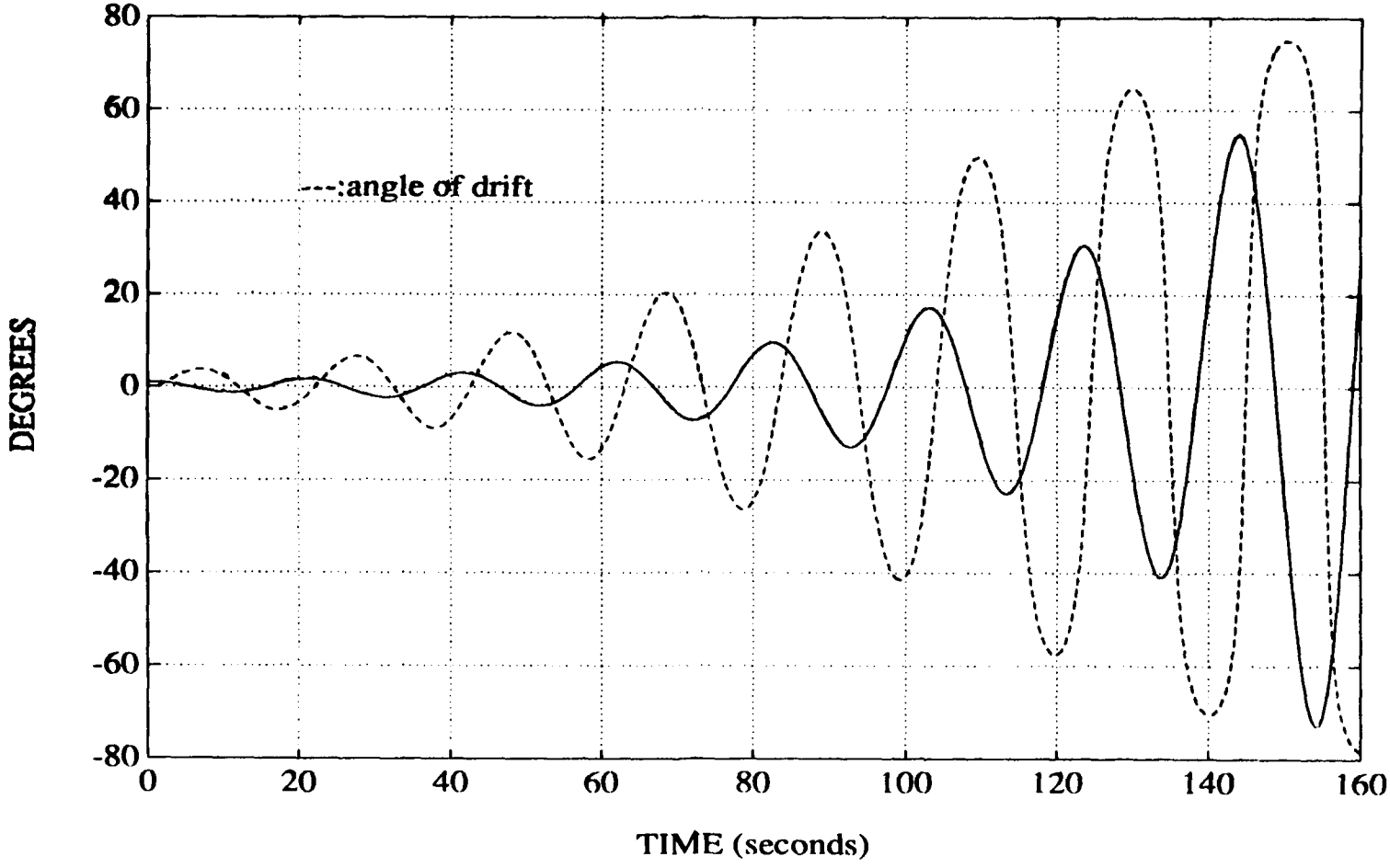

Figure 19: Roll and Angle of Drift vs Time for Configuration 'B' Coupled System
Z_g = 0.04 ft X_g = 1.00 ft Initial Roll Angle = 1.0 degree

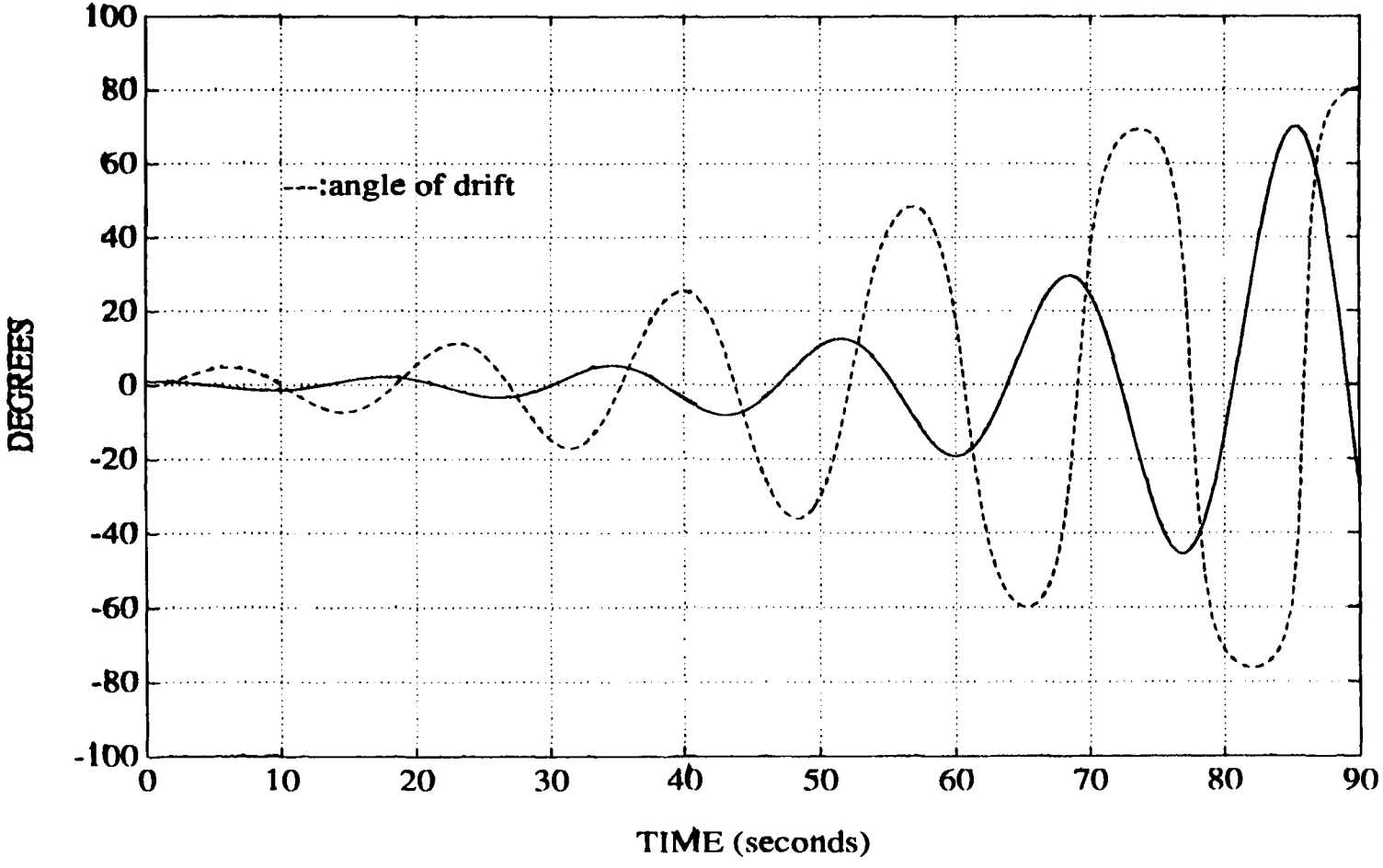

Figure 20: Roll and Angle of Drift vs Time for Configuration 'B' Coupled System
Z_g = 0.04 ft X_g = 1.50 ft Initial Roll Angle = 1.0 degree

magnitude of the discrepancies when the coupling effects are not considered. The comparison below summarizes the results of the figures representing simulations for configuration 'B', where 'C' stands for coupled and 'UC' for uncoupled.

	C	UC	C	UC	C	UC
X_g	0.20	0.20	1.00	1.00	1.50	1.50
Roll Stable	Y	Y	N	Y	N	Y
Drift Stable	Y	N	N	N	N	Y

As was seen before, the effects of the coupling on the system results in complex conjugate eigenvalues with positive real parts. Therefore, the larger values of X_g result in increasingly divergent oscillations instead of the stability predicted by the uncoupled system.

Figure 21 is a three-dimensional presentation of the roll amplitude vs time for configuration 'B' as X_g varies from 0.15 ft to 1.50 ft. This mesh capability of MATLAB allows a comparative view of several solutions, and the behavior of the roll response for the coupled system is easier to discern.

E. NON-LINEAR SIMULATIONS

In order to provide a measure of the accuracy of the results obtained utilizing the linearized equations of motion, a simulation program for the non-linear equations of motion was developed using Hamming's method [Ref. 2]. Hamming's method utilizes a Milne predictor and incorporates a modifier step prior to the correction step. The primary advantage of using Hamming's method is that only two derivative function evaluations are

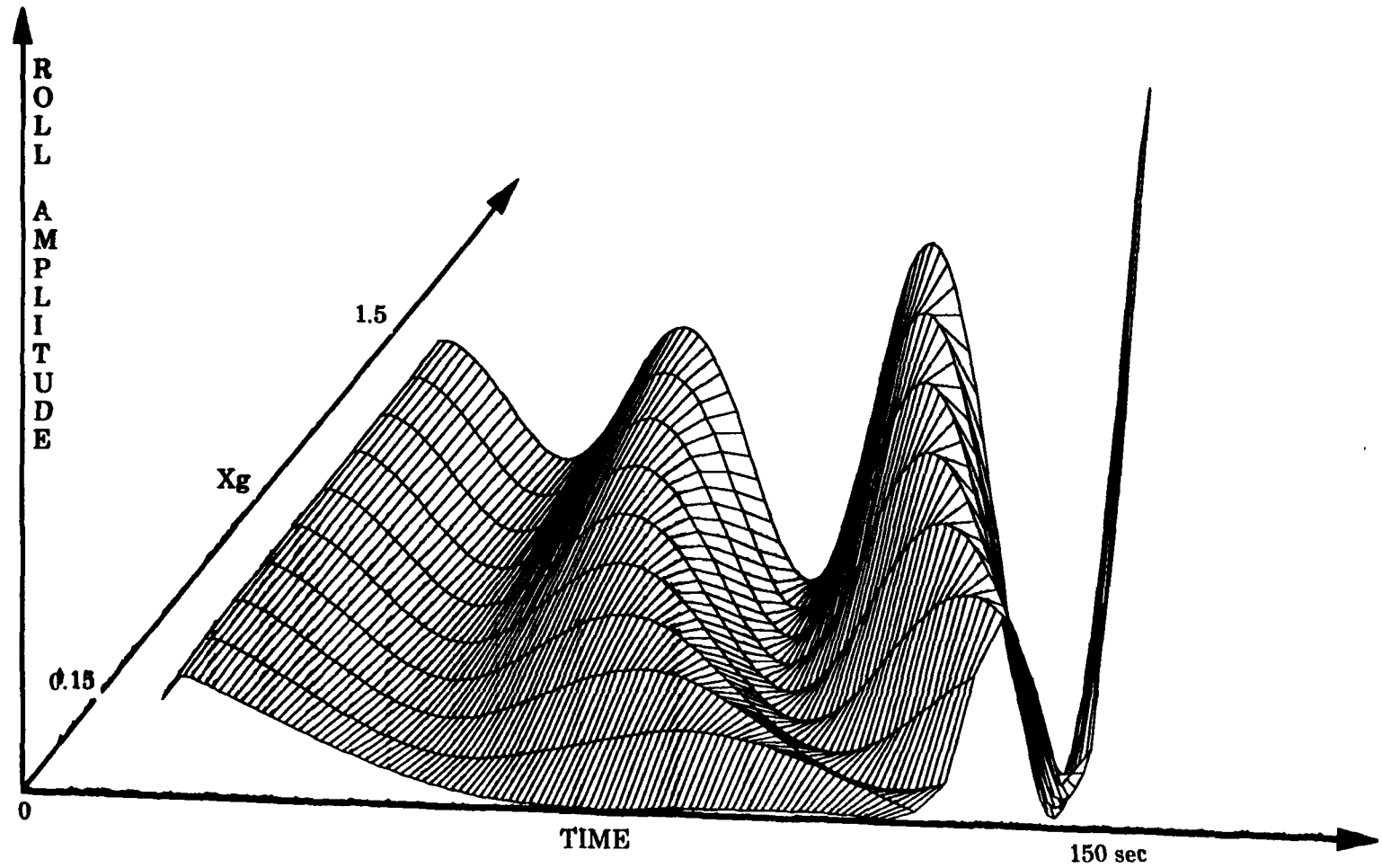

Figure 21: Mesh Plot of Roll Angle vs Time for Configuration 'B' as X_g varies from 0.15 to 1.50 ft

required per step rather than the four or more normally required by other popular methods. The local error is of the same order of magnitude (h^4) as a more time consuming process such as a fourth order Runge-Kutta, but the reduction in function evaluations results in a faster simulation. The formula is presented below, and may also be found in the nonlinear computer program simulation in Appendix A.

HAMMING'S METHOD

$$y(i+1)_{predicted} = y(i-3) + (4h/3)[2f(i) - f(i-1) + 2f(i-2)]$$

$$y(i+1)_{modified} = y(i+1)_{predicted} - (112/121)[y(i)_{predicted} - y(i)_{corrected}]$$

$$y(i+1)_{corrected} = (1/8)[9y(i) - y(i-2) + 3h\{f(i+1)_{modified} + 2f(i) - f(i-1)\}]$$

$$y(i+1) = y(i+1)_{corrected} + (9/121)[y(i+1)_{predicted} - y(i+1)_{corrected}]$$

The first four values must be determined by another method; the Euler linear solution with a small step size 'h' proved sufficient.

Figure 22 represents the simulation for the unstable representation of configuration 'A'. Rather than the exponentially increasing roll angle and the -90 angle of drift computed with the linear simulation, the nonlinear solution predicts an angle of drift that reaches -15 degrees, and then slowly diverges. The roll angle reaches a steady state value of approximately three degrees. Figures 23 and 24 are the nonlinear simulation results for stable configurations of 'A' and 'B', respectively. They are nearly identical to the results obtained using the linear simulation and displayed as Figures 12 and 18.

Figure 25 is the simulation for an unstable configuration 'B'. Quite notable are the steady state roll angle and angle of drift after approximately 250 seconds rather than the exponentially increasing divergence apparent in

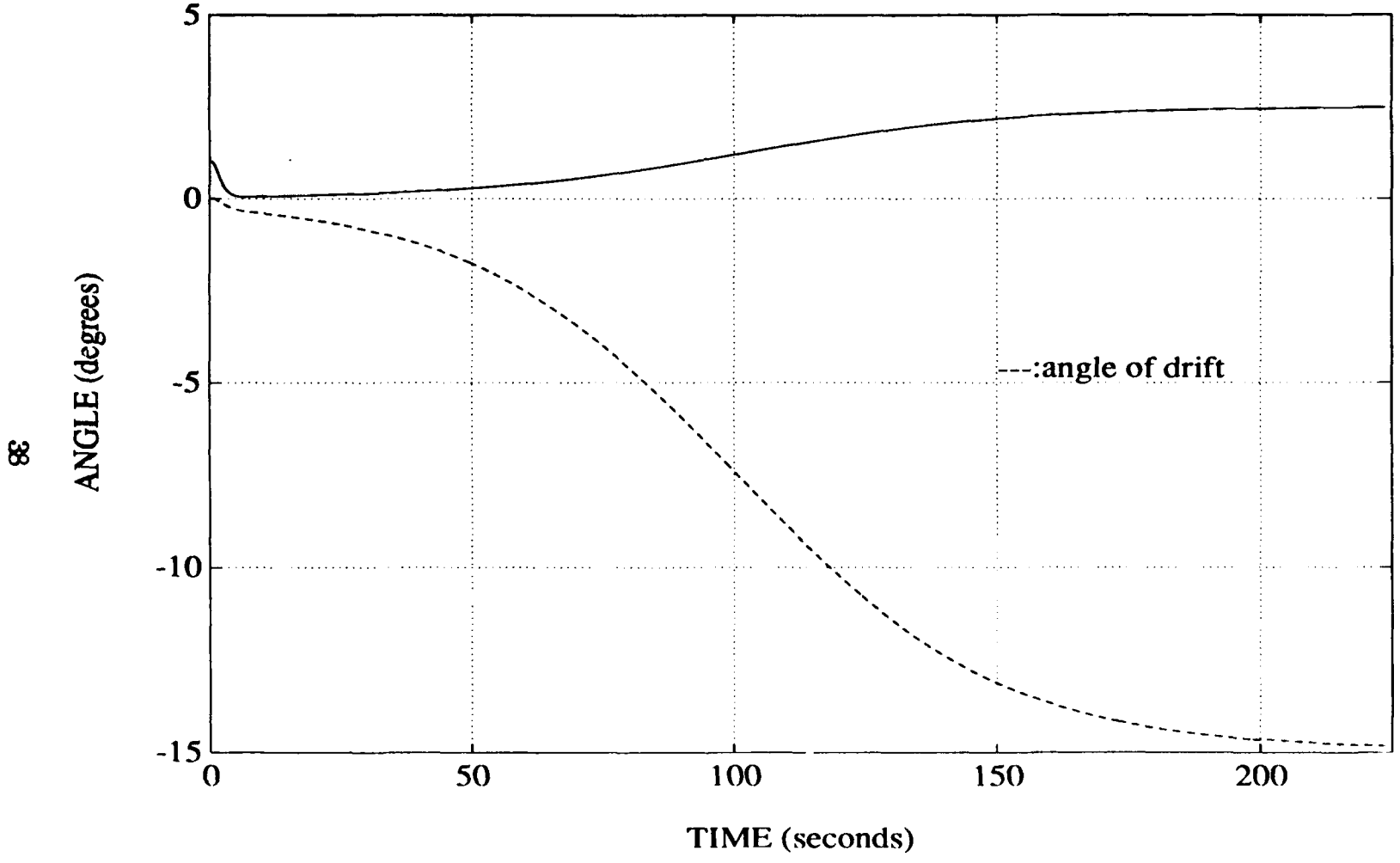

Figure 22: Roll and Angle of Drift vs Time for Configuration 'A' - Nonlinear Simulation
Z_g = 0.20 ft X_g = -0.20 ft Initial Roll Angle = 1.0 degree

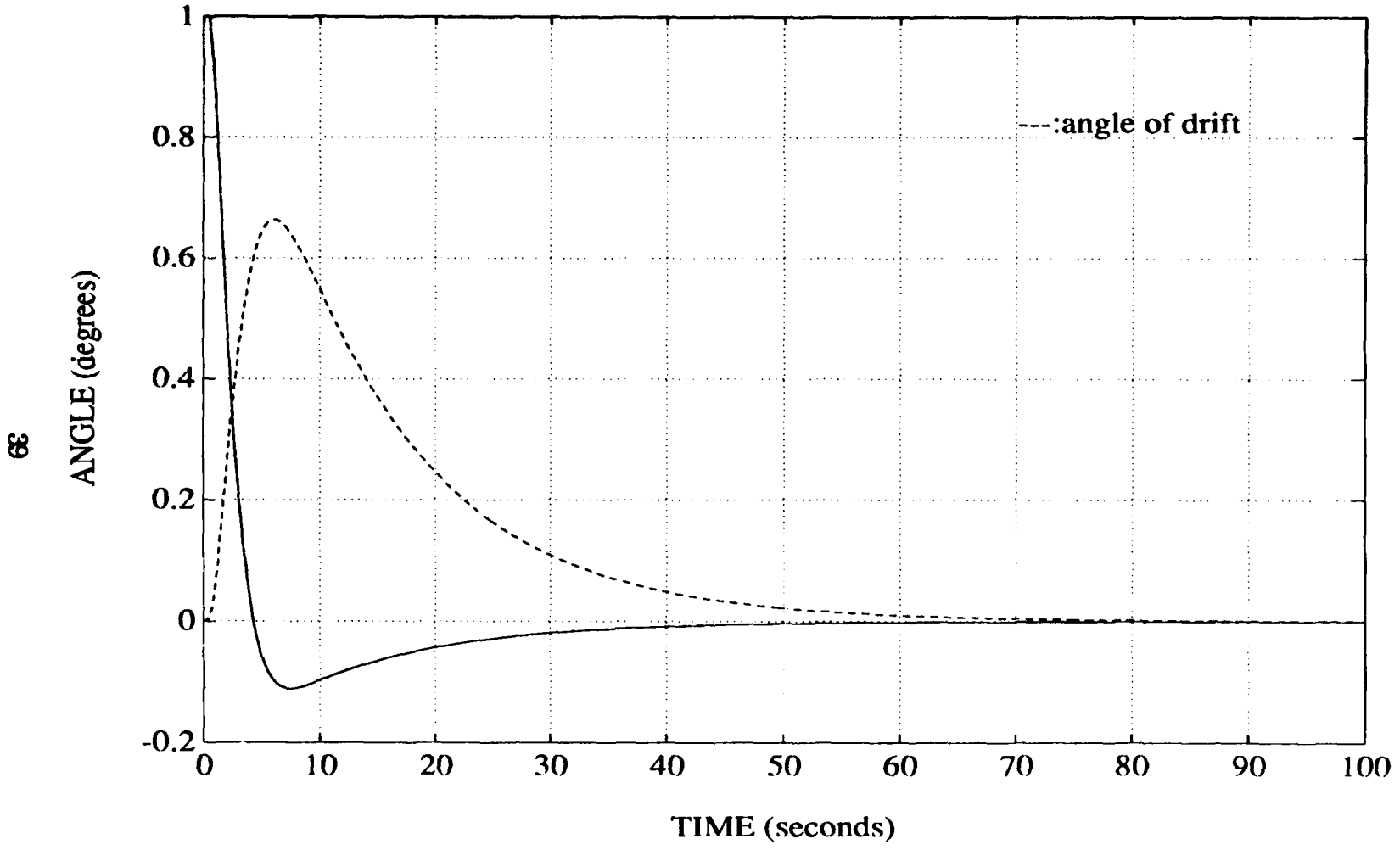

Figure 23: Roll and Angle of Drift vs Time for Configuration 'A' - Nonlinear Simulation
Z_g = 0.20 ft X_g = 0.40 ft Initial Roll Angle = 1.0 degree

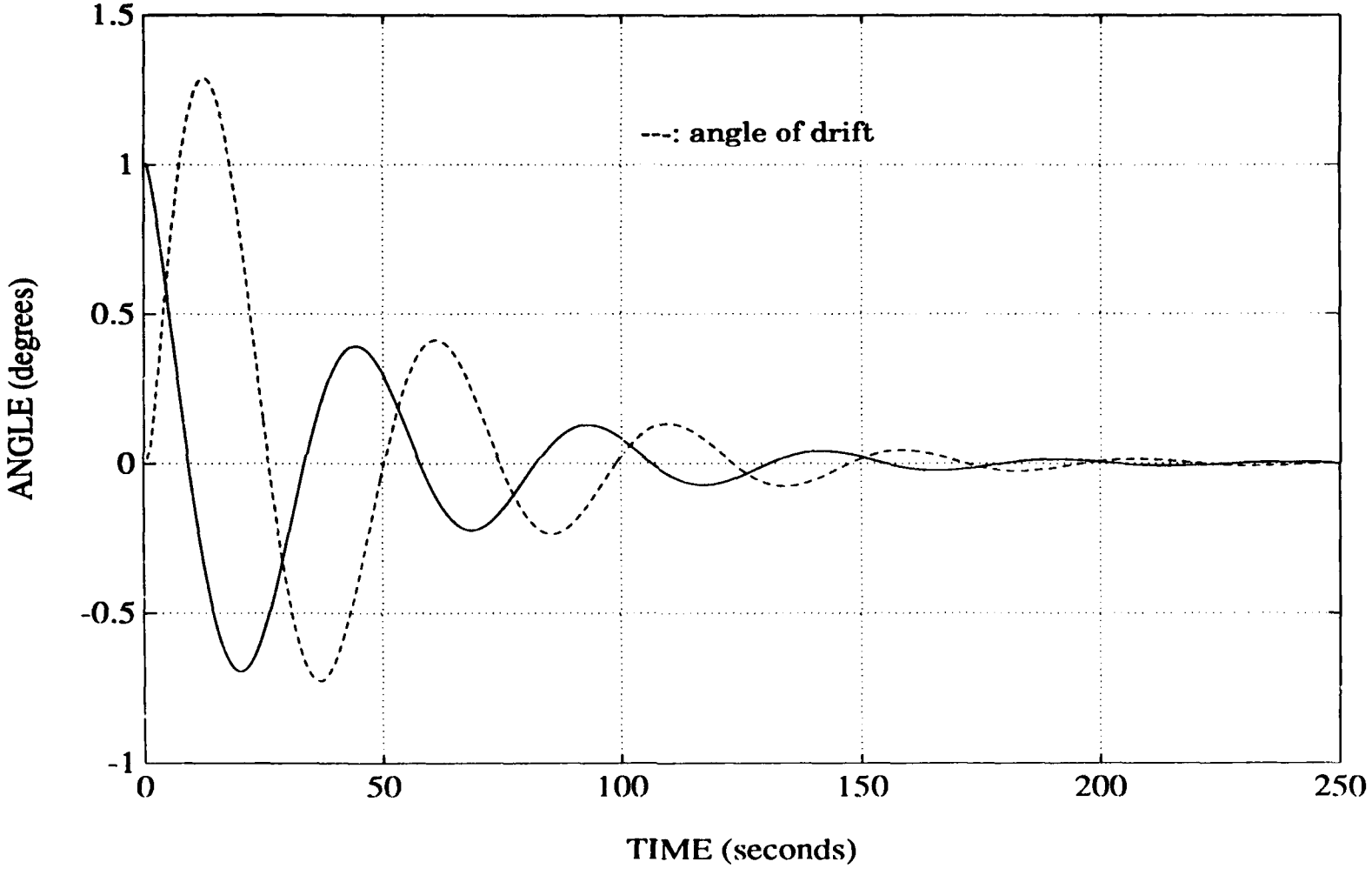

Figure 24: Roll and Angle of Drift vs Time for Configuration 'B' - Nonlinear Simulation
Z_g = 0.04 ft X_g = 0.20 ft Initial Roll Angle = 1.0 degree

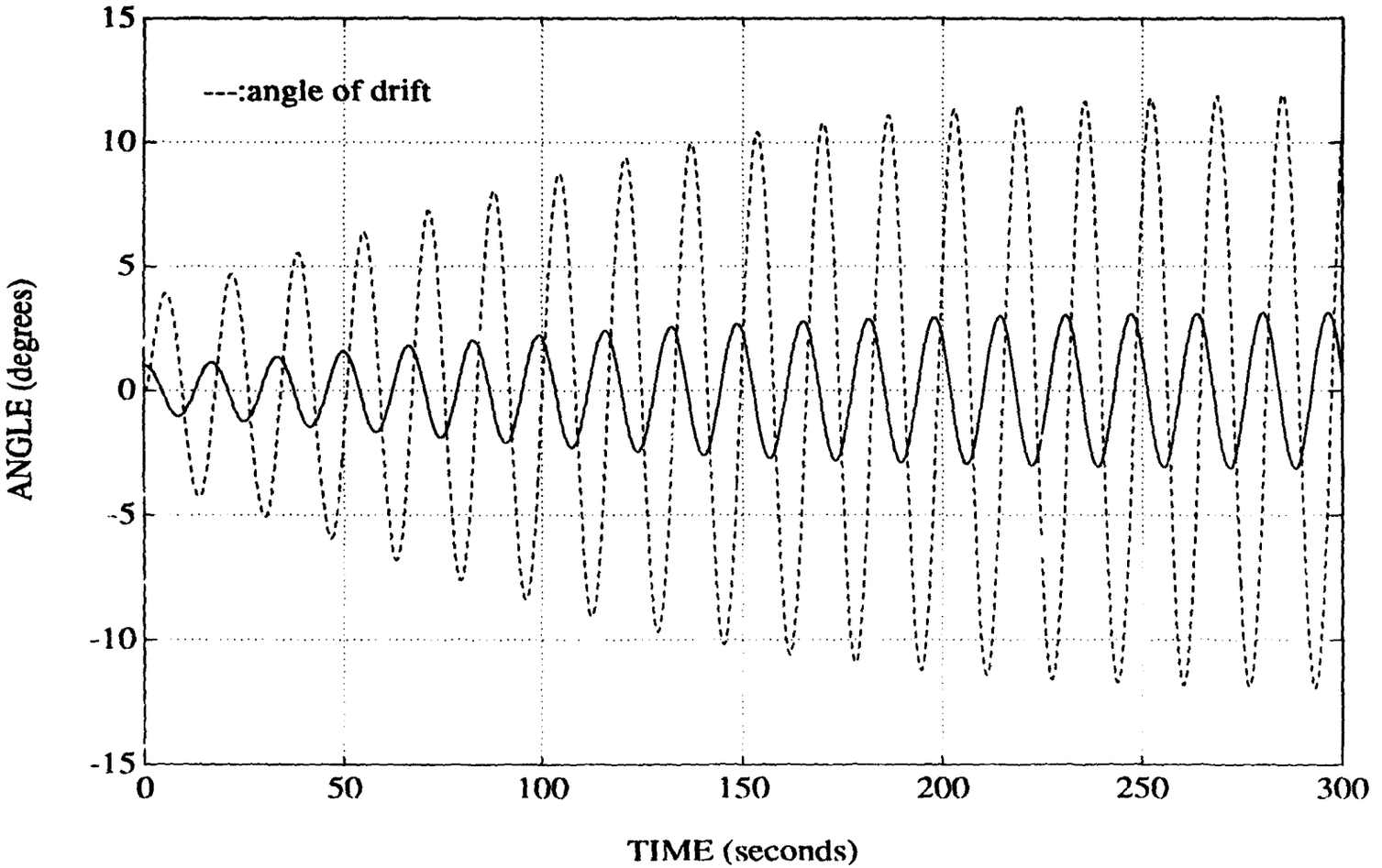

Figure 25: Roll and Angle of Drift vs Time for Configuration 'B' - Nonlinear Simulation
Z_g = 0.04 ft X_g = 1.00 ft Initial Roll Angle = 1.0 degree

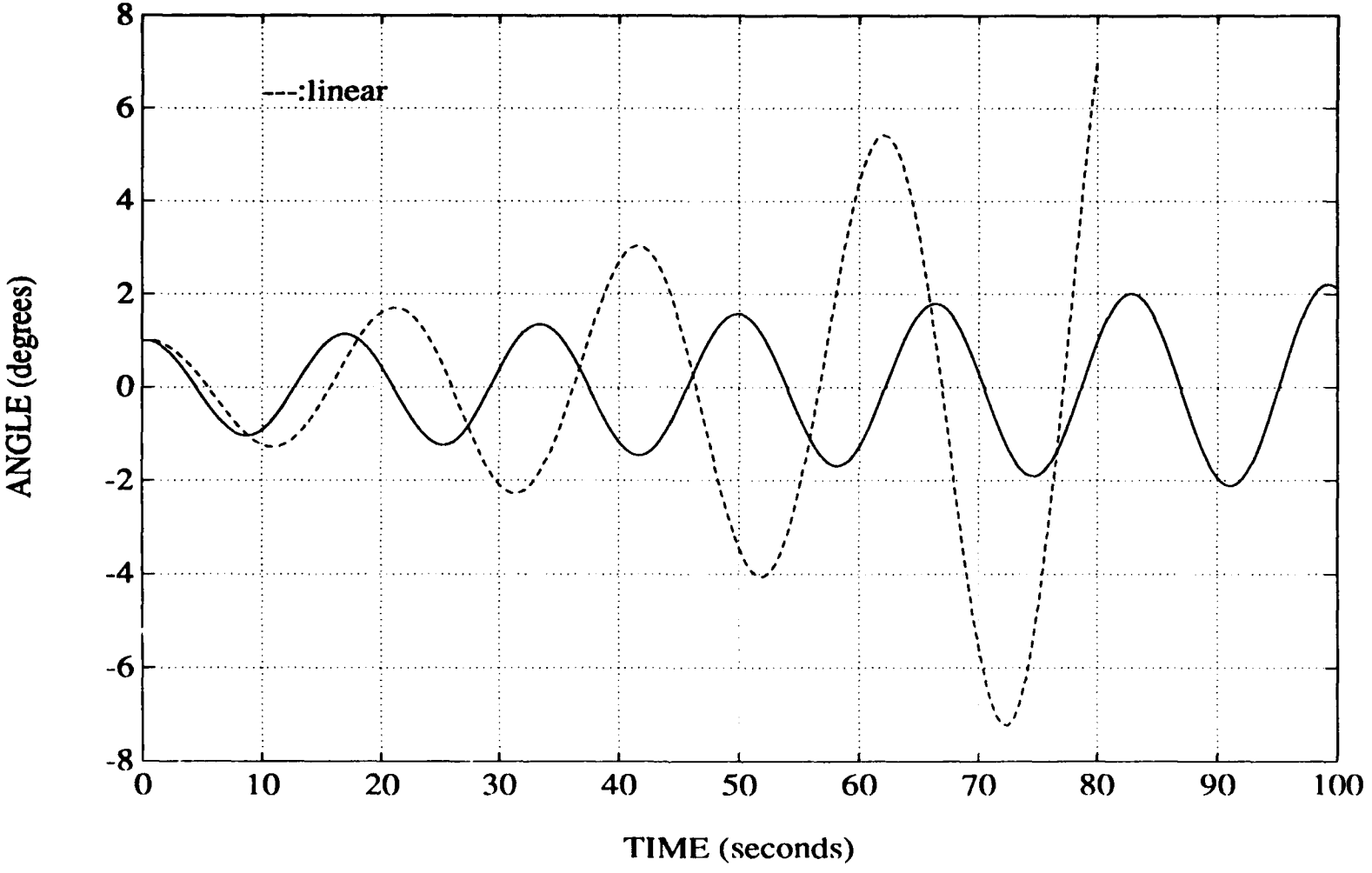

Figure 26: Roll Angle vs Time Comparison Between Linear and Nonlinear Simulations for Configuration 'B'. Z_g = 0.04 ft X_g = 1.00 ft Initial Roll Angle = 1.0 degree

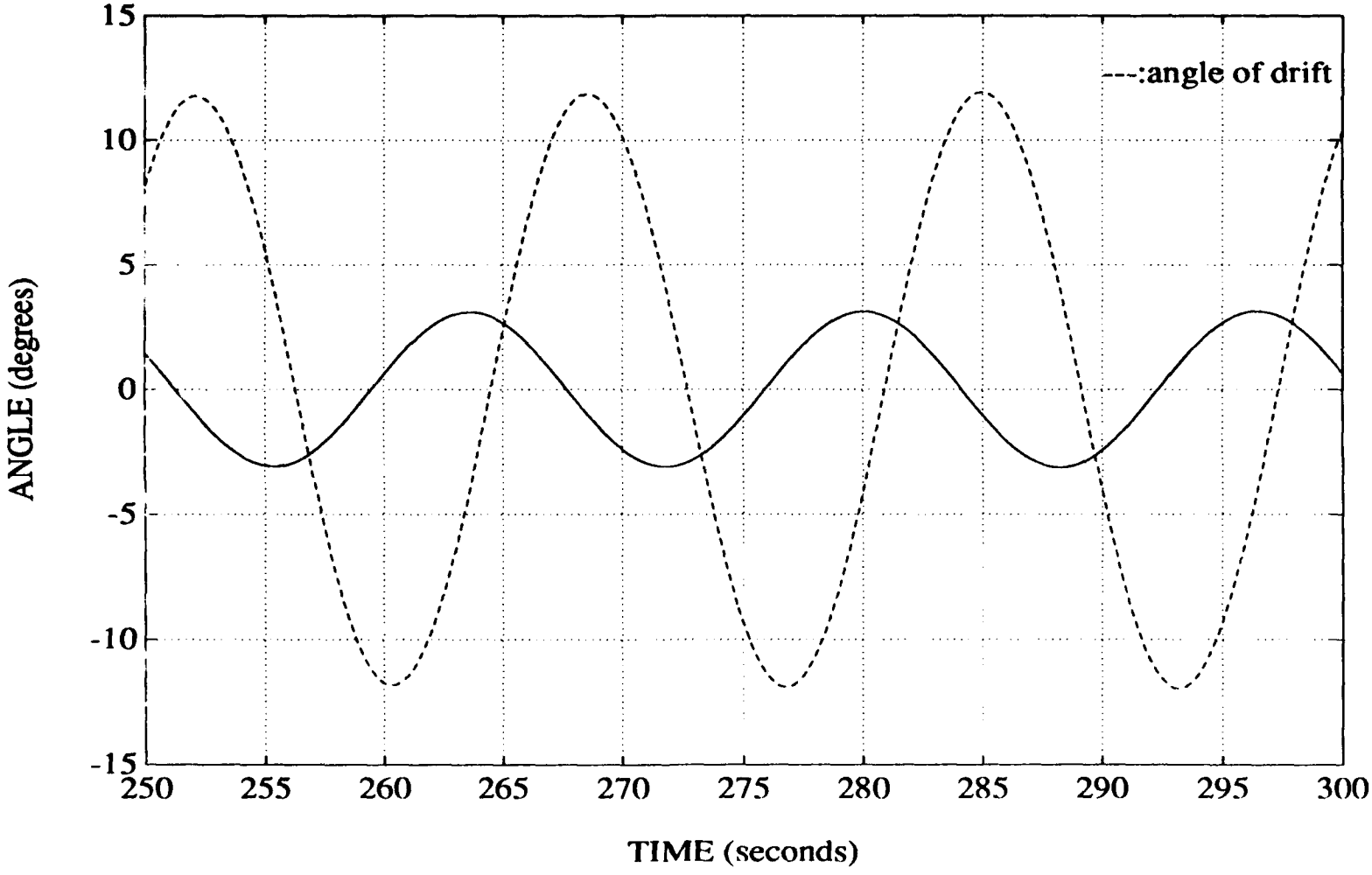

Figure 27: Roll and Angle of Drift vs Time for Configuration 'B' - Enlarged View of Figure 25
Z_g = 0.04 ft X_g = 1.00 ft

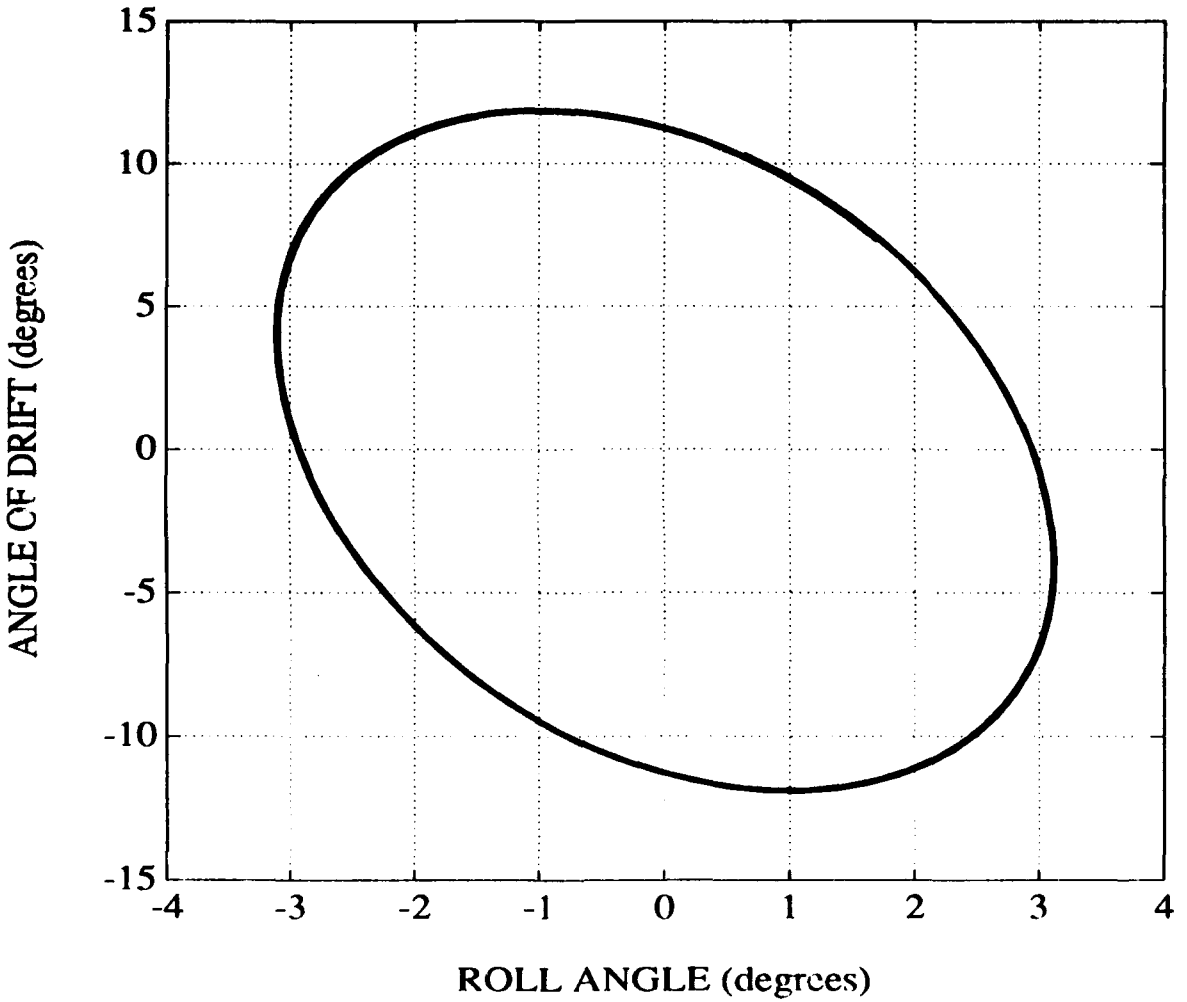

Figure 28: Limit Cycle Phase Plane Trajectory for Roll Angle vs Angle of Drift - Configuration 'B'
Z_g = 0.04 ft X_g = 1.00 ft

the corresponding linear simulation. Figure 26 provides a comparison between the linear and nonlinear solution for angle of roll. The enlarged view of the steady state region provided in Figure 27 better illustrates the constant limits of oscillation. By plotting the roll angle versus the angle of drift, an elliptical trajectory is apparent in Figure 28. This result is similar to the results obtained by Schmidt and Wright in their analysis of high performance aircraft wing-rock [Ref. 5]. They postulate that a possible explanation for the limit cycle is the inertial coupling between a stable longitudinal and an unstable lateral mode. Similar results in the work are attributed to dynamic as well as hydrodynamic coupling. Figures 25 and 28 indicate that the nonlinear interactions for the unstable conditions of configuration 'B' provide a significant amount of damping to the rolling motion. The limiting of the rolling motion accomplished by including the nonlinear terms then serves to limit the buildup of the angle of drift and the result is an eventual stable limit cycle.

The ocean environment can be expected to introduce many combinations of disturbance forces, which may or may not be periodic. A preferred method for simulating many disturbances such as sensor noise, ocean current fluctuation, and vehicle acceleration fluctuations is to model them as 'white noise'. Figure 29 is presented to demonstrate the effects of including constant, zero-mean disturbances in sway and yaw on the marginally stable system of configuration 'B'. The disturbances are developed using MATLAB's random number generator with a uniform distribution. The random numbers are then scaled to simulate values that may be expected. The variance of the sway and yaw acceleration disturbances, respectively, for Figure 29 are 0.003 $(ft/s^2)^2$ and 0.002 $(rad/s^2)^2$. The resulting simulation bears little resemblance

to Figure 24, although the initial conditions and values for X_g and Z_g are the same. With even these relatively minor disturbances acting on the system of configuration 'B', a rather large, non-symmetric oscillation in both roll and angle of drift is evident. Although the system is still stable, with the mean of both the roll angle and angle of drift equalling zero, a limit cycle similar to that of the unstable configuration (Figure 25) has developed. As the angle of drift fluctuates between positive three degrees and negative four degrees, the angle of roll varies between positive and negative two degrees. Increasing the scaling (which increases the variance) for the disturbances would be expected to increase the fluctuations until stability is lost. Similarly, it is true that the small disturbances acting in Figure 29 have a greatly reduced effect on the system of configuration 'A', which has greater stability.

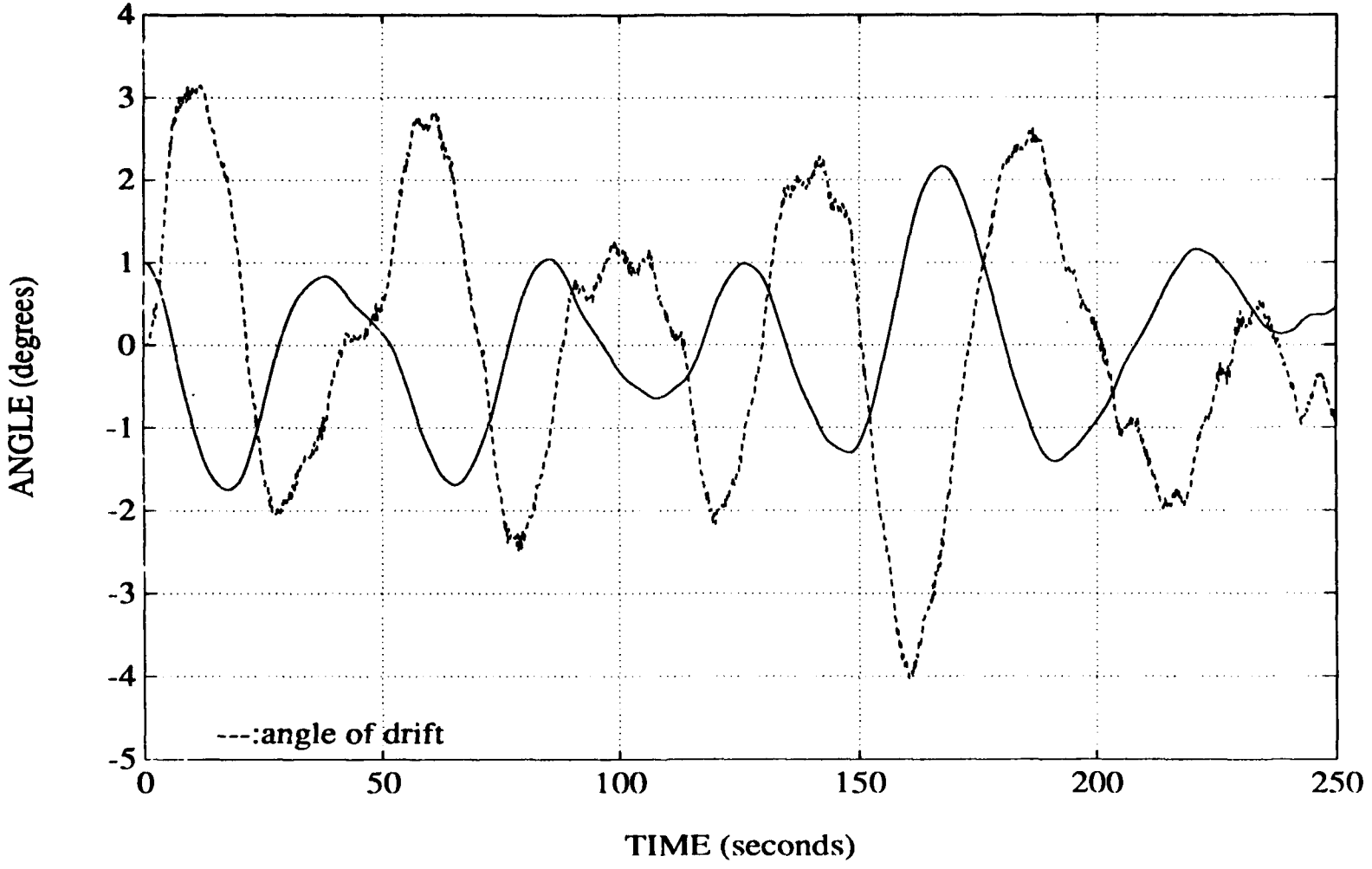

Figure 29: Roll and Angle of Drift vs Time for Configuration 'B' with Constant Zero Mean Sway and Yaw Disturbances. Z_g = 0.04 ft X_g = 0.20 ft Initial Roll Angle = 1.0 degree

IV. PERTURBATION ANALYSIS

A. BACKGROUND

The previous section demonstrates that knowledge of the separation between longitudinal centers of buoyancy and gravity is critical in determining system stability. If this quantity is the dominant factor in a stability analysis, then an approximation for the degree of stability may be developed by applying perturbation theory. Although perturbation results are only approximations, their advantage over numerical methods is in illustrating the degree to which a solution depends on the variable(s) involved. From the fundamental theorem of perturbation theory [Ref. 6], we seek a solution to the characteristic equation $A\lambda^4 + B\lambda^3 + C\lambda^2 + D\lambda + E = 0$ of the form:

$$\lambda(\varepsilon) = \sum_{n=0}^{n=\infty} an\, \varepsilon^n \tag{4.1}$$

where ε is the variable of interest and the solution approximates the numerical solution in the region where ε is small. The constant coefficients $(a_0, a_1, ..., a_n)$ are all independent of ε, and are all equal to zero for small ε.

B. PERTURBATION FORMULATION

Recalling Equations 2.4f - 2.4j, which defined the coefficients of the quartic characteristic equation, it would obviously be desirable to simplify the equations as much as possible prior to formulating the perturbation

approximation. The variable of interest will be defined as:

$$\varepsilon = X_g - X_b \tag{4.2}$$

where the nominal value for X_b is zero and the perturbation will be performed around $\varepsilon = 0$. By comparing Figures 30 and 31 it is clear that by allowing the hydrodynamic coefficients $K_{\dot{v}}$, $K_{\dot{r}}$, $Y_{\dot{p}}$, $N_{\dot{p}}$, Y_p, and N_p to equal zero a very good approximate solution to Equation (2.4e) is obtained for both configurations 'A' and 'B'. This simplification reduces the descriptor coefficients 'f', 'i', 'o', and 'p' from Table 1 to zero, which simplifies the coefficients of the coupled equations of motion to Equations (4.3a) - (4.3e) below.

$$A = (I_{xx} - K_{\dot{p}})[(M - Y_{\dot{v}})(I_{zz} - N_{\dot{r}}) - (MX_g - Y_{\dot{r}})(MX_g - N_{\dot{v}})] + (MZ_g)^2(I_{zz} - N_{\dot{r}}) \tag{4.3a}$$

$$\begin{aligned} B = {} & (K_v U)(MZ_g)(I_{zz} - N_{\dot{r}}) + (MZ_g)^2(N_r - MX_g)(U) - \\ & (MZ_g)(MZ_g + K_r)(MX_g - N_{\dot{v}})(U) - (I_{xx} - K_{\dot{p}})[(M - Y_{\dot{v}})(N_r - MX_g)(U) + \\ & (Y_v U)(I_{zz} - N_{\dot{r}}) - (N_v U)(MX_g - Y_{\dot{r}}) - (MX_g - N_{\dot{v}})(Y_r - M)(U)] - \\ & (K_p U)[(M - Y_{\dot{v}})(I_{zz} - N_{\dot{r}}) - (MX_g - Y_{\dot{r}})(MX_g - N_{\dot{v}})] \end{aligned} \tag{4.3b}$$

$$\begin{aligned} C = {} & (I_{xx} - K_{\dot{p}})[(Y_v U^2)(N_r - MX_g) - (N_v U^2)(Y_r - M)] + \\ & (Z_g W)[(M - Y_{\dot{v}})(I_{zz} - N_{\dot{r}}) - (MX_g - Y_{\dot{r}})(MX_g - N_{\dot{v}})] + \\ & (K_p U)[(M - Y_{\dot{v}})(N_r - MX_g)(U) + (Y_v U)(I_{zz} - N_{\dot{r}}) - \\ & (N_v U)(MX_g - Y_{\dot{r}}) - (MX_g - N_{\dot{v}})(Y_r - M)(U)] + \\ & (MZ_g)[(X_g W)(MX_g - Y_{\dot{r}}) - (N_v U^2)(MZ_g + K_r) + (K_v U^2)(N_r - MX_g)] \end{aligned} \tag{4.3c}$$

$$D = -(Z_g W)[(M - Y_{\dot{v}})(N_r - MX_g)(U) + (Y_v U)(I_{zz} - N_{\dot{r}}) - (N_v U)(MX_g - Y_{\dot{r}}) - (MX_g - N_{\dot{v}})(Y_r - M)(U)] - (K_p U^3)[(Y_v)(N_r - MX_g) - (N_v)(Y_r - M)] + (K_v U)(X_g W)(MX_g - Y_{\dot{r}}) - (MZ_g)(X_g W)(U)(Y_r - M) - (MZ_g + K_r)(U)(X_g W)(M - Y_{\dot{v}}) \quad (4.3d)$$

$$E = (Z_g W)[(Y_v U^2)(N_r - MX_g) - (N_v U^2)(Y_r - M)] - (K_v X_g W U^2)(Y_r - M) + (Y_v X_g W U^2)(MZ_g + K_r) \quad (4.3e)$$

Recalling the definitions of the coefficients for the uncoupled systems:

$$A_L = (M - Y_{\dot{v}})(I_{zz} - N_{\dot{r}}) - (MX_g - Y_{\dot{r}})(MX_g - N_{\dot{v}})$$

$$B_L = -[(I_{zz} - N_{\dot{r}})(Y_v U) + (M - Y_{\dot{v}})(N_r - MX_g)(U) + (Y_r - M)(N_{\dot{v}} - MX_g)(U) + (Y_{\dot{r}} - MX_g)(N_v U)]$$

$$C_L = (Y_v U^2)(N_r - MX_g) - (N_v U^2)(Y_r - M)$$

$$A_R = I_{xx} - K_{\dot{p}} \qquad B_R = -K_p U \qquad C_R = Z_g W$$

Substituting in Equations (4.3a) - (4.3e) yields:

$$A = A_R A_L + (MZ_g)^2(I_{zz} - N_{\dot{r}}) \quad (4.4a)$$

$$B = A_R B_L + B_R A_L + (MZ_g)^2(N_r - MX_g)(U) + (MZ_g)[(I_{zz} - N_{\dot{r}})(K_v U) - (MZ_g + K_r)(MX_g - N_{\dot{v}})(U)] \quad (4.4b)$$

$$C = A_R C_L + C_R A_L + B_R B_L + (MZ_g)[(X_g W)(MX_g - Y_{\dot{r}}) + (K_v U^2)(N_r - MX_g) - (N_v U^2)(MZ_g + K_r)] \quad (4.4c)$$

$$D = C_R B_L + C_L B_R + (K_v U)(X_g W)(MX_g - Y_{\dot{r}}) - (MZ_g + K_r)(X_g W)(U)(M - Y_{\dot{v}}) - (MZ_g)(X_g W)(U)(Y_r - M) \quad (4.4d)$$

$$E = C_R C_L + (Y_v U^2)(X_g W)(MZ_g + K_r) - (K_v X_g W U^2)(Y_r - M) \quad (4.4e)$$

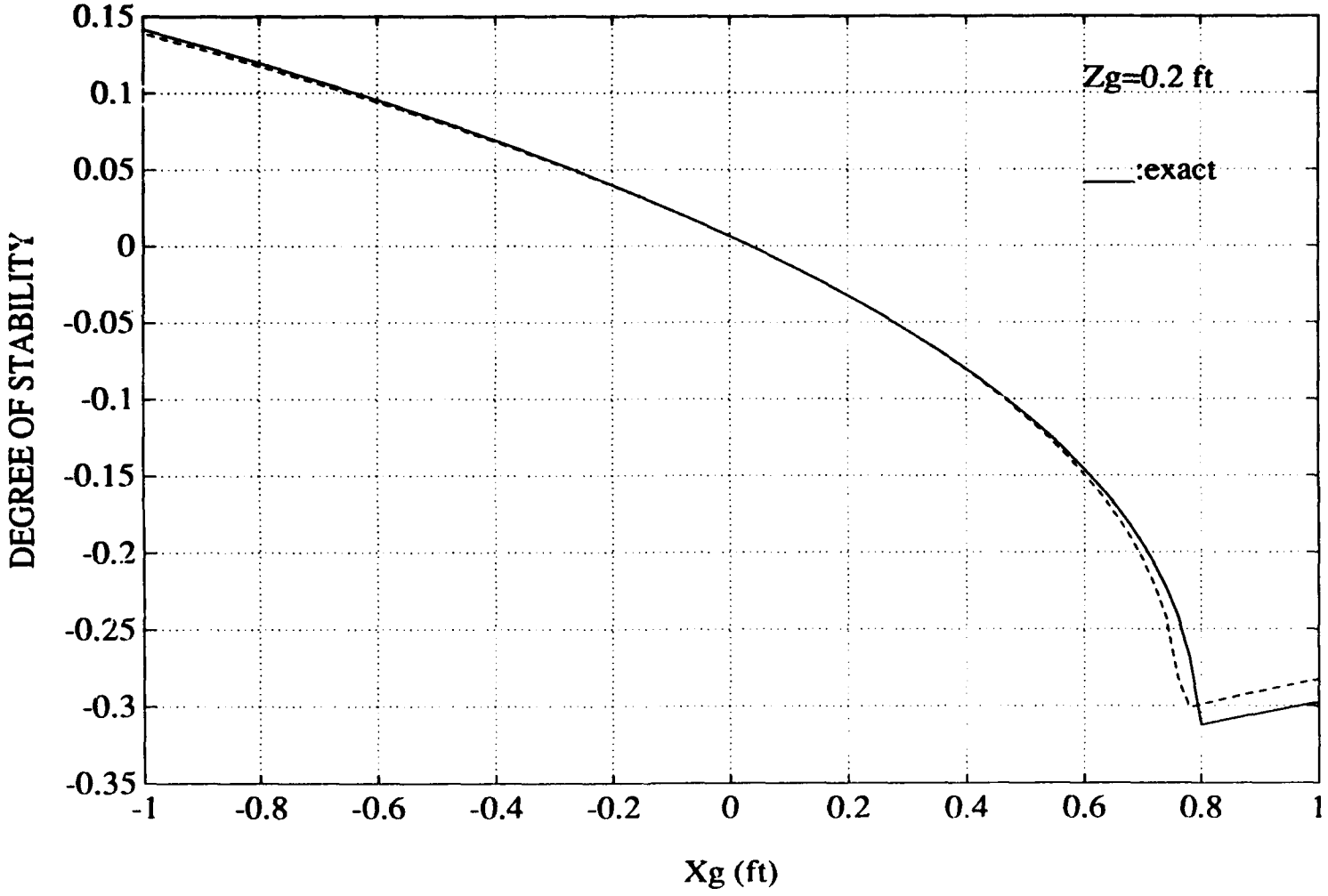

Figure 30: Comparison of Degree of Stability vs X_g with Six Cross Coupling Coefficients Neglected - Configuration 'A'

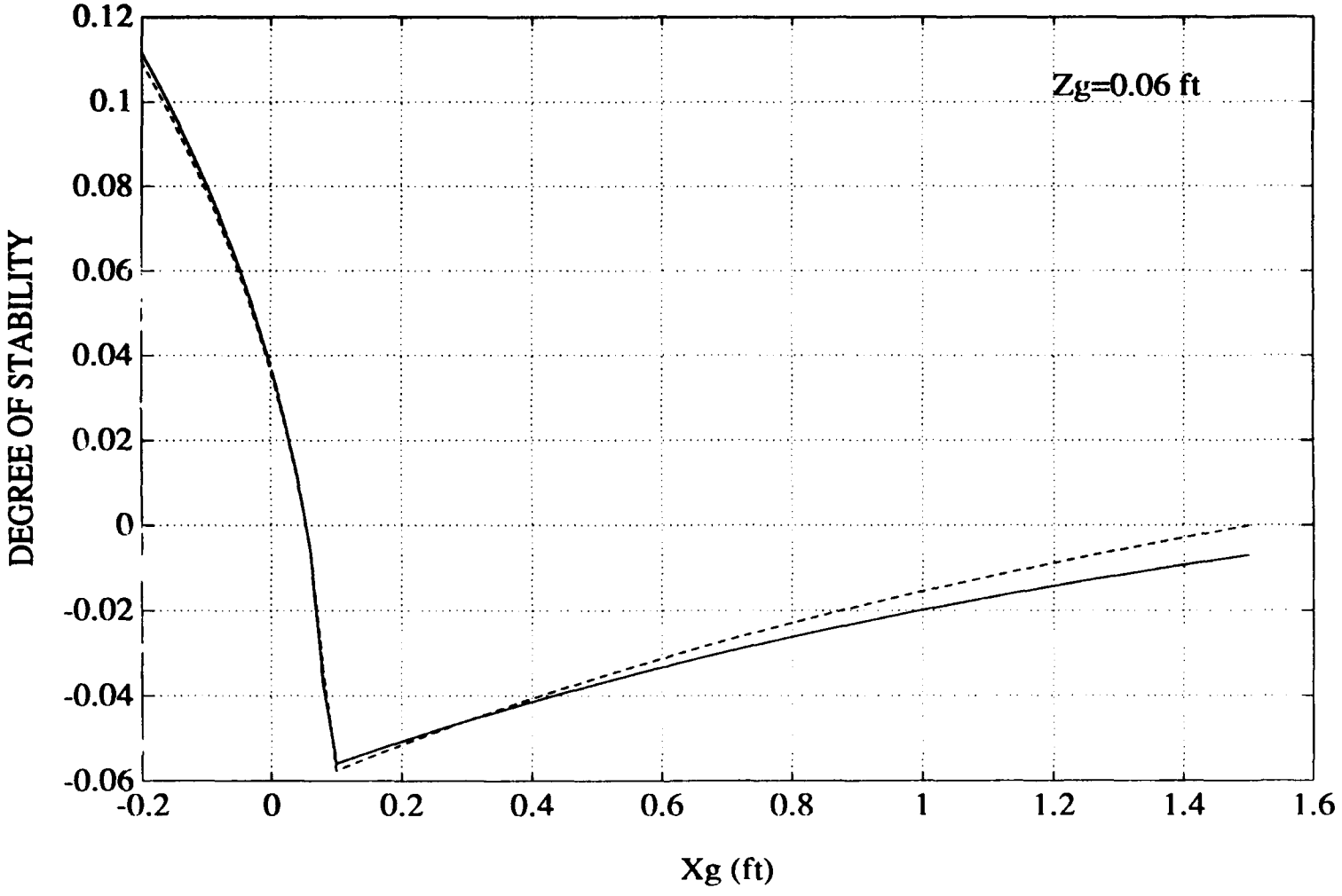

Figure 31: Comparison of Degree of Stability vs X_g with Six Cross Coupling Coefficients Neglected - Configuration 'B'

In order to further simplify these coefficients, terms of order $(Z_g)^2$ and $(X_g)^2$ will be neglected; the effects of doing this are small and may be seen in Figures 32 and 33. This reduces the coefficients to:

$$A = A_R A_L \tag{4.5a}$$

$$B = A_R B_L + B_R A_L + \alpha (X_g) + K1 \tag{4.5b}$$

$$C = A_R C_L + C_R A_L + B_R B_L + \beta (X_g) + K2 \tag{4.5c}$$

$$D = C_R B_L + C_L B_R + \gamma (X_g) \tag{4.5d}$$

$$E = C_R C_L + \delta (X_g) \tag{4.5e}$$

where:

$$\alpha = -M^2 Z_g K_r U \tag{4.6a}$$

$$\beta = -(MZ_g)[(WY_{\dot{r}}) + (MK_v U^2)] \tag{4.6b}$$

$$\gamma = (WU)[MZ_g(Y_{\dot{v}} - Y_r) + K_r Y_{\dot{v}} - K_r M - K_v Y_{\dot{r}}] \tag{4.6c}$$

$$\delta = (WU^2)[(Y_v)(MZ_g + K_r) - (K_v)(Y_r - M)] \tag{4.6e}$$

$$K1 = (MZ_g)[(I_{zz} - N_{\dot{r}})(K_v U) + (N_{\dot{v}} K_r U)] \tag{4.6f}$$

$$K2 = (MZ_g U^2)(N_r K_v - N_v K_r) \tag{4.6g}$$

Carrying through the computations results in the following expressions:

$$(A_R A_L)\, a_0^4 + (A_R B_L + B_R A_L + K1)\, a_0^3 + (A_R C_L + C_R A_L + B_R B_L + K2)\, a_0^2 + (C_R B_L + C_L B_R)\, a_0 + C_R C_L = 0 \tag{4.7a}$$

$$a_1 = \frac{-(\alpha a_0^3 + \beta a_0^2 + \gamma a_0 + \delta)}{(4A)a_0^3 + 3(B - \alpha X_g)a_0^2 + 2(C - \beta X_g)a_0 + (D - \gamma X_g)} \tag{4.7b}$$

$$a_2 = \frac{-a_1^2(C - \beta X_g) - a_1^2 a_0(6A + B - \alpha X_g) - K1 a_0 a_1^2 - 3\alpha a_0^2 a_1 - 2\beta a_0 a_1 - \gamma a_1}{(4A)a_0^3 + 3(B - \alpha X_g)a_0^2 + 2(C - \beta X_g)a_0 + (D - \gamma X_g)} \tag{4.7c}$$

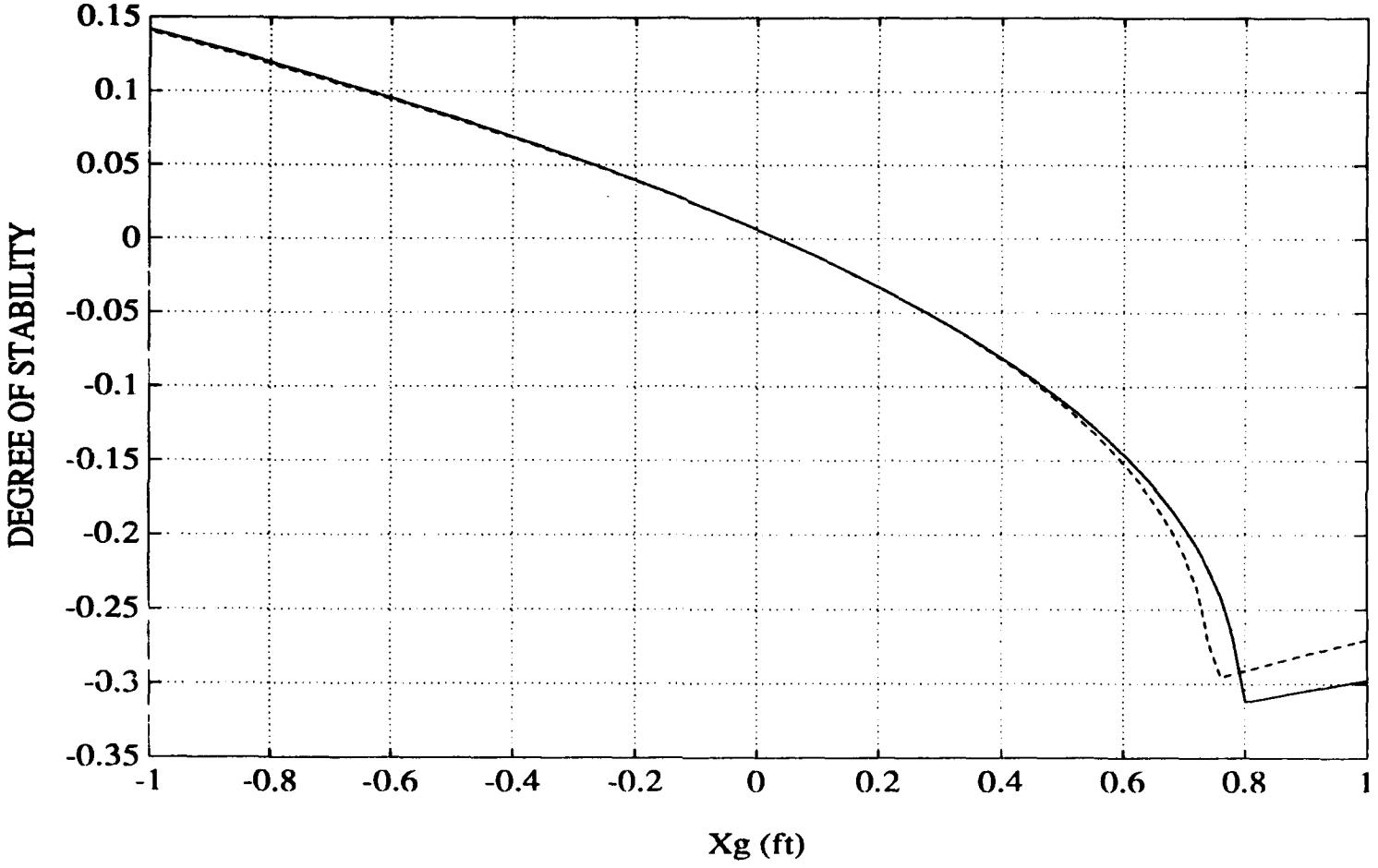

Figure 32: Comparison of Degree of Stability vs X_g Neglecting Higher Order Terms of X_g and Z_g for Configuration 'A'

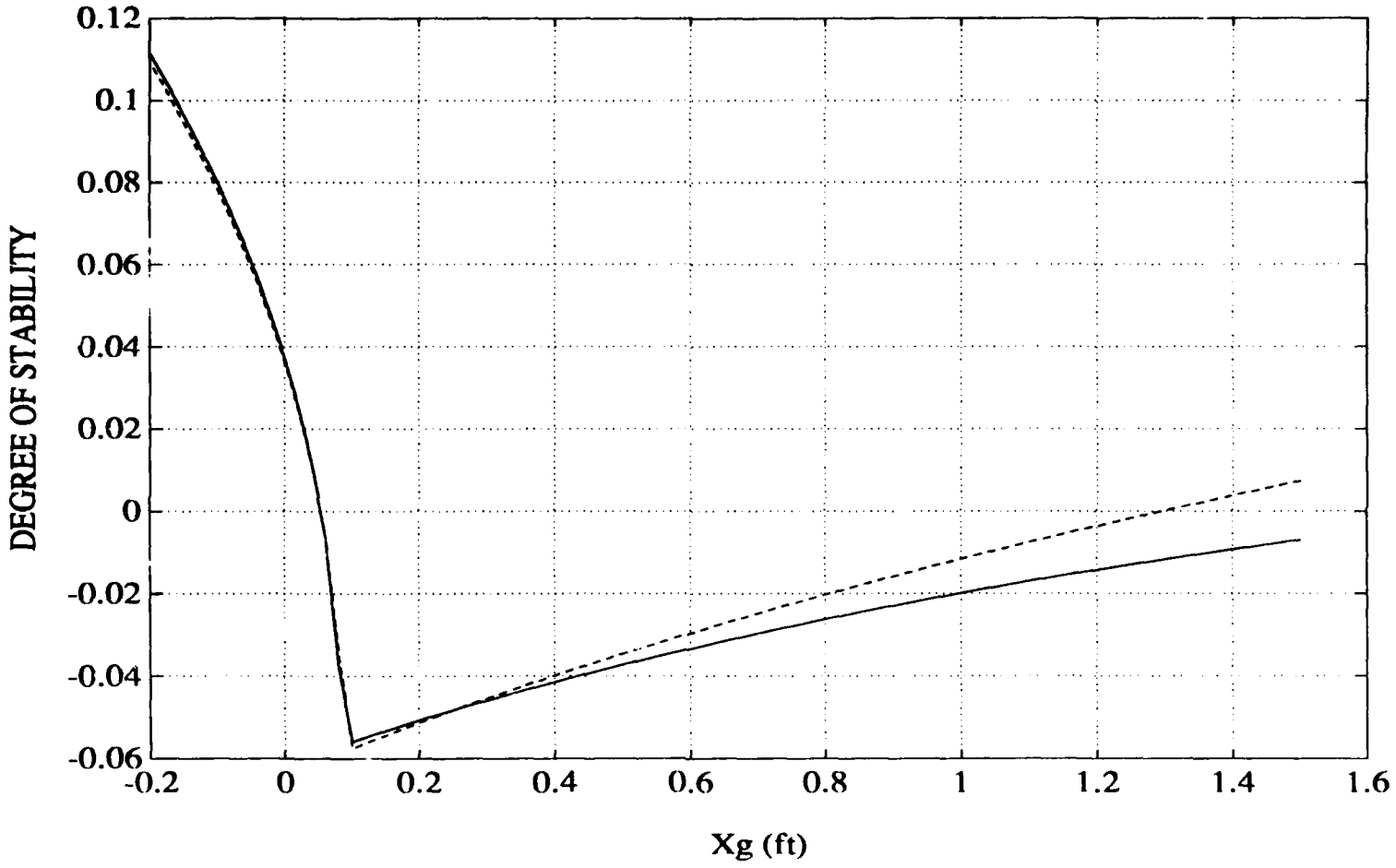

Figure 33: Comparison of Degree of Stability vs X_g Neglecting Higher Order Terms of X_g and Z_g for Configuration 'B'

The characteristic equation $A\lambda^4 + B\lambda^3 + C\lambda^2 + D\lambda + E = 0$ may now be expressed in terms of a second order perturbation which depends on a single variable ε as:

$$\lambda(\varepsilon) = a_0 + a_1 \varepsilon + a_2 \varepsilon^2 \qquad (4.8)$$

Figures 34 through 37 depict the results for both first and second order perturbation analysis about X_g close to zero. Results for both configurations 'A' and 'B' demonstrate that this method for representing the degree of stability in the vicinity of a nominal $(X_g - X_b)$ is quite satisfactory, provided the roots have no complex conjugates. In the region where the roots become complex, the problem is no longer a regular perturbation, and methods to solve the singular perturbation must be developed.

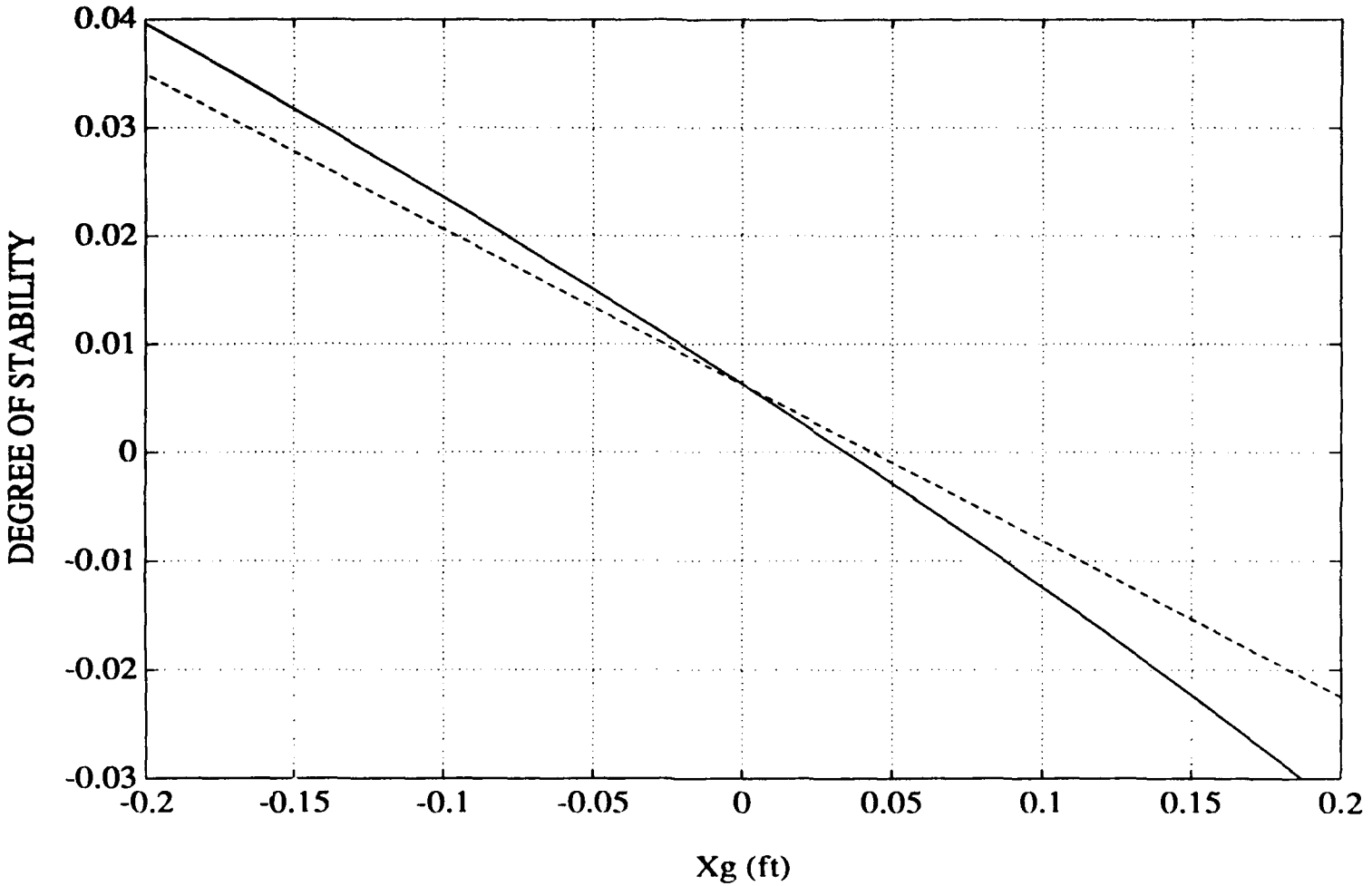

Figure 34: First Order Perturbation Approximation for Configuration 'A'

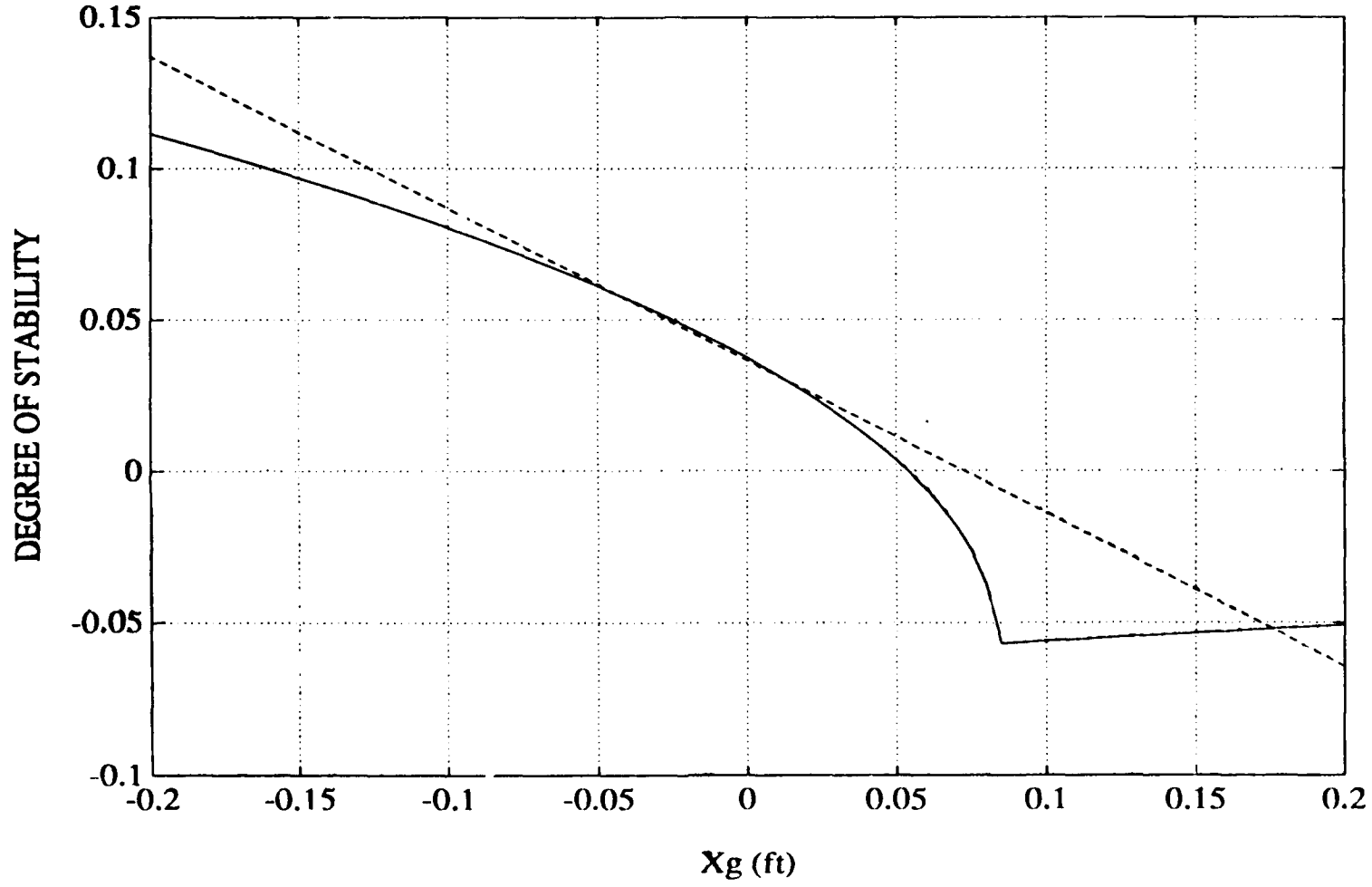

Figure 35: First Order Perturbation Approximation for Configuration 'B'

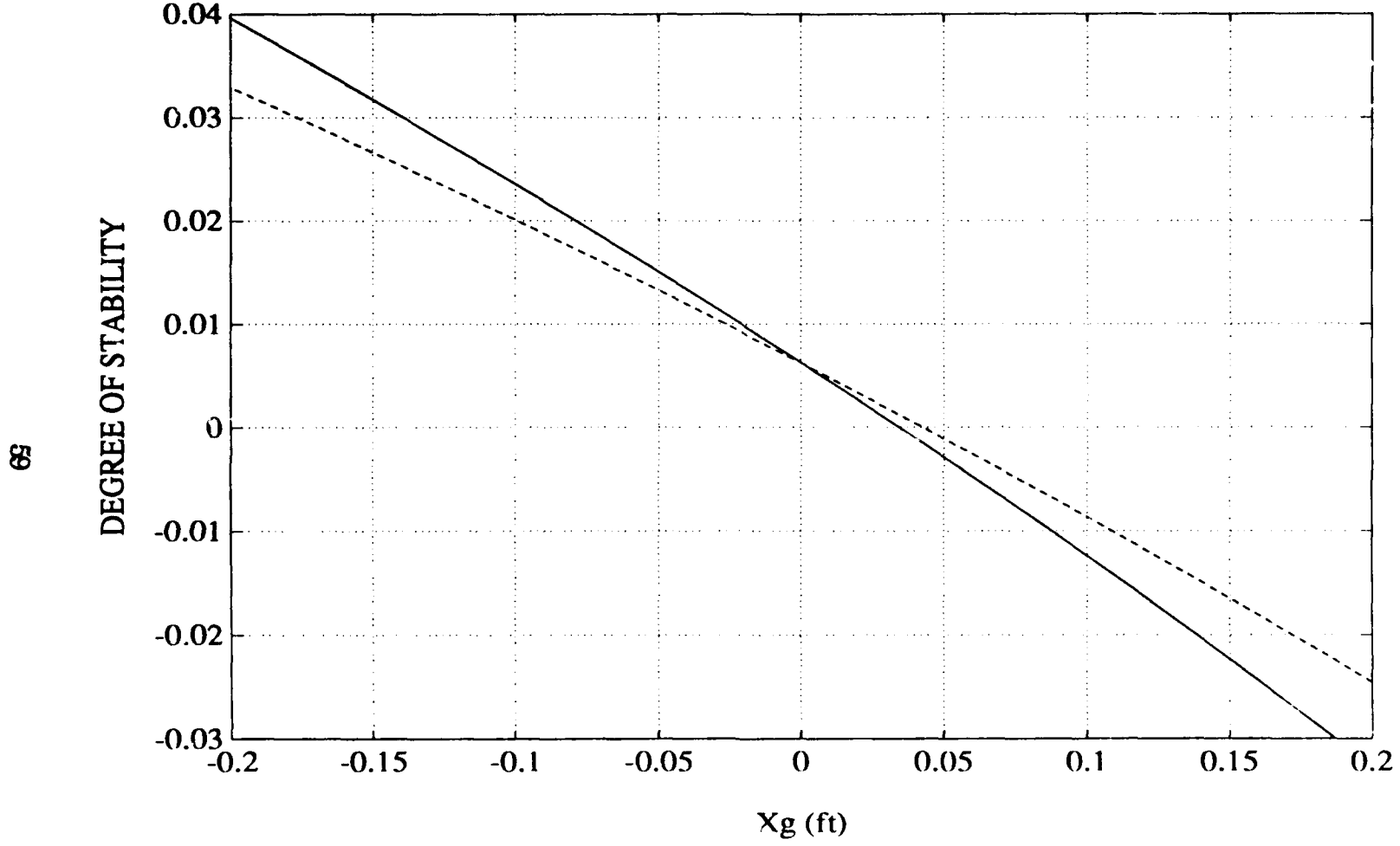

Figure 36: Second Order Perturbation Approximation for Configuration 'A'

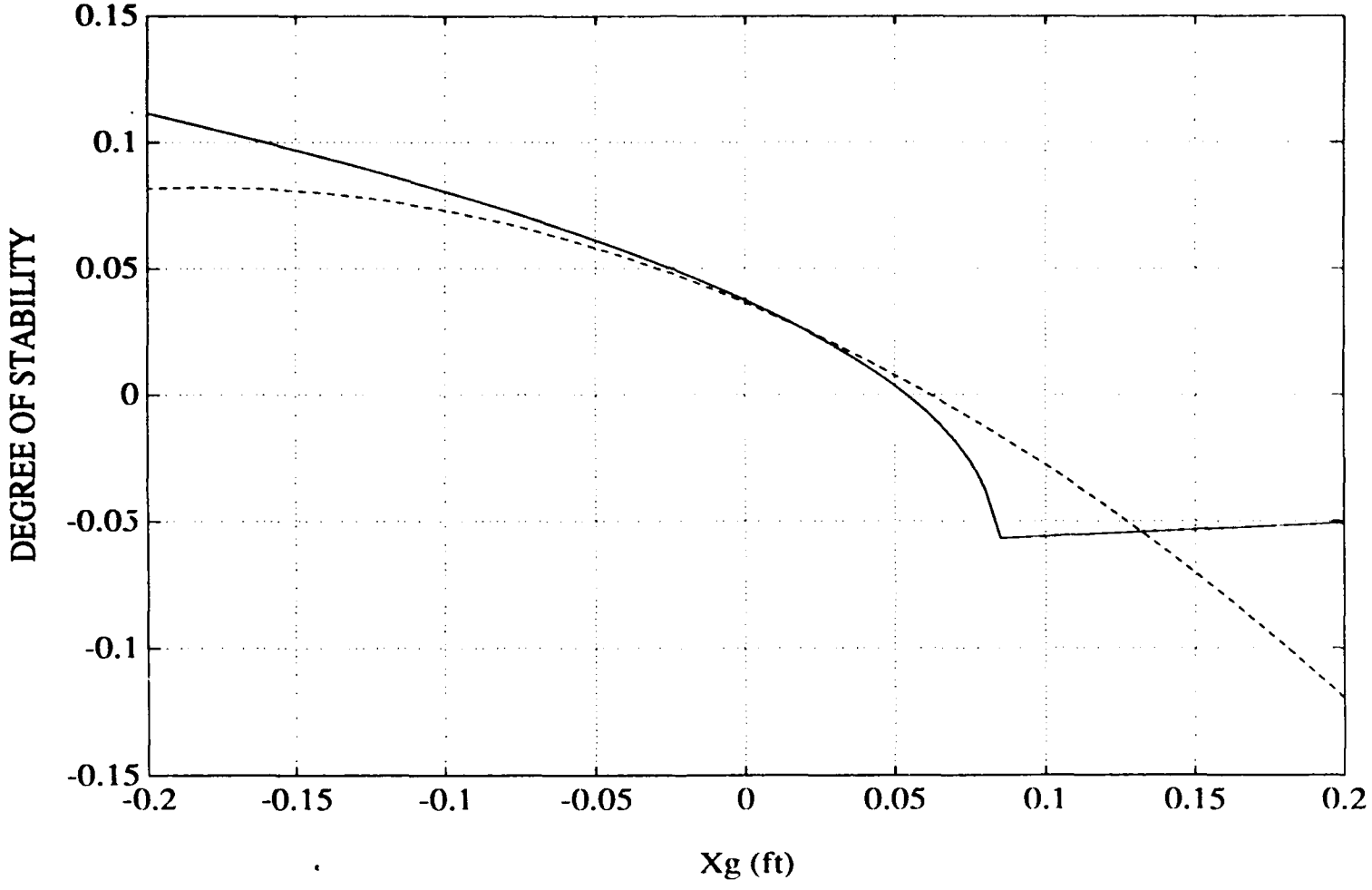

Figure 37: Second Order Perturbation Approximation for Configuration 'B'

V. CONCLUSIONS AND RECOMMENDATIONS

- When considering an inherently stable situation for an analysis of sway, yaw, and roll response, the linear simulations compare favorably with the nonlinear simulations. For a marginally stable or unstable system, only the nonlinear simulation can predict the existence and extent of any non-zero steady states or limit cycles that may occur.
- Obviously, in the design of a submersible, careful attention must be paid to selection of both the metacentric height and the separation between the longitudinal centers of gravity and buoyancy. Instability associated with the dynamic coupling effects can be minimized by increasing the metacentric height. The uncoupled system stability predictions are not reliable when there is separation between X_g and X_b.
- It can be concluded from the analysis that the coupling of roll into sway and yaw for the linearized equations of motion is not very significant when X_g equals X_b.
- Recommendations for future modelling research include an expansion to incorporate coupling effects between the vertical and horizontal planes. It is well known that the coupling between translation and attitude is a severe limitation in the design of submersibles.
- The effects of varying hydrodynamic derivatives and initial conditions, as well as incorporating disturbances in the nonlinear simulations deserve more attention. Additionally, the complexity of the nonlinear system resulting from including the vertical plane is greatly increased. More studies of the nonlinear system resulting from this union are also required.

APPENDIX A

NON-LINEAR SIMULATION PROGRAM:

```
**************************************************************************
% THIS PROGRAM USES HAMMING'S METHOD TO SOLVE A SYSTEM
% OF NONLINEAR EQUATIONS.  SIMILAR TO A FOURTH ORDER
% RUNGE-KUTTA IN TERMS OF LOCAL ERROR, IT REQUIRES ONLY
% TWO FUNCTION CALCULATIONS PER STEP VICE FOUR.

   function[v,phi] = nonlinsim_hamming(U0,Xg,Zg)

% VEHICLE PARAMETERS FOLLOW

  W = 12000.0; Ixx = 1760.0; Iyy = 9450.0; Izz=10700.0; L = 17.425;
  RHO=1.94; G=32.2; M = W/G; BUOY = W; Zb=0.0;  Xb = 0.0;
  ZZ = 0.5*RHO*L^2;

% SWAY HYDRODYNAMIC COEFFICIENTS
    Ypdot  = 1.270E-04*ZZ*L^2;        Yrdot  = 1.240E-03*ZZ*L^2;
    Ypq    = 4.125E-03*ZZ*L^2;        Yqr    = -6.510E-03*ZZ*L^2;
    Yvdot  = -5.550E-02*ZZ*L;         Yp     = 3.055E-03*ZZ*L;
    Yvq    = 2.360E-02*ZZ*L;          Ywp    = 2.350E-01*ZZ*L;
    Ywr    = -1.880E-02*ZZ*L;         Yv     = -9.310E-02*ZZ;
    Yvw    = 6.840E-02*ZZ;

% NOMINAL VALUE FOR Yr =  2.970E-02*ZZ*L
% CONFIGURATION 'A':  Yr = -3.500E-02*ZZ*L
% CONFIGURATION 'B':  Yr = -5.940E-02*ZZ*L

   CC = input('enter model configuration choice; either 1 for A or 2 for B')

  if CC < 2
   Yr = -3.500e-02*ZZ*L;
  else
   Yr = -5.940e-02*ZZ*L;
  end

% ROLL HYDRODYNAMIC COEFFICIENTS
    Kpdot  = -1.01E-03*ZZ*L^3;        Krdot  = -3.37E-05*ZZ*L^3;
    Kpq    = -6.93E-05*ZZ*L^3;        Kqr    = 1.68E-02*ZZ*L^3;
    Kvdot  = 1.27E-04*ZZ*L^2;         Kp     = -1.10E-02*ZZ*L^2;
    Kr     = -8.41E-04*ZZ*L^2;        Kvq    = -5.115E-03*ZZ*L^2;
    Kwp    = -1.27E-04*ZZ*L^2;        Kwr    = 1.39E-02*ZZ*L^2;
    Kv     = 3.055E-03*ZZ*L;          Kvw    = -1.87E-01*ZZ*L;
```

```
% YAW HYDRODYNAMIC COEFFICIENTS
   Npdot  = -3.370E-05*ZZ*L^3;      Nrdot  = -3.400E-03*ZZ*L^3;
   Npq    = -2.110E-02*ZZ*L^3;      Nqr    =  2.750E-03*ZZ*L^3;
   Nvdot  =  1.240E-03*ZZ*L^2;      Np     = -8.405E-04*ZZ*L^2;
   Nr     = -1.640E-02*ZZ*L^2;      Nvq    = -9.990E-03*ZZ*L^2;
   Nwp    = -1.750E-02*ZZ*L^2;      Nwr    =  7.350E-03*ZZ*L^2;
   Nv     = -1.484E-02*ZZ*L;        Nvw    = -2.670E-02*ZZ*L;

% THE FOLLOWING ARE USED FOR EVALUATING THE INTEGRALS
% IN THE SWAY AND YAW EQUATIONS OF MOTION. 'X' IS THE
% DISTANCE IN FEET ALONG THE LONGITUDINAL AXIS AND 'HH'
% IS THE VEHICLE HEIGHT. ALL VALUES ARE IN FEET.

   X(1)=-105.9/12;     X(2)=-104.3/12;     X(3)=-99.3/12;
   X(4)=-94.3/12;      X(5)=-87.3/12;      X(6)=-76.8/12;
   X(7)=-66.3/12;      X(8)=-55.8/12;      X(9)=72.7/12;
   X(10)=79.2/12;      X(11)=83.2/12;      X(12)=87.2/12;
   X(13)=91.2/12;      X(14)=95.2/12;      X(15)=99.2/12;
   X(16)=101.2/12;     X(17)=102.1/12;     X(18)=103.2/12;

   HH(1)=0.0/12;       HH(2)=2.28/12;      HH(3)=8.24/12;
   HH(4)=13.96/12;     HH(5)=19.76/12;     HH(6)=25.1/12;
   HH(7)=29.36/12;     HH(8)=31.85/12;     HH(9)=31.85/12;
   HH(10)=30.00/12;    HH(11)=27.84/12;    HH(12)=25.12/12;
   HH(13)=21.44/12;    HH(14)=17.12/12;    HH(15)=12.0/12;
   HH(16)=9.12/12;     HH(17)=6.72/12;     HH(18)=0.00/12;

% THE INITIAL CONDITIONS ARE SET PRIOR TO INTEGRATION
% BY CALLING A LINEAR INTEGRATION PROGRAM NAMED
% 'EULER'. THE ERRORS ASSOCIATED WITH USING LINEAR
% SOLUTIONS FOR THE FIRST FIVE TIME INTERVAL STEPS ARE
% SMALL AND DO NOT AFFECT THE NONLINEAR SOLUTIONS.

   [p,pdot,v,vdot,r,rdot,phi,phidot] = euler(dt);

   p(1:5)= p;
   pdot(1:5)= pdot;
   pdotmod(5)=pdot(5);

   v(1:5)= v;
   vdot(1:5)= vdot;
   vdotmod(5)=vdot(5);
```

```
r(1:5)= r;
rdot(1:5)= rdot;
rdotmod(5)=rdot(5);

phi(1:5)= phi;
phidot(1:5)= phidot;
phidotmod(5)=phidot(5);

% THE TIME INTERVAL IS 'dt', THE FINAL TIME IS 'tfinal', AND A
% VALUE CALLED 'stopnumber' IS SET TO ALLOW ACCESS TO THE
% DATA AFTER THIS NUMBER OF ITERATIONS.  THE VALUE FOR
% 'stopnumber' MAY BE CHANGED WHILE THE KEYBOARD IS
% ACTIVE TO ALLOW SUBSEQUENT PROGRAM INTERACTION.
% RETURN TO THE PROGRAM IS ACHIEVED BY TYPING 'return'
% FOLLOWED BY THE 'enter' KEY.

dt = input('enter the time interval step size')
tfinal = input('enter the final time')
stopnumber = input('enter the value for stopnumber')

% THIS SECTION ALLOWS FOR RANDOM DISTURBANCES IN SWAY
% AND YAW
 rand('uniform')
vdotdist = rand(1,(tfinal/dt)+1);
vdotdist = 0.05*(vdotdist - mean(vdotdist));
rdotdist = rand(1,(tfinal/dt)+1);
rdotdist = 0.04*(rdotdist - mean(rdotdist));

% THIS SECTION PROVIDES FOR CONTINUATION OF SOLUTIONS.
% IF THE MATRICES BECOME VERY LARGE, IT IS RECOMMENDED
% THAT THE CURRENT VALUES BE SAVED AND A NEW
% SIMULATION BEGUN AS MATLAB SLOWS NOTICEABLY WITH
% LARGE MATRICES.

%  vcorr(5)=      ;     rcorr(5)=      ;
%  pcorr(5)=      ;     phicorr(5)=    ;

%  vpred(5)=      ;     rpred(5)=      ;
%  ppred(5)=      ;     phipred(5)=    ;

%  pdotmod(5)=    ;     rdotmod(5)=    ;
```

```
% COMMENCE INTEGRATION

    for j = 6:(tfinal/dt) + 1;

% THIS SECTION USES A HAMMING PREDICTOR-CORRECTOR TO
OBTAIN VALUES

    vpred(j)=v(j-4)+(4*dt/3)*(2*vdot(j-1)-vdot(j-2)+2*vdot(j-3));
    rpred(j)=r(j-4)+(4*dt/3)*(2*rdot(j-1)-rdot(j-2)+2*rdot(j-3));
    ppred(j)=p(j-4)+(4*dt/3)*(2*pdot(j-1)-pdot(j-2)+2*pdot(j-3));
    phipred(j)=phi(j-4)+(4*dt/3)*(2*p(j-1)-p(j-2)+2*p(j-3));

    if j < 7
      vmod(j) =      vpred(j);
      rmod(j) =      rpred(j);
      pmod(j)=       ppred(j);
      phimod(j)=     phipred(j);
     else
      vmod(j)=       vpred(j)-(112/121)*(vpred(j-1)-vcorr(j-1));
      rmod(j)=       rpred(j)-(112/121)*(rpred(j-1)-rcorr(j-1));
      pmod(j)=       ppred(j)-(112/121)*(ppred(j-1)-pcorr(j-1));
      phimod(j)=     phipred(j)-(112/121)*(phipred(j-1)-phicorr(j-1));
     end

    tmp1mod=vmod(j); tmp2mod=rmod(j);
     [SWAYMOD,YAWMOD]=crossflowintmod(tmp1mod,tmp2mod,X,HH);

    vdotmod(j)=    (1/(M-Yvdot))*((Ypdot+M*Zg)*pdotmod(j-1)+...
                   Yp*U0*pmod(j)+(Yrdot-M*Xg)*rdotmod(j-1)+...
                   Yv*U0*vmod(j)+(Yr-M)*U0*rmod(j)+SWAYMOD);

    vcorr(j)=      0.125*(9*v(j-1)-v(j-3)+3*dt*(vdotmod(j)+2*vdot(j-1)-...
                   vdot(j-2)));

    rdotmod(j)=    (1/(Izz-Nrdot))*(Npdot*pdotmod(j-1)+...
                   (Nvdot-M*Xg)*vdotmod(j)+Np*U0*pmod(j)+...
                   (Nr-M*Xg)*U0*rmod(j)+Nv*U0*vmod(j)+...
                   Xg*W*sin(phimod(j))+YAWMOD);

    rcorr(j)=      0.125*(9*r(j-1)-r(j-3)+3*dt*(rdotmod(j)+2*rdot(j-1)-...
                   rdot(j-2)));

    pdotmod(j)=    (1/(Ixx-Kpdot))*((Kvdot+M*Zg)*vdotmod(j)+...
                   Krdot*rdotmod(j)+Kp*U0*pmod(j)+...
                   (Kr+M*Zg)*U0*rmod(j)+Kv*U0*vmod(j)-...
                   Zg*W*sin(phimod(j)));
```

```
pcorr(j)=       0.125*(9*p(j-1)-p(j-3)+3*dt*(pdotmod(j)+2*pdot(j-1)-...
                pdot(j-2)));

phicorr(j)=     0.125*(9*phi(j-1)-phi(j-3)+3*dt*(pmod(j)+2*p(j-1)-...
                p(j-2)));

v(j)=       vcorr(j)+(9/121)*(vpred(j)-vcorr(j));
r(j)=       rcorr(j)+(9/121)*(rpred(j)-rcorr(j));
p(j)=       pcorr(j)+(9/121)*(ppred(j)-pcorr(j));
phi(j)=     phicorr(j)+(9/121)*(phipred(j)-phicorr(j));

beta(j) = -atan(v(j)/5)*180/pi;

% THIS SECTION HAS THE NON-LINEAR EQUATIONS OF MOTION.
% REMEMBER TO REMOVE THE DISTURBANCES FROM THE SWAY
% AND YAW DERIVATIVES IF THEY ARE NOT DESIRED.

tmp1=v(j); tmp2=r(j);
 [SWAY,YAW] = crossflowint(tmp1,tmp2,X,HH);

vdot(j)=    ((1/(M-Yvdot))*((Ypdot+M*Zg)*pdot(j-1)+Yp*U0*p(j) +...
            (Yrdot-M*Xg)*rdot(j-1)+Yv*U0*v(j)+(Yr-M)*U0*r(j)+...
            SWAY))+vdotdist(j);

rdot(j)=    ((1/(Izz-Nrdot))*(Npdot*pdot(j-1)+(Nvdot-M*Xg)*vdot(j)+...
            Np*U0*p(j)+(Nr-M*Xg)*U0*r(j)+Nv*U0*v(j)+...
            Xg*W*sin(phi(j))+YAW))+rdotdist(j);

pdot(j)=    (1/(Ixx-Kpdot))*((Kvdot+M*Zg)*vdot(j)+Krdot*rdot(j)+...
            Kp*U0*p(j)+(Kr+M*Zg)*U0*r(j)+Kv*U0*v(j)-...
            Zg*W*sin(phi(j)));

if j == stopnumber
 keyboard
end

end
return
```

LINEAR SIMULATION PROGRAM:

```
**************************************************************************
% THIS PROGRAM IS THE LINEAR EQUATION OF MOTION
% INTEGRATION EMPLOYING A SIMPLE EULER METHOD TO
% OBTAIN STARTING VALUES FOR THE NONLINEAR SIMULATION.

  function[p,pdot,v,vdot,r,rdot,phi,phidot] = euler(dt)

% THE MATRIX 'A' CORRESPONDS TO THE DAMPING MATRIX AND
% MATRIX 'B' CORRESPONDS TO THE MASS MATRIX.

  A(1,1) = Kp*U0;          A(1,2) = -((Zg*W)-(Zb*B));
  A(1,3) = Kv*U0;          A(1,4) = (Kr+(M*Zg))*U0;
  A(2,1) = 1.0;            A(2,2) = 0.0;
  A(2,3) = 0.0;            A(2,4) = 0.0;
  A(3,1) = Yp*U0;          A(3,2) = 0.0;
  A(3,3) = Yv*U0;          A(3,4) = (Yr-M)*U0;
  A(4,1) = Np*U0;          A(4,2) = ((Xg*W)-(Xb*B));
  A(4,3) = Nv*U0;          A(4,4) = (Nr-(M*Xg))*U0;

  B(1,1) = Ixx-Kpdot;          B(1,2) = 0.0;
  B(1,3) = -(Kvdot+(M*Zg));    B(1,4) = -Krdot;
  B(2,1) = 0.0;                B(2,2) = 1.0;
  B(2,3) = 0.0;                B(2,4) = 0.0;
  B(3,1) = -(Ypdot+(M*Zg));    B(3,2) = 0.0;
  B(3,3) = M-Yvdot;            B(3,4) = (M*Xg)-Yrdot;
  B(4,1) = -Npdot;             B(4,2) = 0.0;
  B(4,3) = (M*Xg)-Nvdot;       B(4,4) = Izz-Nrdot;

  C = [inv(B)*A];

% INITIAL CONDITIONS

  time(1) = 0.0;
  p(1) = 0.0;              pdot(1) = 0.0;
  phi(1) = 1.0*pi/180;     phidot(1) = 0.0;
  psi(1) = 0.0;            psidot(1) = 0.0;
  v(1) = 0.0;              vdot(1) = 0.0;
  r(1) = 0.0;              rdot(1) = 0.0;
  x(1) = 0.0;              y(1) = 0.0;
  xdot(1) = 0.0;           ydot(1) = 0.0;
  tfinal = 1;
```

```
% THIS SECTION ALLOWS FOR RANDOM DISTURBANCES IN SWAY
% AND YAW FOR THE LINEAR EQUATIONS AS WELL.  MATLAB
% ALLOWS FOR EITHER A UNIFORM OR NORMAL DISTRIBUTION
% OF RANDOM NUMBER.

    rand('uniform')
   vdotdist = rand(1,(tfinal/deltat)+1);
   vdotdist = 0.05*(vdotdist - mean(vdotdist));
   rdotdist = rand(1,(tfinal/deltat)+1);
   rdotdist = 0.04*(rdotdist - mean(rdotdist));

% COMMENCE EULER INTEGRATION

   for j = 2:(tfinal/deltat) + 1;

   p(j) =      p(j-1) + pdot(j-1)*deltat;
   phi(j) =    phi(j-1) + phidot(j-1)*deltat;
   psi(j) =    psi(j-1) + psidot(j-1)*deltat;
   v(j) =      v(j-1) + vdot(j-1)*deltat;
   beta(j) =   -atan(v(j)/U0);
   r(j) =      r(j-1) + rdot(j-1)*deltat;
   x(j) =      x(j-1) + xdot(j-1)*deltat;
   y(j) =      y(j-1) + ydot(j-1)*deltat;

  pdot(j) =          C(1,1)*p(j) + C(1,2)*phi(j) + C(1,3)*v(j) + C(1,4)*r(j);

   phidot(j)=        C(2,1)*p(j) + C(2,2)*phi(j) + C(2,3)*v(j) + C(2,4)*r(j);

   vdot(j) =         C(3,1)*p(j) + C(3,2)*phi(j) + C(3,3)*v(j) + C(3,4)*r(j);

   rdot(j) =         C(4,1)*p(j) + C(4,2)*phi(j) + C(4,3)*v(j) + C(4,4)*r(j);

   psidot(j) =       r(j)*cos(phi(j));

   xdot(j) =         U0*cos(psi(j)) - v(j)*sin(psi(j))*cos(phi(j));

   ydot(j) =         U0*sin(psi(j)) + v(j)*cos(psi(j))*cos(phi(j));

   time(j) =         (j*deltat) - deltat;

   end
   return
```

CROSSFLOW INTEGRAL PROGRAM:

```
*************************************************************************
% THIS IS A NUMERICAL INTEGRATION PROGRAM TO CALCULATE
% THE DRAG FORCES IN THE HORIZONTAL PLANE UTILIZING THE
% TRAPEZOIDAL RULE.  THE CALL TO 'crossflowintmod' IS
% IDENTICAL, ONLY USING DIFFERENT VARIABLE NAMES AND
% VALUES FOR THE MODIFICATION PORTION OF HAMMING'S
% METHOD.

   function[SWAY,YAW]=crossflowint(tmp1,tmp2,X,HH)

  RHO = 1.94;   CDy = 0.35;   SWAY = 0.0;   YAW = 0.0;
  v = tmp1; r = tmp2;

  for k = 1:18;
    if abs(v+X(k)*r) < 1e-6
     UCF(k) = 0.0;
    else
     UCF(k)  = (v+X(k)*r)/(abs(v+X(k)*r));
    end
   CFLOW(k) = CDy*HH(k)*((v+X(k)*r)^2);
   SWAY1(k) = CFLOW(k)*UCF(k);
   YAW1(k)  = CFLOW(k)*X(k)*UCF(k);
  end

  jj = 1:17;
     SWAY = -0.25*RHO*sum((SWAY1(jj)+SWAY1(jj+1)).*(X(jj+1)-X(jj)));
     YAW  = -0.25*RHO*sum((YAW1(jj)+YAW1(jj+1)).*(X(jj+1)-X(jj)));
  return
```

EIGENVALUE CALCULATION PROGRAM:

```
*************************************************************************
% THIS PROGRAM DETERMINES THE FOUR ROOTS FOR THE ROLL
% COUPLED EQUATIONS OF MOTION OVER A RANGE OF Xg.

   function[all_roots,xg] = findroots(U0,Xgmin,stepXg,Xgmax)

  W = 12000.0;   Ixx = 1760.0;   Iyy = 9450.0;   Izz=10700.0;
  L = 17.425;     RHO=1.94;      G=32.2;          M = W/G;
  BUOY = W; Zb=0.0;
  ZZ = 0.5*RHO*L^2;
```

```
% SWAY HYDRODYNAMIC COEFFICIENTS
   Ypdot = 1.27E-04*ZZ*L^2;    Yrdot = 1.24E-03*ZZ*L^2;
   Yvdot = -5.55E-02*ZZ*L;     Yp    = 3.055E-03*ZZ*L;
   Yv    = -9.31E-02*ZZ;

   CC = input('enter model configuration choice; either 1 for A or 2 for B')

  if CC < 2
   Yr = -3.500e-02*ZZ*L;
  else
   Yr = -5.940e-02*ZZ*L;
  end

% ROLL HYDRODYNAMIC COEFFICIENTS
   Kpdot = -1.01E-03*ZZ*L^3;   Krdot = -3.37E-05*ZZ*L^3;
   Kvdot = 1.27E-04*ZZ*L^2;    Kp    = -1.10E-02*ZZ*L^2;
   Kr    = -8.41E-04*ZZ*L^2;   Kv    = 3.055E-03*ZZ*L;

% YAW HYDRODYNAMIC COEFFICIENTS
   Npdot = -3.370E-05*ZZ*L^3;  Nrdot = -3.400E-03*ZZ*L^3;
   Nvdot = 1.240E-03*ZZ*L^2;   Np    = -8.405E-04*ZZ*L^2;
   Nr    = -1.640E-02*ZZ*L^2;  Nv    = -1.484E-02*ZZ*L;

    rows=(abs(Xgmax-Xgmin)/stepXg)+ 1;
   all_roots = zeros(rows,4);    xg = zeros(rows,1);

   Zg = input('enter value for Zg')

   a = (Ixx-Kpdot);            b = (Kp*U0);          c = (Zg*W)-(Zb*BUOY);
   d = (M*Zg)+Kvdot;           e = Kv*U0;            f = Krdot;
   g = (M*Zg*U0) + (Kr*U0);    h = Ypdot + (M*Zg);
   i = Yp*U0;                  j = M - Yvdot;        k = Yv*U0;
   o = Npdot;                  u = Izz - Nrdot;      p = Np*U0;
   m = (Yr*U0) - (M*U0);       x = Nv*U0;

    Xg = Xgmin:stepXg:Xgmax;
   Xb = input('enter either 0.0 or Xg for value of Xb);

   l = (M*Xg) - Yrdot;         q = (Xb.*BUOY)-(Xg*W);
   r = (M*Xg)-Nvdot;           w = (Nr*U0)-(M*Xg*U0);

   A = (((a).*(j*u-l.*r)+(d).*(u*h+o.*l)-(f).*(r.*h+o*j)));

   B = ((e).*(u*h+o.*l)-(d).*(u*i-w.*h+o.*m-p.*l)-(a) * ...
       (j.*w+k*u-l.*x-r.*m)-(b).*(j*u-l.*r)+(f).*(r.*i-x...
       .*h+o*k-p*j)-(g).*(r.*h+o*j));
```

```
C = ((a).*(k.*w-m.*x)+(b).*(j.*w+k*u-l.*x-r.*m)+(c).*...
    (j*u-l.*r)-(d).*(q.*l-w.*i+m.*p)-(e).*(u*i-w.*h+...
    o.*m-p.*l)+(f).*(q.*j-x*i+p*k)+(g).*(r.*i-x.*h+o*k...
    -p.*j));

D = ((g).*(q.*j-x.*i+p*k)-(f.*q*k)+(d.*q.*m)-(e).*(q.*l...
    -w.*i+m.*p)-(c).*(j.*w+k*u-l.*x-r.*m)-(b).*(k.*w-m.*x));

E = ((c).*(k.*w-m.*x)+(e.*q.*m)-(g.*q.*k));

z = [A' B' C' D' E'];

j = 1:rows;      poly(j,:)=z(j,:);      rts = 'roots(poly(jj,:))';

for jj = 1:rows;
all_roots(jj,1:4) = eval(rts)';
end

xg=Xg';
end;
return
```

FIRST AND SECOND ORDER PERTURBATION APPROXIMATION COMPUTER PROGRAM:

```
**************************************************************************
% THIS PROGRAM DEVELOPS THE 1ST & 2ND ORDER PERTURBATION
% APPROXIMATION SOLUTIONS FROM SECTION IV

   function[xlocation,perturbroot1,perturbroot2,xg] =perturbanalysis(U0)

  W = 12000.0;     Ixx = 1760.0;     Iyy = 9450.0;     Izz=10700.0;
  L = 17.425;      RHO=1.94;         G=32.2;           M = W/G;
  BUOY = W;        Zb=0.0;           Xb = 0.0;
  ZZ = 0.5*RHO*L^2;

% SWAY HYDRODYNAMIC COEFFICIENTS
    Ypdot = 0.0;                  Yrdot = 1.24E-03*ZZ*L^2;
    Yvdot = -5.55E-02*ZZ*L;       Yp    = 0.0;
    Yv    = -9.31E-02*ZZ;

    CC = input('enter model configuration choice; either 1 for A or 2 for B')

    if CC < 2
     Yr = -3.500e-02*ZZ*L;
```

```
    else
     Yr = -5.940e-02*ZZ*L;
    end

% ROLL HYDRODYNAMIC COEFFICIENTS
   Kpdot = -1.01E-03*ZZ*L^3;          Krdot = 0.0;
   Kvdot = 0.0;                       Kp    = -1.10F-02*ZZ*L^2;
   Kr    = -8.41E-04*ZZ*L^2;          Kv    = 3.055E-03*ZZ*L;

% YAW HYDRODYNAMIC COEFFICIENTS
   Npdot = 0.0;                       Nrdot = -3.400E-03*ZZ*L^3;
   Nvdot = 1.240E-03*ZZ*L^2;          Np    = 0.0;
   Nr    = -1.640E-02*ZZ*L^2;         Nv    = -7.42E-03*ZZ*L;

    Zg = input('enter value for Zg')

% THIS PERTURBATION PROGRAM SOLVES FOR THE SOLUTION
% ABOUT Xg=0

    Xg = 0.0;

   index = 1;

   for Xg = -1.0:0.05:0.2;

    a = (Ixx-Kpdot);          b = (Kp*U0);          c = (Zg*W)-(Zb*BUOY);
    d = (M*Zg);               e = Kv*U0;            f = Krdot;
    g = (M*Zg*U0)+(Kr*U0);    h = Ypdot + (M*Zg);   i = Yp*U0;
    j = M - Yvdot;            k = Yv*U0;            l = (M*Xg) - Yrdot;
   m= (Yr*U0) - (M*U0);       o = Npdot;            p = Np*U0;
    q = (Xb*BUOY)-(Xg*W);     r = (M*Xg)-Nvdot;     u = Izz - Nrdot;
    w = (Nr*U0)-(M*Xg*U0);    x = Nv*U0;

    Al = (j*u)-(l*r);     Bl = -((u*k)+(j*w)-(m*r)-(l*x));     Cl = (k*w)-(x*m);

    Ar = a;     Br = -b;     Cr = c;

    K1 = d*u*e + d*Nvdot*Kr*U0;
    K2 = d*((Nr*Kv*U0^2)-(Nv*Kr*U0^2));

    alpha    = -M*M*Zg*Kr*U0;
    beta     = -d*((W*Yrdot)+(M*Kv*U0*U0));
     gamma = (d*W*U0*(Yvdot-Yr))+(W*U0*(Kr*Yvdot-Kr*M-Kv*Yrdot));
    delta    = g*Yv*W*U0 - m*Kv*W*U0;
```

```
% P Q R S &T SOLVE THE 4TH ORDER POLYNOMIAL FOR a0

    P = Ar*Al;
    Q = Ar*Bl + Br*Al +K1;
    R = Ar*Cl +Cr*Al +Br*Bl +K2;
    S = Cr*Bl + Cl*Br;
    T = Cr*Cl;

    A = P;
    B = Q+alpha*Xg;
    C = R+beta*Xg;
    D = S+gamma*Xg;
    E = T+delta*Xg;

    z  = [A B C D E];          temp1(index,1:4) = roots(z)';

    xg(index,1) = Xg;          index = index + 1;          end

    zz = [P Q R S T];          temp2(1,1:4) = roots(zz)';
    a0 = temp2(1,4)

% THIS PART SOLVES FOR a1 IN THE 1ST ORDER PERTURBATION

    num1  = -(alpha*(a0^3)+beta*(a0^2)+gamma*a0+delta);
    den1  = (4*P*(a0^3)+3*Q*(a0^2)+2*R*(a0)+S);
    a1    = num1/den1

% THIS PART SOLVES FOR a2 IN THE 2ND ORDER PERTURBATION

    num2a= -(a1^2*(6*P*a0*a0+Q*a0+R)+a1*(gamma+2*beta*a0+...
              3*alpha*a0*a0));
    a2    = num2a/den1

    index = 1;
    for X = -0.8:0.04:0.4;

% PERTURBROOT1 IS  1ST ORDER PERTURBATION APPROXIMATION
    perturbroot1(index) = a0 + a1*X;

% PERTURBROOT2 IS  2ND ORDER PERTURBATION APPROXIMATION
    perturbroot2(index) = a0 + a1*X + a2*X*X;

    xlocation(index) = X;
    index = index+1;
    end
    return
```

LIST OF REFERENCES

1. Yoerger, D.R. and Newman, J.B., "High Performance Supervisory Control of Vehicles and Manipulators", **Intervention '87 Conference and Exposition**, pages 189-192.

2. Gerald, C.F. and Wheatley, P.O., "Applied Numerical Analysis", Addison-Wesley Publishing Company, Fourth Edition, 1989, p. 384.

3. Smith, N.S., Crane, J.W., and Summey, D.C., "SDV Simulator Hydrodynamic Coefficients", NCSC Technical Memorandum 231-78, June 1978, pages 11-16, 20, 24-31.

4. Dorf, R.C., "Modern Control Systems", Addison-Wesley Publishing Company, Sixth Edition, 1992.

5. Schmidt, L.V. and Wright, S.R., "Aircraft Wing Rock By Inertial Coupling", AIAA-91-2885-CP, August 1991, p. 371.

6. Simmonds, J.G. and Mann, J.E., "A First Look at Perturbation Theory", Robert E. Krieger Publishing Company, 1986, pages 12-38.

BIBLIOGRAPHY

Booth, T.B., "Stability of Buoyant Underwater Vehicles, Predominantly Forward Motion", **International Shipbuilding Progress**, Volume 24, November 1977, Nr. 279, pages 297-305.

McKinley, B.D., "Dynamic Stability of Positively Buoyant Submersibles: Vertical Plane Solutions", Master's Thesis, Naval Postgraduate School, Monterey, California, December 1991.

Papoulias, F.A., "Stability and Bifurcations of Towed Underwater Vehicles in the Dive Plane", **Journal of Ship Research**, Volume 36, No. 3, September 1992, pages 255-267.

INITIAL DISTRIBUTION LIST

		No. Copies
1.	Defense Technical Information Center Cameron Station Alexandria, Virginia 22304-6145	2
2.	Library, Code 52 Naval Postgraduate School Monterey, California 93943-5002	2
3.	Department Chairman, Code ME Department of Mechanical Engineering Naval Postgraduate School Monterey, California 93943-5000	1
4.	Professor Fotis A. Papoulias Code ME/Pa Department of Mechanical Engineering Naval Postgraduate School Monterey, California 93943-5000	4
5.	LT Daniel J. Cunningham, II 58 Case Parkway Burlington, Vermont 05401	2
6.	Naval Engineering Curricular Officer, Code 34 Department of Mechanical Engineering Naval Postgraduate School Monterey, California 93943-5004	1